
QCM AND EIS IMMUNOSENSORS

FOR APPLICATIONS TO

FOOD SAFETY AND QUALITY

Martina Cimafonte

Dottorato in Biotecnologie – XXXII ciclo

Università di Napoli Federico II



Dottorato in Biotecnologie – XXXII ciclo

Università di Napoli Federico II



QCM AND EIS IMMUNOSENSORS

FOR APPLICATIONS TO

FOOD SAFETY AND QUALITY

Martina Cimafonte

Dottorando: Martina Cimafonte

Relatore: Prof. Raffaele Velotta

Coordinatore: Prof. Marco Moracci

Settore Scientifico Disciplinare: FIS01/Fisica Sperimentale

She believed she could, so she did

INDEX

RIASSUNTO	1
SUMMARY	6
LIST OF ABBREVIATIONS	7
CHAPTER 1.	9
INTRODUCTION TO BIOSENSING	
1. PRINCIPLE OF A BIOSENSOR	11
2. ANTIBODY AS BIORECEPTOR	13
2.1 STRUCTURE AND IMMUNE RESPONSE	13
2.2 MONOCLONAL AND POLYCLONAL ANTIBODIES	15
3. ANTIBODY IMMOBILIZATION	17
3.1 CONVENTIONAL METHODS	17
3.2 PHOTOCHEMICAL IMMOBILIZATION TECHNIQUE (PIT)	20
4. TRANSDUCTION METHODS	22
4.1 PIEZOELECTRIC SENSOR	22
4.2 ELECTROCHEMICAL SENSOR	23
CHAPTER 2.	25
BIOSENSORS IN FOOD ANALYSIS	
1. FOOD SAFETY	26
2. FOODBORNE AND WATERBORNE PATHOGENS	27
2.1 <i>SALMONELLA</i>	27
2.2 <i>ESCHERICHIA COLI</i>	28
3. PATHOGENIC BACTERIA DETECTION	30
3.1 ISO METHODS	30
3.2 ELISA AND PCR	31
3.3 BIOSENSORS	32
CHAPTER 3.	34
QCM BIOSENSOR FOR <i>SALMONELLA</i> DETECTION	
1. INTRODUCTION	35

1.1 QUARTZ-CRYSTAL MICROBALANCE (QCM)	35
1.2 QCM AS BIOSENSOR	38
2. MATERIALS AND METHODS	41
2.1 CHEMICALS	41
2.2 ANTIBODY PRODUCTION	41
2.3 QCM APPARATUS	44
2.4 GOLD SURFACE PREPARATION	45
2.5 QCM EXPERIMENT	46
3. RESULTS AND DISCUSSION	47
3.1 KINETIC OF THE FUNCTIONALIZATION	47
3.2 DETECTION OF <i>SALMONELLA</i> TYPHIMURIUM	48
3.3 SPECIFICITY TEST	52
CHAPTER 4.	54
EIS IMMUNOSENSOR FOR <i>E. COLI</i> DETECTION	54
1. INTRODUCTION	55
1.1 PRINCIPLES OF ELECTROCHEMISTRY	55
1.2 METHODS FOR BIOSENSOR CHARACTERIZATION	58
1.2.1 CYCLIC VOLTAMMETRY	58
1.2.2 ELECTROCHEMICAL IMPEDANCE SPECTROSCOPY	60
1.3 EIS APPLICATIONS IN BIOSENSING	66
1.4 SCREEN-PRINTED ELECTRODES	69
2. MATERIALS AND METHODS	70
2.1 CHEMICALS	70
2.2 APPARATUS	71
2.3 PREPARATION OF THE BIOLOGICAL SAMPLE	72
2.4 GOLD SURFACE PREPARATION	72
2.5 EXPERIMENTAL PROCEDURE	74
2.6 ENHANCED SENSITIVITY PROTOCOL	75
3. RESULTS AND DISCUSSION	76

3.1 KINETIC OF THE FUNCTIONALIZATION	76
3.2 KINETIC OF THE DETECTION	77
3.3 BLOCKING WITH BSA	79
3.4 DETECTION OF <i>ESCHERICHIA COLI</i>	81
3.5 SPECIFICITY TEST	85
3.6 DATA FITTING	87
CONCLUSIONS	90
BIBLIOGRAPHY	92
APPENDIX	104

RIASSUNTO

Negli ultimi anni, la sicurezza alimentare è diventata un problema di rilievo pubblico in seguito agli enormi cambiamenti che hanno interessato il sistema alimentare caratterizzato non più da uno stretto rapporto tra produzione e consumo ma dalla globalizzazione del cibo ovvero scambi commerciali, merci in viaggio e prodotti esotici provenienti da paesi in cui la legislazione alimentare e agricola potrebbe non essere stringente come quella europea. La sicurezza alimentare è realmente garantita solo se gli alimenti, prima di essere messi in commercio, sono sottoposti a precisi controlli seguendo delle pratiche adeguate che, nel loro insieme, stabiliscono una serie di misure di prevenzione. Se queste misure non sono applicate correttamente, gli alimenti possono essere contaminati da diversi microorganismi patogeni (batteri, virus e parassiti) in grado di causare un elevato numero di infezioni, talvolta anche mortali. L'incidenza di queste infezioni è notevolmente aumentata negli ultimi anni e, attualmente, le malattie di origine alimentare, ma anche idrica, sono classificate tra i problemi più significativi al mondo in quanto incidono negativamente sulla salute dell'uomo. Alcune infezioni possono derivare da acqua non trattata o contaminata da liquami umani o animali, altre da alimenti comuni come latte, formaggio, carne, pollo, frutta e verdure crude contaminati durante il processo di preparazione. Quindi, il monitoraggio dell'acqua e degli alimenti è essenziale per garantire che siano sicuri e adatti al consumo, ovvero che sia i microorganismi patogeni sia le loro tossine siano assenti. Questo è un punto cruciale per preservare il benessere della popolazione, ma nonostante i progressi della sanità, tali malattie sono ancora un problema globale a tal punto che l'Organizzazione Mondiale della Sanità ha posto la sicurezza alimentare tra le sue prime undici priorità. Al fine di prevenire la crescita e l'evoluzione delle malattie di origine alimentare e idrica, è importante sviluppare nuove tecnologie rapide ed economiche per la rivelazione e quantificazione dei più comuni agenti patogeni.

Le infezioni più note sono quelle causate dai batteri *Campylobacter*, *Salmonella* ed *Escherichia coli*, i principali responsabili di malattie gastrointestinali. I sintomi tipici, che generalmente si manifestano tra 12 e 36 ore dopo l'esposizione e durano da 2 a 7 giorni, sono diarrea, nausea, dolore addominale, vomito e febbre. In rari casi, possono provocare malattie più gravi e addirittura la morte. L'Organizzazione mondiale della Normazione (ISO, *International Organization of Standardization*) raccomanda diverse procedure per

l'identificazione di *Salmonella* ed *Escherichia coli* in cibo ed acqua. Questi metodi, analogamente ad altri metodi convenzionali quali ELISA (*enzyme-linked immunosorbent assay*) e PCR (*polymerase chain reaction*), sono laboriosi e richiedono molto tempo in quanto includono varie fasi di pre-arricchimento (da 6 a 58 ore), arricchimento selettivo, procedure di isolamento, caratterizzazione biologica delle probabili colonie e la conferma sierologica finale. I biosensori sono strumenti in grado di superare tali limiti dei metodi convenzionali grazie ai loro principali vantaggi tra cui la semplicità di utilizzo e il breve tempo di analisi. Inoltre, sono dispositivi economici e che, nella maggior parte dei casi, non richiedono un pretrattamento del campione. Un biosensore è composto da tre elementi fondamentali: l'elemento biologico sensibile (ad esempio enzimi, anticorpi, aptameri, recettori cellulari) in grado di riconoscere e legare selettivamente l'analita (ad esempio piccole molecole, batteri, pesticidi, proteine, tossine), l'elemento fisico-chimico chiamato trasduttore o rivelatore che converte l'evento di riconoscimento in un segnale misurabile e, infine, un sistema elettronico (comprendente un amplificatore di segnale, un processore e un display) che elabora il segnale e mostra i dati ottenuti. Quindi, i biosensori sfruttano la specificità intrinseca fornita dalla molecola biologica per determinare e quantificare in modo specifico la presenza di una molecola target (analita) in un campione.

Gli anticorpi monoclonali e policlonali (o immunoglobuline) sono tra gli elementi sensibili più comunemente utilizzati in quanto possono essere preparati per un grande numero di analiti. Essi vengono ottenuti mediante protocolli di immunizzazione e sono selezionati dal sistema immunitario ospite per legarsi in modo efficace a specie aliene come batteri, virus o tossine. Le immunoglobuline di tipo G (IgGs) sono caratterizzate da due siti di legame (*antigen binding sites*) responsabili del riconoscimento selettivo dell'analita (antigene) e che devono essere accessibili quando la IgG è legata al trasduttore fisico. Ciò rende la funzionalizzazione della superficie del trasduttore una fase fondamentale nello sviluppo di un biosensore. Negli anni, molti metodi di funzionalizzazione sono stati proposti. Il metodo più semplice consiste nell'immobilizzare l'anticorpo sulla superficie del sensore mediante adsorbimento. In base al tipo di interazione che si manifesta tra l'anticorpo e la superficie, l'adsorbimento può essere definito fisisorbimento (di tipo fisico) se vengono coinvolti legami deboli di tipo intermolecolare (legami di van der Waals) o chemisorbimento (di tipo chimico) se vengono coinvolti legami forti di tipo intramolecolare. Altri metodi di immobilizzazione sfruttano l'interazione specifica tra due molecole (ad esempio avidina/streptavidina e biotina), legami covalenti

(ad esempio legami zolfo-oro) o l'intrappolamento in matrici polimeriche. Sebbene questi approcci forniscano un'immobilizzazione efficace dell'anticorpo, essi richiedono molto tempo e procedure laboriose e applicabili solo in ambito di laboratorio in quanto necessitano di trattamenti chimici e varie fasi di purificazione. Inoltre, la tossicità di alcuni reagenti chimici utilizzati potrebbe modificare le proprietà biologiche dell'anticorpo, tra cui l'abilità di legare l'antigene specifico. Questi problemi motivano la ricerca di nuove tecniche di funzionalizzazione della superficie che consentono la corretta immobilizzazione dell'anticorpo pur conservando le sue proprietà biologiche e di legame dell'analita in modo da ottenere migliore sensibilità e limiti di rivelazioni più bassi.

Nell'ultima decade, presso il Dipartimento di Fisica dell'Università "Federico II" di Napoli è stata messa a punto una nuova tecnica di immobilizzazione degli anticorpi mediante la loro attivazione con luce UV, denominata *Photochemical Immobilization Technique* (PIT). La tecnica PIT consente l'immobilizzazione di anticorpi su una superficie di oro con i siti di legame ben esposti all'ambiente circostante e al legame con l'antigene. In breve, la PIT si basa sulla fotoriduzione selettiva di ponti disolfuro presenti nelle immunoglobuline prodotta dall'attivazione UV della triade trp/cys-cys. Tale triade è una caratteristica strutturale delle IgGs, infatti ciascuna IgG ne contiene dodici. In particolare, l'energia del fotone viene assorbita dal triptofano (trp) e trasferita a specie elettrofile vicine come la cys-cys portando alla scissione del ponte disolfuro e la formazione di nuovi gruppi tiolici che possono facilmente legare superfici d'oro mediante legame covalente. È stato recentemente dimostrato che solo due delle dodici triadi sono coinvolte in questo processo, ovvero quelle che si trovano nella regione variabile costante, consentendo, quindi, il legame dell'anticorpo sulla superficie con una delle due regioni Fab esposta alla soluzione. La tecnica PIT è stata già ampiamente applicata a superfici d'oro di biosensori piezoelettrici per la rivelazione di proteine (amilasi e gliadina) e piccole molecole tossiche (parathion e patulina) e, recentemente, è stata usata con successo anche per la funzionalizzazione di nanoparticelle d'oro in sospensione colloidale.

In questa tesi, è stata studiata l'applicazione della PIT per lo sviluppo di due immunosensori per la determinazione e quantificazione di batteri patogeni in campioni di origine alimentare. La PIT è stata adottata in combinazione con un trasduttore piezoelettrico per realizzare un immunosensore per il rivelamento sensibile e specifico di *Salmonella Typhimurium* in carne di pollo. In un immunosensore piezoelettrico il segnale ottenuto è attribuibile a variazioni di massa

sulla superficie dell'elettrodo. La microbilancia a cristalli di quarzo (QCM) è il principale biosensore di tipo piezoelettrico e consiste in un disco di quarzo su cui sono depositati due elettrodi di oro (uno per ogni lato del cristallo). Quando la superficie d'oro è ricoperta da anticorpi, precedentemente attivati mediante PIT, la frequenza di risonanza del cristallo di quarzo cambia in base alla variazione di massa che si verifica sulla superficie. Quindi, il cristallo rivestito viene esposto ad una soluzione contenente il campione di pollo contaminato con *Salmonella* causando un'ulteriore variazione di frequenza nel momento in cui gli anticorpi legano i batteri. In particolare, si osserva una diminuzione della frequenza proporzionale alla quantità di *Salmonella* legata. Il protocollo sperimentale dell'immunosensore sviluppato in questa tesi è rapido, economico e non richiede personale specializzato. Inoltre, consente di raggiungere un limite di rivelabilità minore di 10^0 CFU mL⁻¹ con un minimo trattamento del campione, ovvero soltanto due ore di pre-arricchimento a 37°C (rispetto alle 6-58 ore previste dai metodi di rivelazione standard). L'affidabilità di questo immunosensore piezoelettrico è stata dimostrata mediante validazione dei risultati sperimentali con il metodo standard ISO. L'economicità e la rapidità di risposta del biosensore proposto rendono tale metodo analitico adatto per l'ispezione di alimenti con livelli di contaminazione estremamente bassi, senza necessità di lunghe fasi di pre-arricchimento e con tempi di risposta notevolmente ridotti rispetto ad altri biosensori con scopi analoghi. Prove di specificità sono risultate più che soddisfacenti poiché non viene rilevato alcun segnale significativo sostituendo *Salmonella* con *Escherichia coli*.

La versatilità di questa tecnica di funzionalizzazione ha consentito di applicare la PIT anche a sensori elettrochimici basati su spettroscopia di impedenza elettrochimica (EIS) per la rivelazione di *Escherichia coli* in acqua di rubinetto. EIS è una tecnica comunemente utilizzata per l'indagine di proprietà elettriche dei materiali e per studiare i processi elettrochimici che avvengono all'interfaccia elettrodo/elettrolita. Un sistema elettrochimico può essere associato ad un circuito elettrico e i fenomeni fisici e chimici coinvolti nel processo elettrochimico sono associati ai singoli elementi del circuito. Il circuito più utilizzato in *biosensing* è il circuito di Randles costituito da R_s (resistenza della soluzione elettrolitica), C_{dl} (capacità del doppio strato elettrico), R_{ct} (resistenza al trasferimento di carica tra la soluzione elettrolitica e l'elettrodo) e W (impedenza di Warburg). Il parametro R_{ct} dipende criticamente dalle caratteristiche dielettriche e isolanti dell'interfaccia elettrodo/elettrolita e può essere utilizzato come parametro di *sensing* poiché è molto sensibile alle modifiche che

avvengono sulla superficie dell'elettrodo. Talvolta, un CPE (elemento a fase costante) viene introdotto nel circuito equivalente invece di un condensatore ideale C_{dl} per tenere conto della disomogeneità e dei difetti dello strato di materiale biologico, nonché della porosità o rugosità dell'elettrodo. Nella realizzazione del biosensore impedimetrico, sono stati utilizzati semplici elettrodi commerciali (*Screen Printed Electrodes*) che consistono di tre elettrodi (elettrodo di lavoro, di riferimento ed elettrodo ausiliario) depositati su un unico substrato ceramico. La procedura sperimentale consta di quattro fasi: immobilizzazione dell'anticorpo (precedentemente attivato mediante PIT), *blocking* con BSA, rivelazione di *Escherichia coli* in acqua e amplificazione con una soluzione fresca di anticorpo. Lo step di amplificazione, che porta alla formazione di una configurazione di tipo sandwich (anticorpo-batterio-anticorpo) è stato introdotto nel protocollo con lo scopo di amplificare il minimo segnale di impedenza ottenuto dopo la rivelazione di basse concentrazioni di *Escherichia coli*. L'introduzione di questa semplice procedura di amplificazione ha portato alla rivelazione di *Escherichia coli* in acqua di rubinetto con un limite di rivelabilità di 3×10^1 CFU mL⁻¹ conservando la rapidità del metodo, il quale richiede solo un'ora per fornire la risposta. Anche in questo caso, le prove di specificità hanno dimostrato una trascurabile o debole cross-reattività con altri batteri quali *Acinetobacter baumannii* e *Salmonella enteritidis* 706 RIVM.

Per entrambi i biosensori, il limite di rivelabilità risulta essere comparabile o addirittura migliore di altre tecniche utilizzate. Questi risultati dimostrano che la PIT è un metodo di funzionalizzazione efficace anche su elettrodi commerciali ed economici come gli elettrodi *screen printed*. Questo è un risultato importante poiché la maggior parte dei metodi di immobilizzazione convenzionali richiedono pretrattamenti della superficie per ottenere una risposta efficace del sensore. Inoltre, la PIT è un metodo di funzionalizzazione molto rapido poiché sono necessari solo 30 secondi per l'attivazione degli anticorpi e 15-60 minuti per l'intera funzionalizzazione (dipende dal trasduttore). Sebbene questi biosensori risultino non adatti ad un'accurata analisi quantitativa, entrambi si prestano come affidabili dispositivi per analisi qualitative "on-off" di cibo e acqua contaminati. Quindi, la possibilità di monitorare i batteri target con una sensibilità analitica comparabile o di poco maggiore di quella delle tecniche attualmente in uso rappresenta un'opportunità interessante per il controllo degli alimenti finalizzato al miglioramento della sicurezza alimentare.

SUMMMARY

Salmonella and *Escherichia coli* are foodborne pathogens responsible for several illnesses worldwide. Such bacteria, in small amount are not dangerous for human health but, when the food and the water are poorly managed, they can multiply and spread causing foodborne diseases. Standard methods of detecting these bacteria in contaminated food samples, are labour-intensive and time-consuming. Therefore, one of the challenges in food industry is the development of methods for the rapid detection of low level of *Salmonella* and *Escherichia coli*. Immunosensors, based on the interaction antibody-antigen, have proved to be powerful and reliable tools in the detection and monitoring of an ever-increasing number of contaminants in food and water. Conventional antibodies immobilization procedures, based on covalent and non-covalent interactions, require chemical treatments, modification of the surface and does not ensure a correct orientation of the antibodies. To face this issue, at the Physics Department of University of Naples "Federico II", a Photochemical Immobilization Technique (PIT) was proposed in the last decade. PIT is a simple and rapid procedure able to steer antibodies in a convenient orientation of the Fab region once immobilized onto gold surface. In this thesis, PIT was used to realize a QCM-based immunosensor for the detection of *Salmonella* Typhimurium in chicken meat. The simple protocol led to a limit of detection (LOD) less than of 10^0 CFU mL⁻¹ with a pre-enrichment step lasting only 2 h at 37 °C. The reliability of the proposed immunosensor was demonstrated through the validation of the experimental results with ISO standardized culture method. Then, for the first time PIT was used to functionalize gold electrodes in order to develop an impedimetric immunosensor for the detection of *Escherichia coli* in drinking water. The immunosensor exhibited a limit of detection of 3×10^1 CFU mL⁻¹, with no need for pre-concentration and pre-enrichment steps. In both cases, the LODs were comparable or even better than other techniques used to quantify these bacteria and a negligible or slight cross-reaction was observed with other bacterial species. Although not suitable for accurate quantitative analysis, the immunosensors proposed in this thesis lend themselves as very attractive devices for "on-off" qualitative analysis of contaminated food and water. These results demonstrated that PIT is effective proved even on commercial cheap electrodes and this is a major achievement since in most situations careful surface treatments are required to get an effective sensor response.

LIST OF ABBREVIATIONS

Ab	Antibody
BCR	B cell receptor
BPW	Buffered peptone water
BSA	Bovine serum albumin
CE	Counter electrode
CFA	Complete Freund's Adjuvant
CFU	Colony-forming unit
CPE	Constant Phase Element
CV	Cyclic Voltammetry
DNA	Deoxyribonucleic acid
EDC	1-Ethyl-3-(3-dimethylaminopropyl)-carbodiimide
EDL	Electrical double layer
EFSA	European Food Safety Authority
EIS	Electrochemical Impedance Spectroscopy
ELISA	Enzyme-linked immunosorbent assay
FDA	Food and Drug Administration
IHP	Inner Helmholtz Plane
HUS	Haemolytic uremic syndrome
IFA	Incomplete Freund's Adjuvant
Ig	Immunoglobulin
ISO	International Organization of Standardization
LOD	Limit of detection
mAbs	Monoclonal antibodies
MHA	6-Mercaptohexanoic acid

MHB	Muller Hinton Broth
MHDA	16-Mercaptohexadecanoic acid
NHS	N-Hydroxysuccinimide
OHP	Outer Helmholtz Plane
pAbs	Polyclonal antibodies
PBS	Phosphate Buffer Saline
PCR	Polymerase Chain Reaction
PIT	Photochemical Immobilization Technique
QCM	Quartz crystal microbalance
RE	Reference Electrode
SAM	Self-Assembled monolayer
SPE	Screen Printed Electrode
SPR	Surface Plasmon Resonance
TMB	3,3',5,5'-tetramethylbenzidine
TSM	Thickness shear mode
UTIs	Urinary tracts infections
WE	Working electrode
WHO	World Health Organization

Motivation

Reliable, cost-effective and rapid devices are highly required in food industry because the monitoring and the identification of specific contaminants in food products are the key to prevent several problems related to human health. Conventional analytical methods are time consuming and require expensive equipment and skilled workers. In this context, in order to overcome these drawbacks, an increased interest in biosensors has been observed since the end of the 1980s. The application of biosensors in food analysis represents a growing field which prove good reliability for the assay of different analytes. One of the factor which plays a crucial role in the development of a biosensor is the method by which the bioreceptor is immobilized onto the electrode surface. Antibodies are among the most common bioreceptors and conventional antibodies immobilization procedures require chemical treatments, expert personnel for the setup of complex chemical procedures and a previous modification of the surface. To face this issue, at the Physics Department of University of Naples "Federico II", an alternative method to bind antibodies on a metal surfaces has been proposed in the last decade. This technique, named Photochemical Immobilization Technique (PIT), is a user-friendly procedure able to steer antibodies in a convenient orientation of the Fab region once immobilized onto gold surface that is with their binding sites well exposed to the environment. Compared to the conventional methods, PIT is a really quick functionalization method since only 30 seconds are required for the antibodies activation and does not involve previous modification of the surface.

Since PIT has already been used in a number of experiments to develop sensitive and selective piezoelectric immunosensors for the identification of proteins and small molecules, the aim of this thesis is twofold. Firstly, the combination of PIT with the quartz crystal microbalance technology with the aim to realize efficient and reliable detection of bacteria and, then, the use for the first time of PIT-functionalized electrodes to develop an electrochemical immunosensor based on electrochemical impedance spectroscopy (EIS). This thesis is divided in four chapters. A general introduction covering the fundamentals of a biosensor and the advantages of the Photochemical Immobilization Technique (PIT) is presented in Chapter 1. Chapter 2 points out the issue of the food safety and the need to develop biosensors as rapid analytical tools for monitoring food safety while Chapters 3 and 4 describe the development of the two types of immunosensors for the detection of *Salmonella* and *Escherichia coli*.

1. PRINCIPLE OF A BIOSENSOR

A biosensor is an analytical device that measures a physical quantity and converts that into a measurable signal. A sensor consists of three elements: the sensitive biological element (e.g. enzymes, antibodies, aptamers, cell, receptors) also called *bioreceptor* able to selectively recognize and react with the target analyte (e.g. small molecules, bacteria, pesticides, proteins, toxins), the physicochemical element called *transducer* or *detector* which converts the recognition event into a measurable signal and, lastly, an *electronic system* (including a signal amplifier, processor and display) which processes the signal and displays a data output (**FIGURE 1.1**). The output provides a representation of the interaction that occurs between the biological component and the analyte. In fact, the output is proportional to the concentration of the analyte being studied. In the first book dedicated to biosensing,¹ a biosensor was defined as “a device incorporating a biological sensing element either intimately connected to or integrated within a transducer. The usual aim is to produce a digital electronic signal which is proportional to the concentration of a specific chemical or set of chemicals. The apparently alien marriage of two contrasting disciplines combines the specificity and sensitivity of biological systems with the computing power of the microprocessor”. This definition emphasises that, in order to develop an analytical device able to detect and quantify a specific target in a complex matrix, a combination of different research areas such as biology, chemistry or physics is required. The history of biosensors starts with the development of enzyme electrodes by the American biochemist Leland C. Clark (1962), known as the father of the biosensor concept. Clark and co-workers proposed that enzymes could be used as bioreceptors and immobilized on electrochemical detectors to realize the so-called “enzyme electrode”. They published an experiment in which the glucose oxidase (GOX) was entrapped at a Clark oxygen electrode using dialysis membrane.² A schematic representation of a biosensor is shown in **FIGURE 1.1** and, generally, biosensors are classified according to the biological element or the transduction principle.

The performance of a biosensor is experimentally evaluated based on the following parameters:

- *limit of detection* (LOD): the lowest amount of analyte in a sample that can be reliably measured by an experimental procedure;
- *selectivity*: the ability to respond only to the target analyte in a sample containing other contaminants;

- *linear range*: the range of analyte concentrations for which the response changes linearly with the concentration;
- *reproducibility*: the ability to provide identical responses for duplicated experiments;
- *sensitivity*: the ability to discriminate between small differences in analyte concentration;
- *stability*: is the degree of susceptibility to ambient disturbances (e.g. temperature).

Due to their multiple advantages (robustness, fast response, real time detection, low cost, stability, sensitivity, selectivity and reproducibility) biosensors have a variety of applications in different fields including agriculture, food industries, environmental pollution monitoring and medical diagnosis.³⁻⁵ For instance, interesting areas for biosensing are the food quality, which requires rapid and low cost methods to evaluate the presence of contaminants, and the biomedical field where real-time and *in situ* analysis of clinical samples are key objectives.⁶

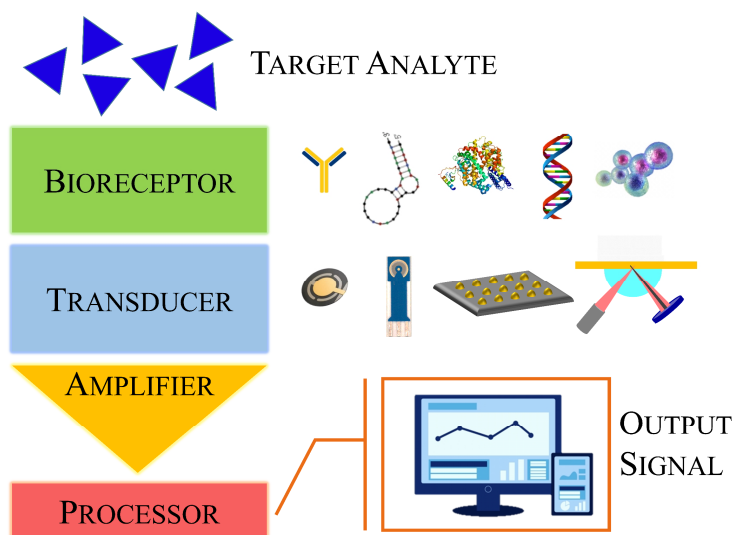


FIGURE 1.1. Sketch of a biosensor. An electrical output is obtained in response to the biological interaction between the target analyte and the bioreceptor.

2. ANTIBODY AS BIORECEPTOR

The biological recognition element, also named bioreceptor, is the crucial component of a biosensor device. The first step in the biosensor construction is the choice of the biorecognition element whose key requirements are the high selectivity and the specificity for the target molecule among a matrix of other biological components. Antibodies are the most commonly used bioreceptors probably because of their availability against a large number of analytes while other bioreceptors are aptamers, DNA, cells and enzymes.⁷ Generally, based on the bioreceptor-antigen interaction process, biosensors can be classified in bio-catalytic (enzyme), immunological (antibody) and nucleic acid (DNA) sensor.⁸ Biosensors based on the antibody-antigen interaction are also called immunosensors. In the following paragraphs, only the main features of the antibodies will be discussed since the immunosensors described in this thesis include them as bioreceptors.

2.1 STRUCTURE AND IMMUNE RESPONSE

Antibodies (Abs), also known as immunoglobulins (Ig), are glycosylated proteins which play a crucial role in the immune system since they are able to tag and neutralize extraneous substances that invade the body such as virus, toxins and bacteria (the so-called antigens). When an extraneous substance enters the body, the immune system identifies it as alien because molecules on its surface differ from those found in the body. In order to remove it, the immune system starts the production of the antibodies. They are produced and secreted by B cells, white blood cells also called B lymphocytes. Each B cell produces a single species of antibody with a peculiar antigen-binding site. When an antigen invades the body, it binds to the membrane proteins of B-cell surface (B cell receptor, BCR) stimulating it to divide and to mature into several identical cells. The mature B cells, known as plasma cells, secrete millions of antibodies into the lymphatic system and blood. Such antibodies circulate and bind the antigens that are identical to the one that triggered the immune response. Immunoglobulins account for about the 20% of the total protein in plasma by mass, thus representing the most abundant components in the blood.

These big Y-shaped proteins have a molecular weight of 150 kDa and consist of four polypeptide chains: two identical heavy chains (H chains) of about 50 kDa and two identical light chains (L chains) of about 25 kDa as shown in **FIGURE 1.2**. Each polypeptide chain has a constant region (C), which does not vary significantly among antibodies,

and a variable region (V), which is specific to each particular antibody. The four chains are connected by a combination of disulphide bonds and non-covalent interactions (i.e. salt bridges, hydrophobic interactions and hydrogen bonds). The two heavy chains are connected to each other by disulphide bridges in the hinge region, a flexible amino acid stretch at the centre of the Y, while the heavy chain is linked to the light one by a disulphide bond. The antigen binding sites of the antibody are at the end of the “arms” of the Y and, since the H and L chains are identical, each antibody has two identical antigen-binding sites.

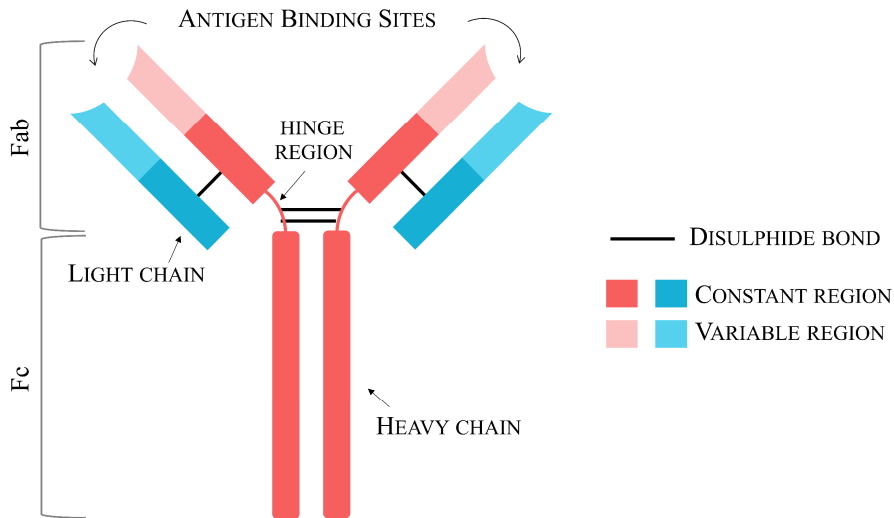


FIGURE 1.2. Structure of IgG consisting of four polypeptide units. Two heavy chains and two light chains joined to form an “Y” shaped molecule.

Two types of light chains, named lambda (λ) and kappa (κ), can be found in the antibodies. There is no difference between antibodies having λ or κ light chains, but usually, a common antibody has either κ chains or λ chains, it does not exist an antibody with one of each. The ratio of this two types is variable, the reason of this variation is still unidentified but it is well known that this ratio varies from one species to another. For instance, in mice a ratio of 20:1 (κ : λ) has commonly found, whereas in humans it is 2:1 and in cattle it is 1:20. By contrast, there are five types of heavy chains denoted by Greek letters as “alpha” (α), “gamma” (γ), “delta” (δ), “epsilon” (ϵ), and “mu” (μ), corresponding to the IgA, IgG, IgD, IgE, and IgM classes or isotypes of antibodies, respectively. Distinct heavy chains differ in size and composition: α and

γ contain approximately 450 amino acids, while μ and ϵ have approximately 550 amino acids. The general structure of all these classes is similar, but the isotype IgG is considered the most abundant immunoglobulin in plasma and has several subclasses (IgG1, IgG2, IgG3 and IgG4 in humans).

Different parts of an antibody have different functions. The top of the Y-shape contains the two antigen binding sites or *paratope* that give to the antibody its specificity towards a specific part of the antigens (*epitope*). This region, called Fab (antigen binding fragment) region, corresponds to the “arms” of the Y and consists of one constant and one variable domain for each heavy and light chain of the antibody. The lower part of the Y plays a role in modulating immune cell activity. This region, called Fc (crystallisable fragment) region, corresponds to the “legs” of the Y and it is the part of the antibody that interacts with cell surface receptors and some specific proteins allowing the activation of the immune system. The Fc region is also the site of binding for secondary antibodies, dye and enzymes which linked to antibodies on the Fc portion for experimental visualization.

The five isotypes (IgM, IgD, IgG, IgA and IgE) have different location and biological properties. IgM is the largest antibody and it is the first to appear in response to initial exposure to an antigen. Initially, an IgM is expressed as monomer on the surface of immature B cells and then secreted as pentameric antibody formed by five Ig monomers and linked via disulphide bonds. IgA is mainly localized in mucosal areas. It is a monomer in the serum but it appears as a dimer termed secretory IgA (sIgA) at mucosal surfaces. IgD acts as membrane immunoglobulin on B cells and participates in immune system stimulation. IgE is present at lowest concentration in peripheral blood but constitutes the main antibody class in allergic responses. Finally, IgG represents the most abundant antibody isotype in blood which, approximately, accounts for the 75% of human adult serum immunoglobulins. It is the main effector molecule of the B cell activity against invading pathogens. In view of their properties, in particular the high specificity and avidity, immunoglobulins are commonly used as powerful bio-recognition element in biosensors development.

2.2 MONOCLONAL AND POLYCLONAL ANTIBODIES

Antibodies can be produced in different ways for practical application such as biology, medicine, bio-sensing, diagnostic testing and therapy. One of the easiest way is the immunization of a mammalian like mouse, rabbit and goat. The selection of the

appropriate immunization strategy strongly depends on the properties of the antigen, including its nature, solubility, purity and availability. The immunization protocol requires the injection of a foreign antigen in the mammal host. Its immune system will respond to such injection producing a big amount of antibodies. It is usually necessary to collect the blood to monitor the antibody response during the experiment and then these blood samples will be purified through chromatographic techniques to obtain the antibodies. When several B cell clones produce antibodies against the injected antigen, these immunoglobulins are known as polyclonal antibodies (pAbs). pAbs are able to bind different epitopes of the antigen. On one side, this property is a huge advantage because provides a successful neutralization of the target, while on the other side, it can result in non-specific interactions since pAbs can bind antigens showing similar epitopes. Clearly, this risk is higher in the detection of large-sized antigens (like bacteria) and negligible with small molecules since in that case the epitope corresponds to the whole antigen. In addition, the production of pAbs is limited by the size of the host mammal. For instance, mice can be immunized only one time because they are commonly killed during the blood collection while bigger animals, such as rabbit and goat, can be immunized several times.

As it concerns the monoclonal antibodies (mAbs), they are produced by identical B cell which are clones from a single parent cell. This means that the mAbs are able to recognize only a specific epitope of an antigen. Unlike pAbs, which are produced in live animals, mAbs are produced *ex vivo* using tissue-culture techniques. As in the case of pAbs production, the process starts with the injection of the antigen into the mammalian. Then, once the animal develops an immune response, B cells are extracted from the host's spleen and fused to cancer cells (i.e. myeloma cells) creating immortalized B cell-myeloma hybridomas. The hybridomas cells, which are able to grow continuously in culture, are screened for the ability to produce specific antibodies for the desired target using enzyme-linked immunosorbent assays (ELISA). This screening step is performed at least three times in order to achieve a stable cell line and, finally, these hybridoma cells are amplified for a large scale antibody production. Such hybridoma technique for the production of monoclonal antibodies, that revolutionized the use of antibodies in health care and research, was developed in 1975 by Kohler and Milstein⁹ winners of the Nobel Prize for physiology and medicine in 1984. Although the production of these antibodies requires the use of a substantial numbers of animals with considerable animal welfare consequences, polyclonal and monoclonal antibodies are both

commonly used as bioreceptors in the development of a biosensor. It is worth highlighting that, in view of the more elaborate procedure claimed for the mAbs production, they are more expensive than pAbs. A polyclonal antiserum can be obtained within a short time (4-8 weeks) with a modest financial investment whereas the production of mAbs takes about 3-6 months and requires more advanced techniques. Thus, the use of pAbs or mAbs depends on the time and money available for the production.

3. ANTIBODY IMMOBILIZATION

The analytical performance of a biosensor is critically dependent on the immobilized antibody (Ab) making the choice of the immobilization procedure a key factor in the development of a biosensor.¹⁰ Ideally, the Ab should be correctly immobilized on the biosensor surface in order to retain its biological function, which means that its binding sites should remain unobstructed and available to bind the target molecule. Over the years, a wide range of immobilization methods have been investigated and the choice of the most suitable depends on the nature of the bioreceptor, the transduction principle and the target molecule.

3.1 CONVENTIONAL METHODS

Adsorption

Physical adsorption of the immunoglobulins onto a solid surface is the easiest immobilization method. Ab molecules can be directly immobilized onto the substrate via passive adsorption after a prolonged incubation.^{11,12} This method occurs through weak and non-covalent interactions between the biomolecule and the surface, such as electrostatic or ionic bonds, hydrophobic interactions and van der Waals forces.^{13,14} If on one hand the adsorption does not require any modification resulting in a very simple immobilization procedure, on the other hand the weak bonds can be easily destroyed by changes in pH or temperature thus making the surface coverage variable over time. In addition, antibodies can adsorb on hydrophobic and hydrophilic substrate by spreading and, as a consequence, the Ab molecules are randomly oriented on the substrate.

Affinity interaction

This non-covalent method is based on the specific interaction between two molecules, one linked to the sensor surface and the other to the molecule that should be immobilized. An example is the specific interaction between avidin and biotin.^{15,16} The avidin, which is able to bind four biotin molecules, can be covalently linked to surfaces functionalized with amino groups by cross-linking its amino or carboxyl functions. Then, biotinylated antibodies can bind the avidin-functionalized substrates with high affinity. This method has several advantages such as the great availability of pre-functionalized antibodies with biotin. Moreover, the biotinylation of Abs does not prejudice their functional activity as the biotin is a small molecule with a molecular weight of 244 Da. But, as in the case of the adsorption method, the interaction biotin-streptavidin can be easily denatured by changes in pH or temperature.

Protein A and G

Antibodies can be correctly immobilized by employing two intermediate binding proteins: protein A and protein G.¹⁷⁻²¹ Such proteins are able to bind to the Fc region of antibodies leaving the antigen-binding sites free for binding to antigen molecules. Protein A is a 46 kDa surface protein, originally found in the cell wall of *Streptococcus aureus*, which binds with strong affinity the heavy chain within the Fc region of immunoglobulins from many mammalian species. Protein A can be either strongly adsorbed to the gold surface or covalently linked to the amino-functionalized substrates via heterobifunctional cross-linking. Protein G, which is a 65 kDa protein expressed in group C or G Streptococci, has higher affinity than Protein A for most antibodies, but it is not able to bind to human IgM, IgA and IgD. Even if the tertiary structure of both proteins is very similar, they have inherent differences such as the optimal pH binding conditions which is 8.2 for protein A and 5 for protein G. Although these biomolecules recognize the Fc region of most immunoglobulins IgG, this interaction is not stable enough for some applications.

Covalent immobilization

In order to covalently bind Abs molecules on a substrate, several chemical strategies have been developed. A common approach is the binding of thiolated antibodies to gold surfaces, which leads to a covalent binding between gold and thiol functions. If the biomolecule

has not intrinsic thiol groups, it is possible inducing them via chemical reaction. For instance, the so-called Traut's reagent (2-iminothiolane hydrochloride) is used to modify amine groups on proteins thus obtaining new sulfhydryl groups for further applications. Another covalent immobilization method requires the modification of the surface with functional groups to which the antibodies will be immobilized. During the last years, considerable attention was given to the functionalization of noble metal surface by organic molecules in order to form self-assembled monolayers (SAMs) which assure an oriented antibodies immobilization thus guaranteeing the accessibility of the antibodies binding sites.^{22,23} Historically, the first self-assembled monolayers were based on alkylsilanes but later, thiols based monolayers have been introduced because thiols are known for being highly reactive towards noble metals and other materials. In particular, the adsorption of sulphur compounds on gold surfaces occurs via the formation of the strong bond S-Au to realize a highly oriented and densely packed monolayer. Many sulphur-based layers have been studied for electrodes modification and the most common used are cysteamine, mercaptoundecanoic acid and mercapto-propionic acid.

Entrapment into polymeric matrix

Another approach is in the entrapment of the antibodies into a polymeric matrix.²⁴⁻²⁷ The procedure consists in the mixing of the antibody with a polymer solution followed by a polymerization or solidification. This very simple approach does not require additional chemical modification but, unfortunately, cannot assure that the binding sites of the entrapped antibodies are correctly oriented and available for bind the analyte. Although some of these methods allow a very efficient antibodies orientation, they present several disadvantages. Above all, these methods are time-consuming and require treatments involving hazardous reagents that can modify the structure and the biological activity of the bioreceptor. In addition, they require a surface modification or pre-treatment for an effective antibodies immobilization than can affect the robustness and reproducibility of the protocol.

Among all the possible strategies, self-assembled monolayers (SAMs) are broadly used as linkers for the immobilization of antibodies onto gold electrode surfaces, but in spite of the many advantages they offer in many applications, there are several issues that should be considered in order to find out and control their physical and chemistry properties.^{22,23,28} SAMs on gold surfaces are usually represented as perfect monolayers, with molecules in a closed packed configuration.

Nevertheless, this concept is far from reality and the control of the quality of SAMs is a key point in many applications. The realization of a well-assembled monolayer strongly relies on the purity of the used solutions and the presence of even a low amount of contaminants, as for instance thiolated precursor molecules that are the typical impurities in thiol compounds, can lead to a non-uniform and, hence, non-ideal monolayer.²⁹ In addition, the electrode surface plays an important role in the realization of SAMs. The analysis of electrode surfaces with different roughness has shown that the rougher substrate exhibits small and variable response as a result of a non-ideal SAM formation, while the smoother surface produces higher and more reproducible response due to the increase of the SAM homogeneity.³⁰ Over the years, several studies have worked to clarify the true nature of the interaction gold-thiols SAMs.^{31–33} Considering these issues, it is worth developing less invasive procedures preserving the functional properties of the immunoglobulin and alternative methods to covalent bind antibodies on gold electrode surfaces in an easier, more rapid and reliable way.

3.2 PHOTOCHEMICAL IMMOBILIZATION TECHNIQUE (PIT)

To face this issue, at the Physic Department of University of Naples “Federico II”, a photochemical approach has been proposed. The Photochemical Immobilization Technique (PIT)^{34,35} is a functionalization method able to tether antibodies (Abs) on metal surfaces (such as gold or other bio-compatible metals) in a proper orientation that is with their binding sites well exposed to the environment.³⁶ This strategy is based on the selective photochemical reduction of disulfide bridges in immunoglobulins (Ig) produced by UV activation of near aromatic amino acid.³⁷

Disulfide bonds, which were established for the first time in the 1960s, are common structures of the four subclasses of IgG. They have a crucial role in the protein folding and stability since they are the result of the oxidation of thiol groups (-SH) of two cysteins thus connecting two parts of the protein and affecting the protein folding. In particular, an immunoglobulin shows the triad cys-cys/trp whereby an aromatic amino-acid (tryptophan) is nearby a disulfide bridge (cys-cys). Briefly, PIT is based on the selective photoreduction of disulphide bridges produced by the UV activation of the trp/cys-cys by means of an UV lamp schematically reported in **FIGURE 1.3a**. The UV photon energy is adsorbed by tryptophan and transferred to near electrophilic species like the close cys-cys resulting in the cleavage of the disulphide bridge and the formation of new thiol (SH) groups able to bind, through a

covalent bond, thiol reactive surfaces like gold ones (**FIGURE 1.3b**). Every immunoglobulin has twelve triads but it has recently been demonstrated that only two of them are involved in this process.³⁸ These triads are located in the constant variable region and allow the attack of the antibody to the surface with one of the two Fab regions exposed to the solution (**FIGURE 1.3c**).³⁸ Considering that the triad of residues trp/cys-cys can be found in every Ig, the PIT is applicable in a wide range of fields. The samples are irradiated for 30-60 s, according to the UV lamp used (for protocol details see Chapter 3 and 4). This time is the result of an optimized protocol that, as confirmed by the Ellman's assay,³⁹ produces a high concentration of UV-activated antibodies while guaranteeing no denaturation of the antibodies as evidenced by their selectivity and efficiency in antigen binding in the developed biosensors. Compared to the conventional methods, PIT is a really quick and user-friendly immobilization method which does not require a previous modification of the surface. In previous works, PIT has been used in a number of experiments to develop sensitive and selective QCM-based immunosensors^{40–43} and colorimetric biosensors.⁴⁴

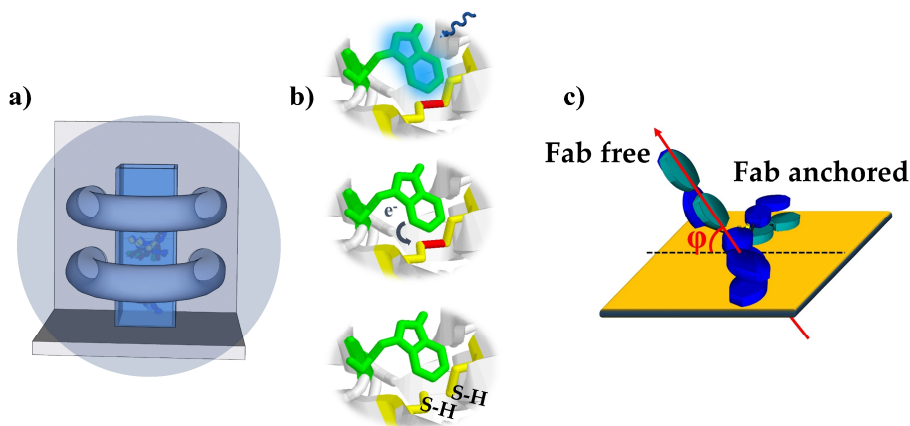


FIGURE 1.3. (a) Sketch of the UV lamp used for the UV activation of the antibodies. (b) Description of the reaction involved in PIT: the UV photon energy is adsorbed by tryptophan and transferred to near cys-cys. The result is the cleavage of the disulphide bridges and the formation of new thiol (SH) groups; (c) Antibody is immobilized onto the surface so that the angle ϕ is 45° on average thereby providing one Fab free and well-exposed to the environment.

4. TRANSDUCTION METHODS

A transducer is a device capable of converting the biological interaction between antibody and the antigen in a measurable signal which is proportional to the concentration of the antigen. Based on the type of the transducer, biosensors may be classified as optical, electrochemical, calorimetric and piezoelectric. Among them, piezoelectric and electrochemical immunosensors are widely used in view of their high sensitivity, selectivity and low cost.^{45–47} This thesis focuses the attention on two transduction methods which are described here.

4.1 PIEZOELECTRIC SENSOR

Mass-based sensors rely on the principle that the output signal is due to mass changes on the electrode surfaces. They are also known as piezoelectric biosensors since piezoelectric crystals are often used in order to precisely detect small changes in the mass caused by substances binding the piezoelectric crystal.⁴⁸ Quartz-crystal microbalance (QCM) is the major type of piezoelectric biosensor⁴⁷ (**FIGURE 1.4a**). In view of its piezoelectricity, a QCM sensor is able to detect the changes in mass by monitoring the inherent variation in the oscillation frequency of the quartz crystal.

The preparation of this transducer is achieved by sandwiching a quartz crystal wafer between two metal electrodes like gold, silver or aluminium. Then, an external oscillator circuit is connected to the electrodes and this circuit leads the quartz crystal to its resonant frequency which depends on the properties of crystal like the cutting edge and thickness. When the metal surface is covered with biological molecules (such as antibodies), the resonant frequency will change according to the mass change that occurs on the surface. Then, the coated crystal is exposed to a solution containing the target of interest causing a further frequency change when the biorecognition event takes place. In particular, a decrease in frequency proportional to the amount of the bound analyte is observed.

The quartz crystals used as a biosensor are mainly 5, 9, or 10 MHz AT-cut and it is reported that, in case of a 10 MHz of AT-cut quartz crystal, the adsorption of mass about 1 ng causes a frequency shift of 1 Hz. Although QCM-based biosensors are less used than optical and electrochemical ones, QCM is a promising sensor technology that enables rapid response, real time monitoring, low cost analysis, portability and allows the direct label-free detection with high selectivity

and specificity in several fields, from the food industry to the medical area.⁴⁹

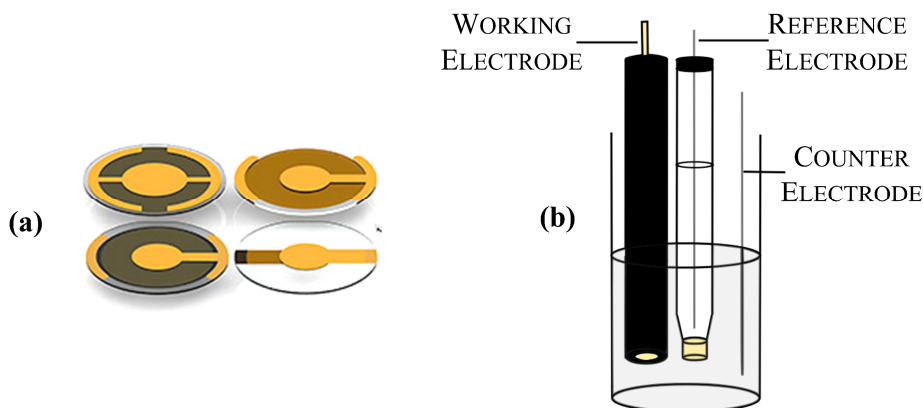


FIGURE 1.4. (a) Different types of a Quartz Crystal Microbalance (QCM) and (b) a traditional three-electrodes cell including working, reference and counter electrodes.

4.2 ELECTROCHEMICAL SENSOR

Electrochemical biosensors are among the most popular sensors for the detection of bacteria and a large number of contaminants. They are a subclass of the chemical sensors which combines the high specificity of the recognition process with the high sensitivity of an electrochemical transducer.⁵⁰ Electrochemical sensors are part of an electrochemical cell which consists of two or three electrodes (see Chapter 4). In a traditional three-electrodes cell (**FIGURE 1.4b**), three electrodes (working, reference and counter or auxiliary) are placed in the same electrolyte solution. According to the nature of the biological recognition that underlies the electrochemical biosensors, they can be classified in biocatalytic and affinity sensors.⁵¹ Biocatalytic biosensors rely on the use of enzymes as recognition element. They are based on the ability of the enzyme to selectively bind the target molecule, thus producing an electroactive species. An example is the glucose sensor, in which the immobilized enzyme “glucose oxidase” catalyses the oxidation of the glucose producing gluconic acid and hydrogen peroxide. The hydrogen peroxide, that is released as product of the reaction, is oxidized at the surface of the electrode thus producing electrons which are detected as an electrical current. On the other

hand, affinity biosensors consist of a biological element (antibody, DNA, aptamer) which can selectively bind its respective target with high affinity. In this case, the produced electrochemical signal is related to the bioreceptor-analyte interaction and it is proportional to the concentration of the analyte.

Depending on the electrical response, electrochemical biosensors can be classified as amperometric, potentiometric, impedimetric and conductometric sensors. Amperometric devices were the first type to be developed and have been using as glucose biosensors for over 35 years.⁵² They measure the current resulting from the oxidation or reduction of the electroactive species at the surface of the working electrode while a potential is applied between the electrodes.⁵³ Typically, the current is measured while the potential is maintained constant at the working electrode and this is referred to as *amperometry*. If the current is measured during controlled potential scanning, this is defined *voltammetry*. Potentiometric biosensors measure the potential of an electrochemical cell when zero or no significant current flows in it. These sensors usually use a two electrodes system. An example is an ion selective electrode for the determination of ions such as K^+ , Na^+ , Ca^{2+} and Cl^- . Impedimetric biosensors are the most commonly used for the quantification of biomolecular interactions such as antigen-antibody or protein-protein. The surface of the electrode is modified with a specific biorecognition element and, when it interacts with its specific analyte, the recognition event causes a change in the impedance. Lastly, a conductometric biosensor monitors the change in conductivity of a solution as the solution changes during the course of the chemical reaction.⁵⁴

2

BIOSENSORS IN FOOD ANALYSIS



<http://foodsafetytrainingcourse>

1. FOOD SAFETY

Food and waterborne diseases, often referred to as food poisoning, are generally caused by eating or drinking food, water and beverages contaminated by the presence of chemicals (pesticides and toxins) and pathogens (bacteria and viruses). In recent years, the incidence of these infections has hugely increased due to the globalization of the food which means the manufacturing and transport of the food to and from different regions locally and worldwide.⁵⁵ Nowadays, foodborne and waterborne illnesses are classified among the most significant public health problems in the world. Thus, the issue of the food safety has become a problem of public interest in both developed and under-developed countries since the sub-quality of the food and the contamination of the water are related to an increase of human diseases and even mortality.⁵⁶

In 2015, the World Health Organization (WHO) reported that each year 420000 people, mostly children below the age five, suffer from these infections and die because of the consumption of contaminated food and water.⁵⁷ Some infections can be derived from the sources, like untreated or polluted water. Mainly, water contaminated with human or animal sewage will cause a food poisoning illness. Safety agencies usually suggest to avoid suspicious water. For instance, it is not recommended to drink water in areas with poor water supplies except after boiling it or bottled water. Other foodborne diseases come from food. Common food such as milk, cheese, meat, chicken, fruit and raw vegetables become contaminated during the food preparation process, before reaching the supermarket or by a food handler with unclean hands.

Bacteria, viruses, fungal, bacterial toxins and pesticides are the main cause of food poisoning. These pathogens are dangerous for the human health and responsible for severe illnesses which may range from temporary to long-term diseases, acute organ damage and even cancer. However, food quality monitoring is essential to ensure that the water and the food produced by the food industry are both safe and suitable for consumption. This is a crucial point for preserving the well-being of the population, but in spite of the advances in healthcare, such diseases are still a global problem to such an extent that the WHO has placed the food safety as one of its top 11 priorities. In order to manage the growth and evolution of food and waterborne diseases, it is important to develop devices for rapid detection of pathogenic contamination that would replace the conventional methods.

2. FOODBORNE AND WATERBORNE PATHOGENS

Pathogenic bacteria are among the major causative agents of foodborne and waterborne infections. Some bacteria, in small amounts, are not dangerous for human health because the human body is able to fight them off. When the food and the water are poorly managed, these bacteria can multiply and spread causing several diseases such as food poisoning. Unfortunately, contaminated food and water may not look, taste or smell different from uncontaminated ones thus increasing the possibility to become infected.

The most important pathogenic organisms are *Bacillus cereus*, *Campylobacter jejuni*, *Clostridium botulinum*, *Clostridium perfringens*, some strains of *Staphylococcus aureus*, *Escherichia coli*, *Brucella*, *Listeria monocytogenes*, *Salmonella* spp., *Shigella*, *Vibrio cholerae*, *Yersinia enterocolitica* and *Aeromonas* spp.⁵⁸ These bacteria produce toxins and other cell metabolites that cause fatal diseases. There are different symptoms of food poisoning which usually develop from 30 minutes to several days after consumption of contaminated water or food. In the next paragraphs, an overview of *Salmonella* and *Escherichia coli*, which are the most widespread bacteria commonly found in food and water, is reported.

2.1. *Salmonella*

Salmonella genus are rod-shaped and Gram-negative bacteria belonging to the family of *Enterobacteriaceae*⁵⁹ isolated in 1885 by two American veterinarians, Salmon and Smith. The name was subsequently adopted in honour of Dr Salmon. Over the years, many others *Salmonella* were isolated and the classification or serotyping is the result of several studies about the interaction between bacterial surface antigens and antibody. Currently, more than 2500 serotypes have been described and each *Salmonella* serotype has a particular lipopolysaccharide or O antigen, a flagellar or H antigen or a capsular or K antigen. The genus *Salmonella* consists of two species: *Salmonella bongori* (*S. bongori*) and *Salmonella enterica* (*S. enterica*). *Salmonella* bacteria typically live in animal and human intestines, in particular *S. enterica* has six subspecies which are mainly found in warm-blooded animals and in the environment while *S. bongori* is restricted to cold-blooded animals, particularly reptiles. Members of the genus *Salmonella* are non-spore forming and facultative anaerobic bacilli with a cell diameter between 0.7 and 1.5 μm , length from 2 to 5 μm and peritrichous flagella all around the cell body.⁶⁰ They are

sensitive to heat, usually grow at temperature range of 5-47 °C (with optimum temperature of 35-37 °C) and get killed at temperature of 70 °C or above. However, the optimal pH range for its growth is between 6.5 and 7.5. Worldwide, *Salmonella* species are foodborne pathogens and second only to *Campylobacter spp.* for causing serious gastrointestinal illnesses.⁶¹ They invade only the gastrointestinal tract and provoke a symptomatic infection known as *Salmonellosis*, which is the most common example of disease transmitted from animals to humans in both developing and developed countries.

People can become infected as a consequence of a failure of personal hygiene after contact with infected animals or people and through the consumption of untreated food of animal origin. Particularly, raw and uncooked eggs, poultry meat, vegetables and fruits are considered to be primary sources of human *Salmonellosis*.^{62,63} These foodstuffs may be contaminated with *Salmonella* during slaughter, processing and production in contaminated environment. As with other infections, its course and outcome depend on several factors including bacteria species, inoculating dose and the immune status of the host. *Salmonellosis* in humans is mainly caused by *S. enterica* subsp. Typhimurium or *S. enterica* subsp. Enteritidis and the typical symptoms are diarrhea followed by nausea, abdominal pain, vomiting and fever. These symptoms occur between 12 and 36 hours after exposure and last from two to seven days. The infection, which does not normally require an antibiotic treatment, can be pretty dangerous for people with a weakened immune system who are more likely to develop severe infections. In such cases, a prompt medical attention is required.

2.2. *Escherichia coli*

Originally known as *Bacterium coli commune*, *Escherichia coli* is a Gram-negative bacterium of the genus *Escherichia* and member of the bacterial family of *Enterobacteriaceae*. A number of genera within the family are human intestinal pathogens (e.g. *Salmonella*, *Shigella*, *Yersinia*). Many others are normal colonists of the human gastrointestinal tract (e.g. *Escherichia*, *Enterobacter*, *Klebsiella*), but these bacteria may occasionally be associated with different diseases. It was identified for the first time in 1885 by the German paediatrician and bacteriologist Theodor Escherich, which isolated it from the faeces of new-borns. *E. coli* is a rod-shaped gut bacterium, natural inhabitant in the in gastrointestinal tract of humans and warm-blooded animals. *E. coli* has been considered a “commensal” organism in the large intestine for many years since it lived in a mutually beneficial association with

hosts. This idea changed in 1935 when a strain of *E. coli* was shown to be the cause of an outbreak of diarrhea among infants. In fact, although most *E. coli* strains are harmless and rarely cause a disease, a few strains, such as Shiga Toxin-producing *E. coli* (STEC), can be pathogenic and responsible for a broad spectrum of diseases, including severe diarrhoea, urinary tracts infections (UTIs), inflammations and neonatal meningitis.⁶⁴ In rare cases, these strains are also responsible for haemolytic-uremic syndrome, peritonitis, mastitis, septicaemia and gram-negative pneumonia. These pathogenic varieties of *E. coli* produce toxins that make them able to live in the human body, particularly in those parts normally not inhabited by *E. coli*, and able to damage host cells.

The intestinal pathogens can be classified in six well-described categories: enteropathogenic *E. coli* (EPEC), enterohaemorrhagic *E. coli* (EHEC), enterotoxigenic *E. coli* (ETEC), enteroaggregative *E. coli* (EAEC), enteroinvasive *E. coli* (EIEC) and diffusely adherent *E. coli* (DAEC). Over 700 serotypes of *E. coli* are recognized and, as *Salmonella* and other bacteria, can be categorized based on elements that can produce an immune response in animals, namely O antigen (part of the lipopolysaccharide layer), H antigen (capsule) and K antigen (flagella). The antigenic type is important to distinguish the small number of strains that actually cause diseases. For instance, the serotype O157:H7 is uniquely responsible for causing haemolytic uremic syndrome (HUS). Humans may be exposed to *E. coli* infection primarily by eating contaminated food, such as raw or undercooked ground meat products and unpasteurized milk. An increasing number of outbreaks are also associated with the consumption of contaminated fruits and vegetables whereby the contamination is mainly due to the contact with faeces from animals (domestic or wild) at some stage during cultivation or handling. Also waterborne transmission has been reported. Water can become contaminated by faeces and the infections occur from drinking polluted water and from swimming in contaminated pools. Most healthy adults usually recover from *E. coli* illness within a week, but in a small portion of patients (particularly young children and older adults) the infection may lead to a life-threatening disease such as haemolytic uremic syndrome. Symptoms of *E. coli* infection typically begin three or four days after exposure to the bacteria, though you may become ill as soon as one day after to more than a week later.

The peculiar characteristic of *E. coli* is its ability to adapt to the habitat; it can grow in media with only glucose as solvent and under both anaerobic and aerobic conditions. Under anaerobic conditions it will grow by means of fermentation, producing characteristic "mixed

acids and gas" as end products. *E. coli* bacteria cells are able to survive outside the body for a limited amount of time, which makes them ideal indicator organisms to test environmental samples for faecal contamination. As a consequence, the presence of *E. coli* in water is considered as a possible indicator of the microbiological water quality deterioration and the presence of *E. coli* in processed food products can indicate faecal contamination.⁶⁵

3. PATHOGENIC BACTERIA DETECTION

3.1 ISO METHODS

The detection of pathogenic bacteria is an important issue for ensuring food safety, security and public health. Some strict rules are established by safety agencies such as US Food and Drug Administration (FDA), the European Food Safety Authority (EFSA) and International Organization of Standardization (ISO) which define the maximum level for certain contaminants in food and water in order to keep a high level of quality. The isolation and identification of *Salmonella* and *E. coli* can be performed by using conventional culture methods recommended by the International Organization of Standardization (ISO). The approved method for *Salmonella* detection in food and animal foodstuffs is ISO-6579-1:2017.⁶⁶ It includes pre-enrichment steps of the samples followed by selective enrichment. From each enrichment medium, plating onto two agar media plates is carried out after 24 h and 48 h of incubation. Then, the biochemical characterization of probable colonies and their final serological confirmation are performed. For the confirmation, it is recommended that at least five colonies have to be identified in the case of epidemiological studies.

As it concerns *Escherichia coli*, ISO 9308-2:2012 is the approved method for the enumeration of *E. coli* and coliform bacteria in water. This method, which can be applied to all types of water (including water with suspended matter), relies on the growth of target organisms in a liquid medium and the calculation of the "Most Probable Number" (MPN) of organisms by reference to MPN tables. When this test is used for the enumeration of *E. coli* in marine water, a 1:10 dilution in sterile water is typically required because of the high concentration of salts. This method is based on the detection of *E. coli* through the expression of the enzyme β -D-glucuronidase and, consequently, it does not detect many of the enterohemorrhagic strains of *E. coli*, which do not typically

express this enzyme. This test provides a confirmed result with no requirement for further confirmation.

Certainly, these methods are very sensitive and cheap, but even unsuitable for testing a large number of samples, labour-intensive and time consuming since they require 2–3 days to yield initial results and up to 7–10 for the confirmation because they rely on the ability of microorganisms to multiply and to produce visible colonies.⁶⁷ Furthermore, while waiting for test results without shipping the foodstuffs could have a strong negative impact on the business profitably, the alternative of missing possible positive result for pathogenic contamination, obviously, implicates costly recalls of goods, human suffering and loss of reputation.⁶⁸

In this context, the development of rapid, cost-effective and automated methods for the identification and, eventually, quantification of bacteria such as *S. Typhimurium* and *E. coli* is urgent. These methods, integrated with preventive strategies such as Hazard Analysis Critical Control Points (HACCP), could significantly improve the safety of the food chain, from raw to processed foods.⁶⁹ Such an issue has been addressed by adopting a number of strategies,⁷⁰ but the goal is far from being accomplished since the current regulation for food analysis requires that alternative methods should have sensitivity and specificity of at least 99%, be rapid and not requiring specialized personnel to carry out the analysis.⁷¹ These strategies can be classified as immunology-based assays (ELISA), nucleic acid-based assays (PCR) and biosensors.

3.2 ELISA AND PCR

ELISA (*enzyme-linked immunosorbent assay*) is a plate-based assay designed for detecting and identifying many substances (such as peptides, proteins, antibodies, hormones and pathogens) in a complex matrix.⁷² It relies on the specific affinity between the antigen and monoclonal or polyclonal antibodies.⁷³ In the simplest form of an ELISA assay, an antigen is immobilized on a solid surface and a matching antibody is applied over the surface so that it can bind to the antigen. This antibody is linked to an enzyme, and in the final step, a substance containing the substrate of the enzyme is added. The reaction enzyme-substrate produces a measurable signal that usually is a colour change. Other names, such as enzyme immunoassay (EIA), are also used to describe the same technology.

PCR (*polymerase chain reaction*) is a nucleic acid-based assay widely used in the determination of microbial pathogens.^{74–76} The PCR

involves the use of many critical steps (DNA extraction, PCR amplification and detection of amplicons) and each procedure must be carefully designed and performed. In contrast to the other culture-based methods, PCR allows the detection of different pathogens in a single multiplex reaction. Moreover, since PCR is based on DNA amplification, false-positive or -negative results may easily occur and a further confirmation step is requested.

These methods are robust and have specificity and sensitivity comparable to the conventional methods (culture based techniques) but, although are less time-consuming, they require expensive equipment and chemical reagents, skilled workers, initial sample pre-treatment, accurate primer designing and specific labelled secondary antibody which make the application of these methods limited only to the laboratory environment.⁷⁷⁻⁷⁹ Moreover, the results provided by these methods are easily influenced by intrinsic characteristics of the food such as background microbiota, sample matrix and inhibitory substances (heavy metals, proteins, fats, carbohydrates, antibiotics and organic compounds⁸⁰).

3.3 BIOSENSORS

Detection techniques based on biosensors are considered powerful instruments to quickly detect foodborne pathogens and their toxins, able to overcome the limitations of the conventional methods due to their multiple advantages such as low cost, high-sensitivity, fast response, robustness, real time detection and simple operation.⁸¹ Biosensors have been increasingly gaining popularity thanks to their intrinsic selectivity that allows an accurate and rapid detection of pathogens in foodstuffs. Unlike the complex and lengthy methods, they require minimal or no sample purification and can be applicable on a wider scale as, for instance, in selecting the correct direction for finished products: sale at retail market or industrial treatments to eliminate pathogens bacteria.⁷¹ The application of biosensor technology offers, hence, a promising solution for portable, rapid and sensitive detection of pathogens in the food industry. Moreover, biosensors are frequently employed for both the identification of many substances and the determination of parameters such as aroma and freshness.⁸²

An ideal biosensor should have high sensitivity and selectivity for the target analyte, high electrode stability and, so that it works successfully, it should respond quickly in real time detection of the target. Many types of biosensors have been developed over the years. A useful classification is to divide them into two groups: direct and

indirect biosensors.⁸³ The direct recognition sensors (or “label-free”) rely on the direct measurement of the biological interaction between the analyte and the bioreceptor. On the other hand, the indirect detection sensors require a secondary element (called label) for the detection of the analyte. Examples are enzymes (such as the glucose oxidase) and fluorescently tagged antibodies that enhance the detection of a sandwich complex. For instance, a common type of indirect detection sensor could be an electrochemical transducer capable of measuring the oxidation or reduction of an electroactive compound on the secondary ligand. Although direct detection methods are simpler and faster, they typically yield a higher limit of detection than indirect detection methods.

In each group, different types of transducers can be employed and, currently, considerable attention is given to the devices based on surface plasmon resonance (SPR)^{84–86}, cantilever⁸⁷, photochemical immunoassay (PEC)⁸⁸, piezoelectric^{89,90} and electrochemical transducers.^{91–94} However, nanomaterial-based sensors are gaining an increasingly crucial role in the development of sensors in the food industry because of the high versatility of the used nanomaterials.⁹⁵ Thus, AuNP based immunosensors and magnetic nanoparticles-derived biosensor are considered the most attractive approach for detecting and removing food contaminants.⁹⁶

For all of these technologies, the recognition element plays a crucial role. Biosensors based on antibody-antigen interaction (the so-called immunosensor) are broadly investigated and, electrochemical and QCM-based immunosensor have emerged as sensitive techniques for bacteria detection due to the multiple advantages.^{97–100}

3

QCM BIOSENSOR FOR *SALMONELLA* DETECTION



1. INTRODUCTION

1.1 QUARTZ-CRYSTAL MICROBALANCE (QCM)

In recent years, Thickness Shear Mode (TSM) resonators have received an increasing interest from scientific community mainly due to their multiple applications in various disciplines of science and technology including surface characterization and detection of numerous analytes (metals, chemical substances, environmental pollutants, biomolecules and pathogens).^{101,102} Quartz Crystal Microbalance (QCM) is a shear mode device consisting of a thin disk of quartz with coated electrodes (**FIGURE 3.1a**), in which the elastic wave propagates in a direction perpendicular to the crystal surface. QCMs have been traditionally used for thin film deposition control under vacuum and gas phase for 60 years, but about 40 years ago this device was proven to be applicable also in liquid environment allowing the use of quartz crystal microbalances in the development of sensor for liquid samples analysis. The QCM technology relies on the *reverse piezoelectric effect*, a physical principle first discovered by Jacques and Pierre Curie in 1880. They observed that for a certain crystalline material, notably quartz, the application of a mechanical stress produces an electrical polarization (*direct piezoelectric effect*). By contrast, if an electric field is applied to the same crystalline material the result is a mechanical deformation (*reverse piezoelectric effect*) (**FIGURE 3.1b**).

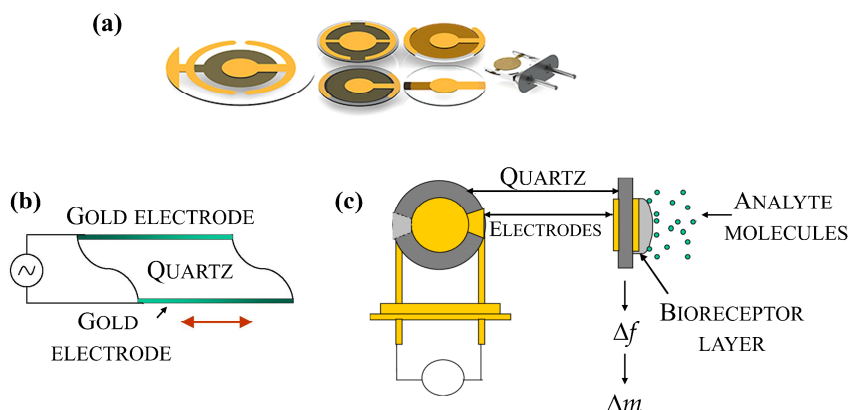


FIGURE 3.1. (a) different QCM electrodes, (b) shear deformation at the fundamental frequency and (c) schematic representation of the QCM principle: the frequency shift is proportional to the mass adsorbed onto surface electrode.

The term “quartz crystal microbalance” was coined by the German physicist Gunter Sauerbrey in the 1950s.¹⁰³ He demonstrated that, when a voltage is applied to a quartz crystal, it oscillates at a specific resonance frequency and the mass change (Δm) that occurs on the electrode surface is directly related to the change in frequency (Δf) of the oscillating crystal, as shown by the Sauerbrey’s linear equation:

$$\Delta m = -C\Delta f \quad (3.1)$$

where C is a constant related to the resonant frequency, the active crystal area, the density and the shear modulus of quartz. In practice, this equation can be used to calculate the mass of thin layers tethered to a QCM crystal surface, taking in account that QCM is a device able to detect from nanogram to microgram level changes in mass.

The application of an oscillating electric field to the gold electrodes leads to the generation of two shear waves in the crystal. These waves, produced in view of the piezoelectric properties of the QCM, overlap resulting in the deformation of the quartz. A shear wave propagates through the quartz crystal and is reflected on its faces. If the total phase shift is an integer multiple of 2π constructive interference will lead to crystal resonance. For a QCM resonator the subsequent resonance conditions are valid:

$$h_s = N \frac{\lambda}{2} \quad (3.2)$$

$$f_N = \frac{Nv_s}{2h_s} \quad (3.3)$$

where h_s is the thickness of the crystal, N the mode number, λ the acoustic wavelength, f_N the resonance frequency and v_s is the shear wave velocity.

The shear wave velocity (v_s) is defined as:

$$v_s = \sqrt{\frac{\mu_q}{\rho_q}} \quad (3.4)$$

where μ_q ($2.947 \times 10^{11} \text{ g cm}^{-1} \text{ s}^{-2}$) is the shear quartz modulus and ρ_q (2.648 g cm^{-3}) is the density.

The resonance condition is verified only at specific frequencies where kinetic (U_k) and potential (U_p) peak energies are perfectly

balanced. When a small amount of mass is attached on the gold electrode, U_k rises and the resonant frequency shifts to the value required to keep the U_k and U_p values balanced.

U_k and U_p can be defined by the following expressions:

$$U_k = \frac{\omega^2 u_{x^0}^2}{2} \left(\rho_s + \frac{\rho_q h_s}{2} \right) \quad (3.5)$$

$$U_p = \frac{\mu_q k^2 u_{x^0}^2 h_s}{4} \quad (3.6)$$

where u_{x^0} is the surface displacement amplitude, ρ_s is the surface density of the adsorbed material and k is the wavenumber.

Since $U_k = U_p$, combining the equations (3.5) and (3.6), the following relationship is obtained:

$$\left(\frac{\omega_0}{\omega} \right)^2 = 1 + \frac{2\rho_s}{\rho_q h_s} \quad (3.7)$$

where ω_0 and ω are the basal and the final angular resonance frequencies, respectively.

In particular ω_0 is obtained when $\rho_s = 0$, i.e. in absence of adsorbed material and can be described as:

$$\omega_0 = 2\pi f_0 = \frac{\pi}{h_s} \sqrt{\frac{\mu_q}{\rho_q}} \quad (3.8)$$

For small values of ρ_s , Equation 3.8 can be linearly approximated as follows:

$$\frac{\Delta f}{f_0} = - \frac{\rho_s}{\rho_q h_s} \quad (3.9)$$

This expression states that the relative shift in the oscillation frequency is equal to the relative mass shift due to the material adsorption. The Sauerbrey's equation descends from the combination of the expressions 3.2, 3.3, 3.4 and 3.9:

$$\Delta f = - \frac{2f_0^2 \rho_s}{\sqrt{\rho_q \mu_q}} = - \frac{2f_0^2 \Delta m}{A \sqrt{\rho_q \mu_q}} \quad (3.10)$$

where A is the area of the electrode and Δm is the deposited mass.

The Sauerbrey's equation is used to estimate the amount of mass deposited on the gold electrode surface and it is only valid when the change in mass is less than 2% of the crystal mass. For greater change in mass, the Sauerbrey's equation becomes inaccurate thus losing the linear relationship between Δf and Δm . For the Sauerbrey's equation, the mass on the gold electrode surface should be rigid and thin, for instance elastic subjects such as metallic coatings, metal oxides and thin adsorbed layer which do not dissipate energy during the oscillation.¹⁰¹ As it concerns the adsorption of viscoelastic films or soft molecules from liquid sample, dissipation phenomena have to be examined. Kanazawa and Gordon¹⁰⁴ showed the influence of the liquid on the resonance frequency of the quartz and the Sauerbrey's equation has to be modified as:

$$\Delta f = - \sqrt{f_0^3 \frac{\rho_l \eta_l}{\pi \mu_q \rho_q}} \quad (3.11)$$

where ρ_l and η_l are the density and the viscosity of the liquid, respectively.

The cut angle of a quartz crystal affects the resonant frequency. Typical special cuts would include AT-cut, BT-cut, SC-cut, IT-cut and FC-cut crystals. Usually, AT- or BT-cut are preferred in order to facilitate the propagation of the acoustic wave perpendicular to the surface of the QCM. AT-cut quartz refers to quartz cut at an angle of 35° 15' from the optical axis while BT-cut quartz to an angle of 49°00'. AT-cut quartz crystal, fabricated for the first time in 1934, is the most widely used and its major advantage is that it has nearly zero frequency drift at room temperature and, hence, it is only subject to minimal changes in frequency due to variations in temperature. Since thin crystals with high resonant frequency and sensitivity are very breakable, the most common used QCMs have a diameter of about 1 cm.

1.2 QCM AS BIOSENSOR

The possibility to attach biological molecules (such as antibodies, aptamers, enzyme, cells etc.) to the gold surface electrode enables the QCM to act as a biosensor since the functionalization makes the surface bioselective. The first use of a QCM as immunosensor was reported by Shons in 1972,¹⁰⁵ where a piezoelectric quartz crystal microbalance was modified for the determination of antibody activity in solution. In particular, anti-BSA (bovine serum albumin) antibodies were detected by coating the QCM surface with BSA. Over the years,

many researchers have applied QCM as transducer in biosensing and, nowadays, QCM-based biosensor are considered a reliable alternative to the conventional methods due to the ease of use, portability and the high sensitivity to mass deposition on the electrode surface.

Several QCM applications concern the detection of pathogenic bacteria in which the working principle is represented by the interaction between the biological molecule immobilized on the gold electrode and the target bacteria that leads to an increase of the mass onto the electrode and consequent decrease of the QCM resonance frequency as it is shown by the negative sign in the Sauerbrey equation (3.1 or 3.10). Thus, the frequency change is proportional to the mass change, which is related to the analyte concentration.

As it is shown in **TABLE 3.1**, QCM-based immunosensors reported for the detection of *Salmonella* fail to achieve very low limit of detection unless ballasting procedures (by antibodies or even by functionalized nanoparticles) and separation techniques are carried out. Pathirana *et al.*¹⁰⁶ reported a rapid and sensitive method for the detection of *Salmonella* by using the Langmuir–Blodgett method to immobilize polyclonal antibodies. The results indicate a limit of detection of few hundred cells/mL in less than 100 s and with a linear response between 10^2 - 10^7 cells/mL. A QCM-based immunosensor for the detection of *Salmonella* Typhimurium with simultaneous measurements of the resonant frequency and motional resistance has been described.¹⁰⁷ The immobilization of the antibody onto crystal gold surface was achieved via protein A interaction and, when analysing chicken meat sample, the limit of detection was 10^2 CFU mL⁻¹ using anti-*Salmonella* modified magnetic beads both as a separator/concentrator during the pre-treatment and as a marker for signal amplification. Recently, Salam *et al.*¹⁰⁸ described the application of a QCM integrated with a microfluidic system and modified with monoclonal antibodies for rapid and real time detection of *Salmonella* Typhimurium. The bacteria were detected using direct, sandwich and sandwich assay with antibody conjugated gold nanoparticles and the highest sensitivity (LOD = 10-20 CFU mL⁻¹) was obtained with gold-nanoparticles. The direct and sandwich assay allowed to achieve LODs of 1.83×10^2 CFU mL⁻¹ and 1.01×10^2 CFU mL⁻¹, respectively.

A similar limit of detection (7.9×10^3 CFU mL⁻¹) was obtained in less than 1 hour by using a QCM-based aptasensor.⁹⁰ After the modification of the electrode with SAMs of MHDA, an aptamer was immobilized on the electrode surface via EDC/NHS activation. This aptasensor was able to detect 10^3 CFU mL⁻¹ of *S. Typhimurium* in less than 1 hour and without any pre enrichment. In order to reduce the limit

of detection in food sample, Ozalp *et al.*¹⁰⁹ reported the development of a sensitive and specific aptasensor for the detection of *Salmonella* by integrating magnetic beads as purification system. Such a magnetic separation system could efficiently capture cells in less than 10 min and the feeding of captured bacteria to a QCM flow cell system showed specific detection of *Salmonella* cells at 100 CFU mL⁻¹ from model food sample (i.e. milk).

TABLE 3.1. QCM-based immunosensor for *Salmonella* detection

Bioreceptor	Immobilization method	LOD (CFU mL ⁻¹)	Reference
Antibody	Langmuir-Blodgett	10 ²	106
Antibody	Protein A	10 ²	107
Antibody	EDC-NHS	10–20	108
Aptamer	SAMs of MHDA EDC-NHS	10 ³	90
Aptamer	SAMs of MHA Amine	10 ²	109

EDC:1-Ethyl-3-[3-dimethylaminopropyl]-carbodiimide hydrochloride); NHS: N-Hydroxysuccinimide; MHDA: 16-Mercaptohexadecanoic acid; MHA: 6-Mercaptohexanoic acid

In this chapter, a simple, reliable, fast, sensitive and specific protocol based on Quartz-Crystal microbalance (QCM) for the detection of *Salmonella* Typhimurium in chicken meat is described. The proposed method, which exploits PIT as effective surface functionalization technique, allows us to directly detect samples with a LOD less than 10⁰ CFU mL⁻¹ requiring a pre-enrichment step lasting only 2 hours at 37 °C. The reliability of the proposed immunosensor has been demonstrated through the validation of the experimental results with ISO standardized culture method. The cost-effectiveness of the procedure and the rapidity of the QCM-based biosensor in providing the qualitative response make the analytical method described here suitable for applications in food inspection laboratory and throughout the chain production of food industry.

2. MATERIALS AND METHODS

2.1 CHEMICALS

Phosphate buffer saline (PBS) was purchased from Microgem (Naples, Italy). Fisher 344 rats were obtained from Harlan, Italy. Anti-*Salmonella* polyclonal antibody (pAbs) were prepared through a procedure described in the next paragraph and anti-*Salmonella* solutions ($50 \mu\text{g mL}^{-1}$) were prepared in a 0.01 M PBS solution (pH 7.4). Goat Anti-Rat HRP was supplied from Abcam, UK. Sodium Chloride (NaCl), Tween 20, bovine serum albumin (BSA), sulphuric acid (H_2SO_4 98%), hydrogen peroxide (H_2O_2), Freund's adjuvant, 3,3',5,5'-Tetramethylbenzidine (TMB), 2% skimmed milk powder were purchased from Sigma-Aldrich (Italy). Buffered peptone water (BPW) was from A.E.S. Laboratoire Groupe, France. NAb™ Protein G Spin Kit, NanoDrop 2000 spectrophotometer, Chromogenic Agar Base (CM1007), Tryptone Bile X-Gluc (TBX Agar, CM0945) was purchased from Thermo Fisher Scientific (USA). The quartz crystal oscillators (AT10-14-6-UP-01) were from Novatech S.r.l. (Naples, Italy). Specificity of anti-*Salmonella* pAbs was assessed using ANOVA Test from GraphPad Software, La Jolla, CA, USA. The microfluidic setup involves a fluidic cell, silicon tubes and a 10 mL syringe. The total volume of the circuit is about 200 μL while the cell volume is about 30 μL .

2.2 ANTIBODY PRODUCTION

Polyclonal antibodies against *Salmonella* were produced in Fischer 344 rats. Each animal received two intraperitoneal injections at two weeks' interval of heat killed *Salmonella* Typhimurium bacteria at the concentration of 10^7 CFU mL^{-1} in 0.9 % NaCl (300 μL), emulsified with an equal volume of incomplete Freund's adjuvant. Freund's adjuvant is considered one of the most effective adjuvants commonly used to trigger a humoral antibody inflammatory response for the production of high titer antibodies. There are two types of Freund's adjuvant: complete and incomplete. Complete Freund's Adjuvant, or CFA, is a water in oil emulsion, which also contains inactivated mycobacteria (*Mycobacterium tuberculosis* is most frequently used). Incomplete Freund's Adjuvant, or IFA, is the same water in oil emulsion, but does not contain the mycobacteria pathogen. After 1 week from the last injection, animals were sacrificed, and peripheral blood was collected. The serum, which has the same composition of the blood plasma but without clotting factors, contains proteins (e.g. antibodies,

electrolytes and small molecules) and it was separated from clotted blood by centrifugation at 5000 rpm for 5 min. The immunoglobulins were then purified by using NAb™ Protein G Spin Kit. The eluted anti-*Salmonella* pAbs level was analysed by means of NanoDrop 2000 spectrophotometer. All procedures were approved by Italian Minister of Health (authorization n° 891/2015-PR) and were performed in accordance with relevant guidelines and regulations. The purified antibody aliquots were stored at -20°C for later use.

Before evaluating cross-reactivity of IgG antibodies against major foodborne pathogens, the pAbs titer was measured by ELISA. Briefly, 100 µL of *Salmonella* Typhimurium (10^5 CFU mL⁻¹) in pure PBS were seeded in a 96-well plate. After incubation overnight at room temperature, the wells were washed 3 times with 0.05% Tween 20 (v/v) in pure PBS; quenched with 100 µL of 1% BSA (v/v) in pure PBS and incubated at room temperature for 1 h. Then, 100 µL of anti-*Salmonella* pAbs at different dilutions (1:20; 1:50; 1:60; 1:80; 1:100; 1:150) were added to the wells and the plate was incubated at room temperature for 3 h using a constant shaking (100 rpm). Subsequently, the wells were rinsed 3 times with 0.05% Tween 20 (v/v) in pure PBS and incubated 1 h at room temperature with 100 µL of Goat Anti-Rat HRP diluted 1:5000. Then, wells were washed 3 times with 0.05% Tween 20 (v/v) in pure PBS and 50 µL of 3,3',5,5'-Tetramethylbenzidine (TMB) were added. The plate was incubated again, in the dark, at room temperature for 20 min. The reaction was stopped by the addition of 0.16 M H₂SO₄ (100 µL) to all wells and the titer was determined through the measurement of the optical absorbance at 450 nm (Biorad microplate reader model 680, USA).

Subsequently, an immunoabsorption protocol was carried out to avoid any possible cross-reaction of anti-*Salmonella* pAbs with *Escherichia coli* bacteria. Briefly, in 1.5 mL eppendorf tube, quenched with 2% skimmed milk powder, 50 µL of pure PBS containing *E. coli* at the concentration of 10^8 CFU mL⁻¹ were mixed with 1 mL of anti-*Salmonella* pAbs diluted 1:50. The eppendorf was incubated at room temperature overnight, under constant shaking (100 rpm) and later centrifuged at 13400 rpm for 5 min. The supernatant, containing the antibodies which have not interacted with *E. coli*, was collected and the anti-*Salmonella* pAbs level was determined by NanoDrop 2000 spectrophotometer.^{110–112}

To evaluate the sensitivity and specificity of pAbs, an ELISA test was carried out according to the above protocol. In details, 100 µL of different concentrations of the foodborne pathogens (*E. coli*, *Yersinia*

enterocolitica, *Campylobacter jejuni*, *Shigella dysenteriae*, *Salmonella* Enteritidis, *Salmonella* Typhimurium and monophasic *Salmonella* Typhimurium) were diluted in PBS, ranging from 10^7 CFU mL⁻¹ to 10^4 CFU mL⁻¹, and seeded in a 96-well plate. The polyclonal antibodies used was diluted 1:50 in PBS and the sensitivity and specificity of antibodies were evaluated measuring optical absorbance at 450 nm. All the bacteria used for this test were provided by Istituto Zooprofilattico Sperimentale del Mezzogiorno of Portici (Naples). The results, shown in **FIGURE 3.2**, exhibits the high reactivity of anti-*Salmonella* pAbs against three different *Salmonella* strains compared to non-*Salmonella* strains ($p < 0.001$). Rather than a drawback, the significant reactivity with other *Salmonella* strains is a strength feature of our pAbs since both the monophasic variant of *S. Typhimurium* and *S. Enteritidis* are hazardous for human health, so that possible positive response of the biosensor coming from the presence of these two strains would be beneficial for food analysis in practical use.

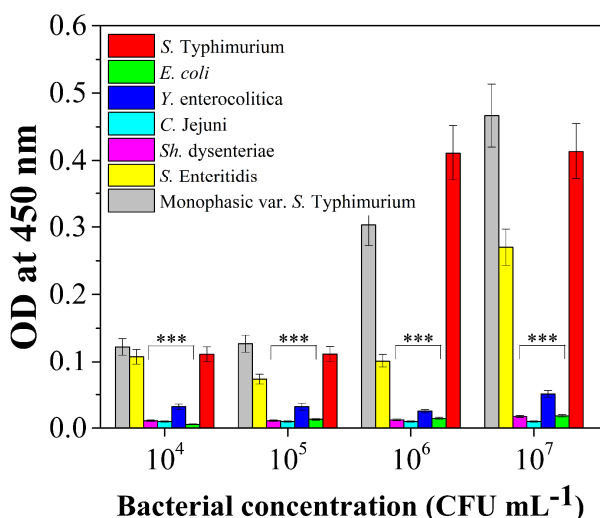


FIGURE 3.2. Anti-*Salmonella* pAbs specificity against different selected foodborne pathogens: *Escherichia coli*, *Yersinia enterocolitica*, *Campylobacter Jejuni*, *Shigella dysenteriae*, *Salmonella* Enteritidis, *Salmonella* Typhimurium and the monophasic variant of *Salmonella* Typhimurium. Results are presented as mean value \pm standard deviation and each experiment is repeated three times. *** p value < 0.001 .

2.3 QCM APPARATUS

The QCM device is a μ Libra (from Technobiochip, Italy) and the quartz oscillators (AT10-14-6-UP-01) were from Novaetech S.r.l. (Naples, Italy). They are AT-CUT quartz with a fundamental frequency of 10 MHz where the crystal and the gold electrode diameters are 1.37 cm and 0.68 cm respectively. **FIGURE 3.3** shows the experimental setup. The QCM wafer, mounted on its support, was placed on the electronic console of μ Libra connected via USB cable to the computer and the resonance frequency of the oscillator was monitored by producer-released software. In order to convey the analyzed solutions onto the sensor surface, the QCM was integrated in a microfluidic circuit consisting of a cell containing the oscillator, a 10 mL syringe and Tygon tubes with a diameter of 1 mm (for both the input and output channels) designed for biological samples. The solution volume in contact with the electrode was about 30 μ L, but considering all its components the total volume of the circuit was about 200 μ L. A 10 mL syringe was used to draw 1 mL volume repeatedly (for five times); in more details, the syringe draws conveyed fresh solution to the cell and were separated each other by a time interval of three minutes that showed to be long

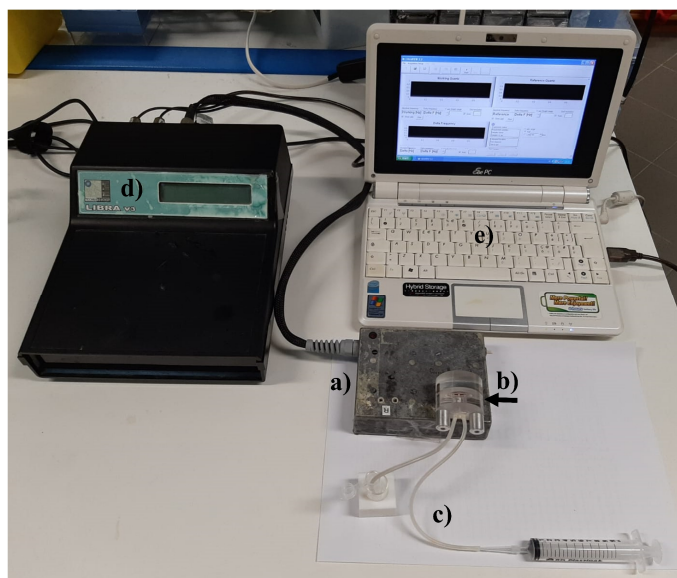


FIGURE 3.3. QCM apparatus. **a)** electrode console; **b)** cell containing the electrode; **c)** tygon tubes and 10mL syringe; **d)** frequency reader; **e)** computer for data acquisition.

enough to reach a temporary frequency stabilization. No further frequency change was observed after five syringe draws so that 1 mL was the volume to be changed for reaching the equilibrium (frequency stabilization); since it was changed by sucking 200 μ L every three minutes the whole step took 15 min to be completed.

2.4 GOLD SURFACE PREPARATION

An essential requirement for an effective immobilization of the antibodies is a clean gold electrode. Clean gold surfaces exposed to ambient conditions will quickly collect several impurities from the environment that can affect the functionalization. Among the various contaminants, likely hydrocarbon pollutants are the most common. These contaminants can be removed from the Au substrates by using strong oxidizing agents such as aqua regia solution, piranha solution and ozone plasma treatment. The so-called “piranha solution” is a mixture of sulphuric acid (H_2SO_4) and hydrogen peroxide (H_2O_2) frequently used in microfabrication laboratories to remove the photoresist in photolithographic process, to clean organic matters off surface electrodes and to hydroxylate (add OH groups) most surfaces making them highly hydrophilic. Many different mixture ratios can be considered. The traditional composition is 3 parts of concentrated sulphuric acid (H_2SO_4) and 1 part of 40% hydrogen peroxide (H_2O_2). Other protocols use a 4:1 or 7:1 ratio. A related mixture, called “base piranha solution” is a 3:1 mixture of ammonia water and hydrogen peroxide. Both are equally dangerous when hot, although the reaction in the acid piranha is self-starting whereas the base piranha must be heated to 60 degrees before the reaction takes off.

For our experiments the gold surfaces were cleaned by immersing the oscillator for 1 min in a glass beaker containing a “piranha solution” in the typical 3:1 ratio. Then, the QCMs were washed with Milli-Q water and left to dry in air. The whole cleaning procedure, strong enough to remove any organic residues from the gold surface, was performed in the hood with great care and using specific equipment (such as gloves, lab coat, etc.) since the piranha solution is highly corrosive and an extremely powerful oxidizer. The piranha solution preparation consists in pouring the hydrogen peroxide in the glass beaker, containing the sulphuric acid, slowly. It is worth using a glass beaker and avoiding plastic vessels or tweezers because the involved reaction, which is extremely exothermic, can reach temperatures up to 120 °C and plastic containers can melt. If the solution is made rapidly, it will instantly boil realising large amounts of corrosive fumes. Once the mixture has

stabilized, it can be further heated to sustain its reactivity. The hot and often bubbling solution removes organic compounds from the substrates and oxidizes most metal surfaces. After the cleaning, the quartz crystal was mounted on the support, being careful in avoiding touching the gold surface with tweezers or gloves, and a new functionalization step was carried out by PIT. This cleaning procedure can be repeated up to 3-4 times because the quartz disk become progressively more fragile to handle and has to be changed.

2.5 QCM EXPERIMENT

The first step of the experiment is the reaching of the basal frequency stabilization by conveying PBS 1X solution at pH 7.4. PBS is a salty solution widely used in biological research containing sodium chloride, sodium phosphate, and (in some formulations) potassium chloride and potassium phosphate. It is used for all phases since it helps to preserve a constant pH and to avoid frequency shift due to different solution densities. Then, the gold electrode of quartz crystal was functionalized with anti-*Salmonella* pAbs UV activated by Photochemical Immobilization Technique (PIT). As described in details in Chapter 1, PIT is a quick reproducible technique which allows the immobilization of the antibodies onto gold surfaces in an upright orientation that means with their binding sites exposed to the environment. In this experiment the PIT was carried out by irradiating a solution of $50 \mu\text{g mL}^{-1}$ anti-*Salmonella* pAbs for 1 min by a HERAEUS amalgam type NNI 40/20 lamp emitting at 254 nm with a power average of 40 W. The lamp was approximately 20 cm long and had a diameter of 1 cm, so the effective irradiation intensity for the antibodies activation was about 0.7 W/cm^2 . Then, the immunoglobulin solution was conveyed on the gold electrode by means of five draws of $200 \mu\text{L}$ with an incubation time of 3 minutes. The proteins were adsorbed onto the sensor surface thus resulting in the first drop of frequency. After reaching again the stabilization, the circuit was washed with PBS buffer solution to remove the non-specifically bound antibodies. In the next step BSA was used as blocking reagent to fill free spaces on the gold electrode in order to avoid non-specific interaction between the sensor surface and the further flowing molecules. In such a case, five volumes of $200 \mu\text{L}$ of a BSA solution ($50 \mu\text{g mL}^{-1}$) were piped in the circuit. It is worth highlighting that if the conveying of BSA solution does not result in a variation of the resonance frequency of the QCM, the gold surface is quite fully covered by immobilized antibodies confirming the efficiency of the functionalization technique. The last step is the detection of

Salmonella in chicken meat samples purchased from a local supermarket. Firstly, the chicken meat was tested to confirm the absence of *Salmonella* according to ISO 6579-1: 2017. Later, 25g of chicken was contaminated with *Salmonella* Typhimurium at different concentration in the range 10^0 - 10^5 CFU mL⁻¹ and were placed in sterile stomacher bag containing 225 mL of buffered peptone water. These bags were placed into a stomacher device for 90 seconds and incubated for 1 or 2 hours at 37 °C, the so-called pre-enrichment step. After the incubation, 15 mL of each sample (included a chicken meat sample without *Salmonella* contamination) were collected and centrifuged at 2000 rpm for 15 min to remove part of food debris. 1 mL of supernatant, containing bacterial cells, was centrifuged at 13400 rpm for 5 min at room temperature. The bacterial pellet was suspended in pure PBS (1 mL) and conveyed on the QCM sensor for the analysis by means of five syringe draws. The antigen binding results in a second frequency shift and a final washing step is used to remove weakly bounded bacteria. Each bacteria concentration was tested in triplicate.

In order to evaluate the specificity of the immunosensor for the detection of *Salmonella*, the chicken meat samples were infected with a non-target bacterium (*E. coli*, 10^4 CFU mL⁻¹) alone or in combination with *S. Typhimurium* (both bacteria at 10^4 CFU mL⁻¹). All the sample were pre-enriched for 2 hours at 37 °C and later, analysed at QCM immunosensor. Before the pre-enrichment step, the samples contaminated or not were diluted and spotted on *Salmonella* Chromogenic Agar Base (CM1007) or Tryptone Bile X-Gluc (TBX Agar, CM0945) for *S. Typhimurium* or *E. coli* isolation, respectively. The plates were then incubated at 37 °C (*S. Typhimurium*) or 44 °C (*E. coli*) for 24 h. This procedure allowed us to validate the presence and the concentration of the bacteria in food samples.

3. RESULTS AND DISCUSSION

3.1 KINETIC OF THE FUNCTIONALIZATION

The kinetic of the functionalization was studied to optimize the performance of the QCM sensor. A solution of anti-*Salmonella* pAbs with a concentration of 50 μ L mL⁻¹ was conveyed to the electrode by means of a 10 mL syringe and the number of syringe draws necessary to completely cover the sensor surface by immobilized antibodies was studied. The frequency shift (Δf) was monitored after each draw, that means at time intervals of 3 minutes and the resulting Δf are shown in **FIGURE 3.4** where its behaviour with the time is well fitted by an

exponential function with a time constant of 3.7 ± 0.2 Hz. As the first volume (200 μL) of the antibody solution was conveyed to the electrode, a first drop in the frequency shift (~ 90 Hz) was observed. After 3 minutes of incubation, a second volume (200 μL) gave rise to a frequency drop of ~ 125 Hz till obtaining a frequency shift of ~ 150 Hz after five draws. Since no further frequency change was observed after five syringe draws, the whole functionalization procedure can be considered accomplished after five draws that means 15 minutes in total. Moreover, we observed that no significant frequency shift was achieved after the blocking step with BSA suggesting that the saturation of Δf shown in **FIGURE 3.4** corresponds to an electrode fully covered by antibodies.

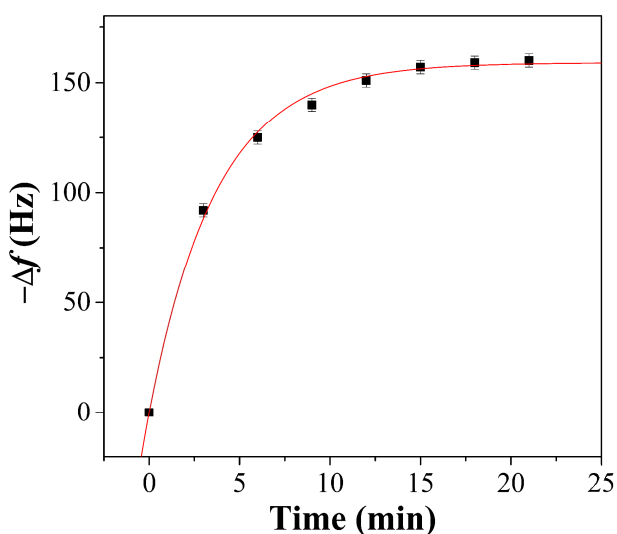


FIGURE 3.4. Kinetic of the antibody immobilization. Δf is shown as a function of the time showing an exponential kinetic with a constant time of 3.7 ± 0.2 . The errors of Δf are slightly noticeable because they are almost within the thickness of the experimental points.

3.2 DETECTION OF *SALMONELLA* TYPHIMURIM

The response of the QCM (i.e. the frequency change) is proportional to the mass tethered to the surface so that, through the measure of the frequency shift, we measure the concentration of the analyte in the solution because the frequency drop is the result of the biological interaction between antibodies and antigen. To establish a relationship between *S. Typhimurium* concentrations and QCM

frequency signal changes, a *Salmonella* binding assay was carried out using QCM immunosensor. Different concentrations of *S. Typhimurium*, ranging from 10^0 CFU mL⁻¹ to 10^5 CFU mL⁻¹, were selected for the test. At each concentration corresponds a QCM frequency variation which is explained by the Sauerbrey equation (3.10). As an example, in **FIGURE 3.5** is reported the QCM sensorgram obtained with a concentration of *Salmonella* 10^0 CFU mL⁻¹.

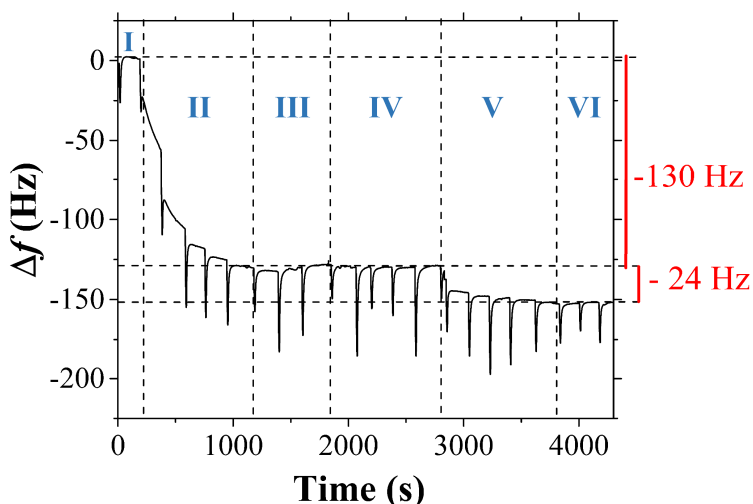


FIGURE 3.5. QCM sensorgram and detection of *S. Typhimurium*. Food sample contaminated with a concentration of bacteria 10^0 CFU/mL with a pre-enrichment step of 2h at 37 °C.

First, antibody aliquots of 1 mL containing $50 \mu\text{g mL}^{-1}$ of anti-*Salmonella* polyclonal antibodies were irradiated by means of the UV lamp for 1 minute. Then, the experimental procedure consists of the following steps. The fluidic cell containing the electrode was washed with 1X PBS (pH 7.4) until the basal frequency stabilization was reached (step I). Then, the surface was functionalized by conveying to the QCM, the solution of previously UV-activated anti-*Salmonella* polyclonal antibodies ($50 \mu\text{g mL}^{-1}$) resulting, after five draws of syringe, in the first drop in frequency of 130 Hz at about 1100 s, which is due to the antibody immobilization onto the sensor surface (step II). When the electrode reached the stabilization, the cell was washed with PBS (step III) to remove possible antibodies not tethered onto gold surface, so checking for the efficiency of the functionalization. A blocking step was carried out using a BSA solution ($50 \mu\text{g mL}^{-1}$) to avoid non-specific interaction between the antigen and the electrode (step IV). During this blocking phase the oscillator frequency remains constant and the lack

of significant frequency change in the blocking step suggests that the gold surface is most completely covered by antibodies. Once the QCM achieved the new stabilization, the sensor was ready for the analysis of the chicken meat samples infected with *S. Typhimurium*. 1 mL aliquot of the sample (prepared as described in paragraph 2.5) was conveyed in the fluidic circuit and the immobilized antibodies recognized the bacteria resulting in a frequency shift (step V). A final washing step with PBS 1X was performed to eliminate all the elements which did not interact with the antibodies or with the gold surface (step VI). This washing did not lead to any frequency change; thus, the lack of detachment from the surface emphasises once again the stability of the interaction between bacteria and UV-activated anti-*Salmonella* pAbs and, hence, demonstrates the effectiveness of PIT as a gold functionalization method. The difference in frequency between the values before the conveying of the *Salmonella* incubated sample and after the washing with PBS was due to the binding of the bacteria by the antibodies immobilized onto the sensor surface and corresponds to $\Delta f = -24$ Hz at about 4000s. Since the response of the QCM is related to the mass tethered to the electrode, this second drop in frequency is a measure of the amount of the analyte caught by the immobilized antibodies. The sensorgram (**FIGURE 3.5**) refers to a chicken sample initially contaminated with 10^0 CFU mL⁻¹ of *S. Typhimurium* after 2 h of pre-enrichment step at 37 °C, a time leading to approximately 10^2 multiplication factor by assuming a replication time of 20 min.¹¹³ It is worth noticing that the spikes in the plot are due to the syringe draws and do not affect the measurement of the frequency shift.

Moreover, the initial concentration (10^0 CFU mL⁻¹) was checked in three independent experiments by spotting 10 μ L of the samples analysed by QCM at different dilutions. One of these cases is shown in **FIGURE 3.6** where the top left section (dilution 1:10) contains three spots each containing 5 CFU/10 μ L.

In order to evaluate the performance of the QCM sensor, we measured the dose-response curve that is reported in **FIGURE 3.7**, in which the values on x-axis refer to the initial *Salmonella* concentration selected for the contamination of the chicken sample (range from 10^0 to 10^5 CFU mL⁻¹). The samples were analysed after 1 and 2 hours of pre-enrichment. This step, which is also included in the ISO standardized method (ISO-6579-1:2017),⁶⁶ is necessary to assist the isolation of the *Salmonella* and to allow the detection of low numbers of bacteria in environmental samples where *Salmonella* is often accompanied by a considerably larger number of other members of *Enterobacteriaceae* or other families.

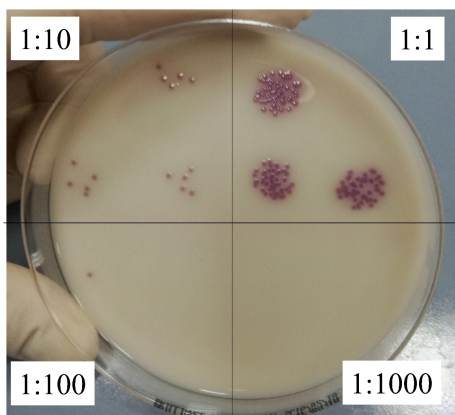


FIGURE 3.6. Spot dilution of the sample before the pre-enrichment step on *Salmonella* Chromogenic Agar Base after overnight incubation. Each section shows the dilution factor.

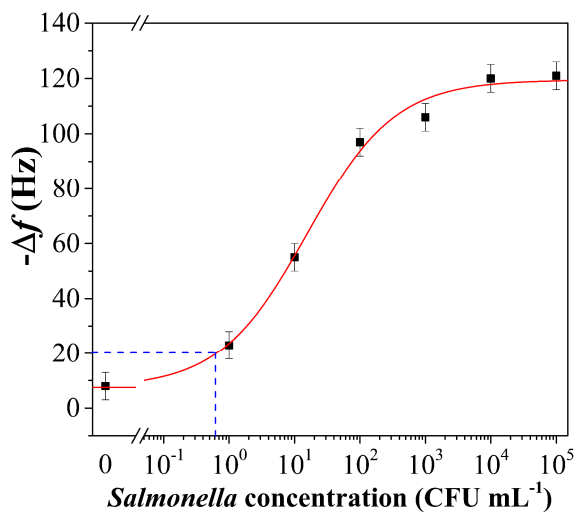


FIGURE 3.7. Dose-response curve of the QCM immunosensor referred to samples of chicken meat contaminated with different concentrations of *Salmonella* Typhimurium. The curve is the best fit of the experimental value obtained by a logistic function.

Firstly, 1 hour of pre-enrichment step was applied. In such a case the immunosensor was able to detect *Salmonella* only in the range 10^2 - 10^5 CFU mL⁻¹ (data not shown), whereas 2 hours of pre-enrichment enable to decrease the lower limit down to 10^0 CFU mL⁻¹ (see **FIGURE 3.7**). With the longer pre-enrichment, it was possible to observe a frequency shift induced by the step V of the protocol (i.e. bacteria binding) for all the samples infected, whereas no significant frequency shift could be detected with uncontaminated chicken sample (negative control). Each point of the dose-response curve (**FIGURE 3.7**) represents the mean triplicates of measurements carried out in several days, in different environmental conditions and using different electrodes. The curve shows a linear range of three decades from 10^0 to 10^3 CFU mL⁻¹ before reaching a saturation profile at the highest concentrations. The frequency shift measured for the negative sample was 8 ± 4 Hz and, probably, it was due to non-specific interaction of the food constituents with the biosensor surface. Such a value for the blank does not prevent us from estimating a very low limit of detection of our biosensing procedure. In fact, the concentration that provides a signal corresponding to 3σ of the background noise is lower than 10^0 CFU/mL, a concentration that can be safely considered the LOD of the proposed biosensor.

3.3 SPECIFICITY TEST

In order to prove the sensor specificity, the same experimental procedure was used to test the QCM response when the sample is contaminated with a non-target bacterium such as *Escherichia coli* (*E. coli*). Since *E. coli* is among the most spread bacteria in food and water, it is essential to consider its possible cross-interference when the purpose is the development of a high sensitive immunosensor for the detection of *Salmonella*. **FIGURE 3.8** shows the sensorgrams obtained when chicken meat samples were contaminated by *S. Typhimurium*, *E. coli* and a mixture of them. At a concentration of 10^4 CFU mL⁻¹ (before the pre enrichment step at 37°C for 2 hours), where *Salmonella* exhibited a response of 115 Hz (black line), *E. coli* showed no significant detectable frequency shift (17 Hz, red line). In particular, the frequency shift detected in the case of *Salmonella* chicken meat sample was comparable to that reported in the dose response curve (**FIGURE 3.7**). Therefore, the sensor response was tested in samples infected with both *S. Typhimurium* and *E. coli* and the drop frequency was 95 Hz (blue line). Such a value was lower than that provided by *Salmonella* infected sample (115 Hz) and this difference was probably due to a

competition between the two bacteria (*S. Typhimurium* and *E. coli*) during the enrichment step, when both are present in the food matrix. The initial bacterial concentrations selected for the test were also supported by microbial count carried out on the same sample. Once again, the high specificity of the anti-*Salmonella* pAbs, even when they are photoactivated, is highlighted thus demonstrating, by this way, the effectiveness of the proposed QCM sensor in detecting *Salmonella* in a real food matrix as chicken meat.

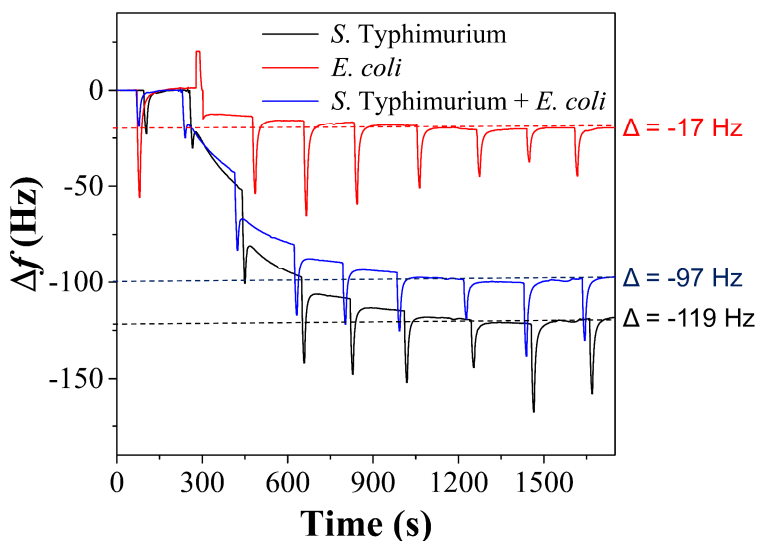


FIGURE 3.8. QCM biosensor specificity. Sensorgrams of *Salmonella* Typhimurium (black curve), *Escherichia coli* (red curve) and both bacteria (blue curve) contaminated chicken meat samples, after the pre-enrichment step (2h at 37 °C). Each bacterial concentration was at 10^4 CFU mL⁻¹ before the pre-enrichment step.

4

EIS IMMUNOSENSOR FOR *E. COLI* DETECTION



1. INTRODUCTION

1.1 PRINCIPLES OF ELECTROCHEMISTRY

Electrochemistry is a branch of the chemistry that concerns with chemical reactions involving charged particles and electrons transfer, the so-called redox reaction (oxidation and reduction). This subclass of the chemistry, which has a number of different applications in various fields such as research and industry, correlates the chemical reactions to electrical currents in order to identify substances in a solution or at an electrode surface. Redox reactions usually take place at the interface electrode-electrolyte in an electrochemical cell.

A cell consists of two parts: the electrodes and the electrolyte solution in which the electrodes are immersed. The electrolyte solution contains charged species such as ions that ensure the electron transfer at the interface of the electrode. Electrochemical measurements can be run in a two- or three-electrodes configuration (**FIGURE 4.1**). The simplest configuration for an electrochemical cell requires only two electrodes which are the working and the reference electrodes. The *working electrode* (WE) is the actual sensor surface where the bio-receptor is immobilized to specifically bind the analyte and the reduction and oxidation reactions take place. The WE can be made of an inert and conductive material (Ag, Au, Pt, silicon and glassy carbon). The *reference electrode* (RE) is an electrode with a stable and well-known potential which is used to provide a stable potential reference point. The RE is required to be inexpensive, non-toxic and with a high stability

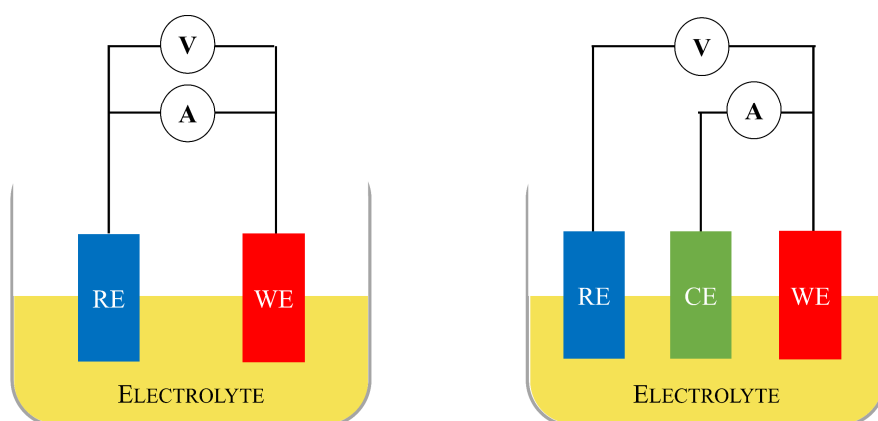


FIGURE 4.1. Schematic representation of an electrochemical cell in a two- and three-electrodes configuration

which is normally achieved by employing a redox system with a constant concentration of the reducing and oxidizing species. Silver/silver chloride (Ag/AgCl) electrode is the most widely used reference electrode. The RE should hold a constant potential during an electrochemical reaction, since the potential of the WE is monitored relative to the reference electrode.

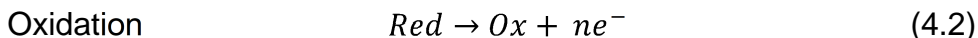
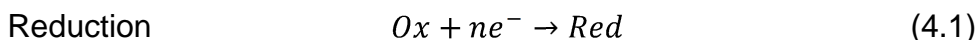
The main trouble of the two electrodes configuration is that, when an external potential is applied, both the perturbation and the subsequent current response are measured between the WE and the RE. However, the current flowing changes the potential of the RE and it can no longer be considered a reference. To deal with this problem, an additional electrode is introduced to the electrochemical cell, namely the *counter* or *auxiliary* electrode (CE). In this cell setup, the potential is applied between the working and the reference electrode and the resulting current flows exclusively between the counter and the working electrode (**FIGURE 4.1**). This separation guarantees that the RE is not involved in the exchange of current thus providing a reference potential for the application of an external voltage. The counter electrode consists of an inert material (typically platinum or gold) which does not involve any reaction. The potentiostat is a device connected to the electrodes, which applies a voltage to WE with respect to RE and measures the current flowing between the WE and the CE.

The electrode/electrolyte interface is the place where electrochemical reactions occur. When two different phases come in contact, for instance when an electrode is immersed in an electrolyte solution, charge accumulation and separation occur at the interface electrode/electrolyte thus resulting in the formation of the so-called electrical double layer (EDL). The excess charge on the surface electrode is compensated by the accumulation of counter-ions (i.e. ions of the opposite charge) in the solution and the concentration of these ions decrease with the distance from the electrode. Thus, one layer of charges is located on the metal surface of the electrode and the other layer is inside the electrolytic solution. Over the years, several models have been proposed to model the EDL. The last one was proposed by Stern in 1924 and, on the strength of the previous Helmholtz and Gouy-Chapman models, it offers a more accurate and realistic description of a double layer by taking into account the finite size of the counter-ions and their binding properties at the surface.¹¹⁴

An electrochemical reaction involves the transfer of electrons between two substances inducing the change of oxidation state of these species. This reaction can occur through the application of an external potential and is responsible for generating the so-called faradaic

currents. In fact, the redox reactions follow the Faraday's law which states that the amount of species produced by an electrochemical reaction is directly proportional to the quantity of current that passes through the electrolytic cell. Although the faradaic process is the main interest of an electrochemical investigation, processes generating a current without charge transfer (non-faradaic processes) must be considered. Non-faradaic currents are not generated by electrochemical reactions, but are due to the adsorption of ions present in the solution at the surface of either positively or negatively charged electrode. Such currents are also called capacitive currents since this phenomenon can be associated to a capacitor. Both faradaic and non-faradaic processes can take place at an electrode surface.

The two processes involved in a redox reaction are the oxidation and the reduction of the electroactive species. In one case (oxidation) the species loses electrons while in the second (reduction) the species gains electrons:



where *Ox* and *Red* are the oxidised and reduced form of the electroactive species and *n* is the number of electrons involved in the reaction. The redox reaction can be homogenous or heterogeneous depending on the phase of the species involved in the exchange of electrons that can be the same (homogenous) or different (heterogeneous). The most common heterogeneous case is the electron transfer between solid and liquid phases such as the process that takes place at the electrolyte/electrode interface. The concentrations of the oxidised and reduced species at the electrode surface are correlated to the electrode potential by the Nernst Equation:

$$E = E^{0'} + \frac{RT}{nF} \ln \frac{C^{Ox}}{C^{Red}} \quad (4.3)$$

where $E^{0'}$ is the formal potential of the redox probe, *R* is the universal gas constant, *T* is the temperature (in Kelvin), *n* is the number of exchanged electrons, *F* is the Faraday constant, C^{Ox} and C^{Red} are the concentrations of the oxidised and reduced species.

The reduction and oxidation currents involved in the redox reaction follow the Faraday's law and can be described as:

$$\text{Reduction} \quad i_{Red} = -nFAk_R C^{ox} \quad (4.4)$$

$$\text{Oxidation} \quad i_{Ox} = nFAk_{Ox} C^{Red} \quad (4.5)$$

where k_R and k_{Ox} are the rate constants for the reduction and oxidation processes and A is the electrode area. Assuming that at the equilibrium $C^{ox} = C^{Red}$ the two values of current are identical and the exchange current i is expressed as:

$$i = nFAkC \quad (4.6)$$

The equation (4.6) states that, in an electrochemical cell, the current is directly proportional to the concentration of the electroactive species.

1.2 METHODS FOR BIOSENSOR CHARACTERIZATION

1.2.1 CYCLIC VOLTAMMETRY

Cyclic Voltammetry (CV) is an analytical method well-known for its versatile application in a number of areas, such as the investigation of the electron transfer process of a given electroactive species. CV measurement is performed by applying at the working electrode a varying potential and measuring the resulting current. In particular, the potential difference between the working and the reference electrode is linearly swept in time from a starting potential to a vertex one and back again. By sweeping the potential, the electroactive species in the solution can be oxidized or reduced at their respective potential thus resulting in a flowing current which is measured as a function of the applied potential. The current-potential waveform, called cycling voltammogram (CV), is shown in **FIGURE 4.2**. When a single redox couple exists in the electrochemical cell, which means a species that can be oxidised or reduced in the selected potential range (e.g. $\text{Fe}(\text{CN})_6^{3-}/\text{Fe}(\text{CN})_6^{4-}$), the applied potential produces both reduction and oxidation currents depending on the direction of the potential scan. As the potential is swept negatively (to more reductive values) the reduction process occurs. The reduction of the electroactive species causes an exchange of electrons between the electrode and the bulk

electrolyte thus resulting in an increase of current (cathodic current, I_{pc}) which reaches the maximum value at the cathodic peak potential (E_{pc}). To rationalize this event, it is necessary to consider that, during the scanning, the potential reaches a value whereby the working electrode changes from a condition of equilibrium to a condition where the redox reaction is favourable. The E_{pc} is reached when all of the substrate at the surface of the electrode is reduced. After the I_{pc} peak, the current decreases because of the depletion of the reducing species until the switching potential is attained. Then, the potential is positively swept (to more oxidative values) and the oxidation process starts thus generating an anodic current (I_{pa}) with a maximum peak at the anodic peak potential (E_{pa}) which is reached when all of the substrate at the surface of the electrode is oxidized. Then, the anodic current decreases due to the pauperization of the oxidising species until the potential reaches the initial value.

In the case of a reversible system with a single redox species, the anodic or cathodic peak current can be further described by the Randles-Sevcik equation:

$$I_p = 0.4463 nFAC \left(\frac{nFvD}{RT} \right)^{\frac{1}{2}} \quad (4.7)$$

where n is the number of electrons involved in the redox process, F is the Faraday's constant, A is the active area of the working electrode, C is the bulk concentration of the electroactive species, v is the potential scan rate, D is the diffusion coefficient of the species reduced or oxidised, R is the universal gas constant and T is the temperature. The Equation (4.7), valid for both anodic and cathodic currents, shows that the current is directly proportional to the electroactive species in solution. For a reversible reaction the anodic peak current is equal to the cathodic one and the separation between the two peaks is given by the following equation valid at 25 °C:

$$\Delta E_p = E_{pa} - E_{pc} = \frac{59}{n} mV \quad (4.8)$$

where E_{pa} is the anodic peak potential, E_{pc} is the cathodic peak potential and n is the number of electrons involved in the redox reaction. When the conditions deviate from the reversibility, the ΔE_p increases and the values of I_{pc} and I_{pa} are incongruent.

Moreover, from the CV it is possible to obtain the *Formal Reduction Potential* of the redox probe which is the mean of the E_{pc} and E_{pa} values:

$$E^{0'} = \frac{E_{pa} + E_{pc}}{2} \quad (4.9)$$

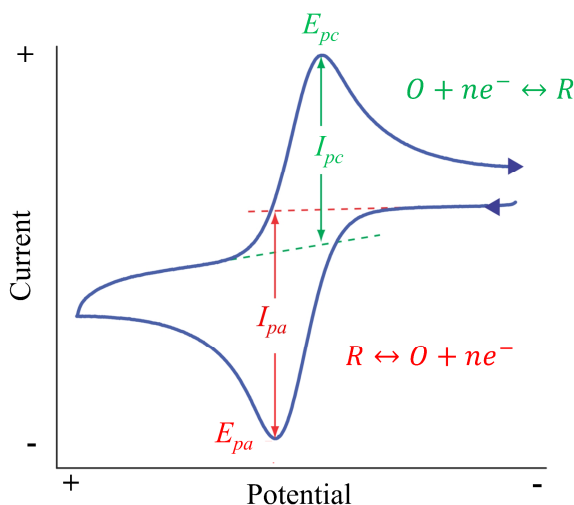


FIGURE 4.2. Cyclic voltammogram of a fully reversible reaction.

1.2.2 ELECTROCHEMICAL IMPEDANCE SPECTROSCOPY

Electrochemical Impedance Spectroscopy (EIS) is one of the most complex techniques in electrochemical research commonly applied in different fields including corrosion analysis, batteries, fuel cells and, widely used as detection technique to investigate the recognition events at electrode/electrolyte interface.^{115–117} Since its introduction, it has drawn particular attention mainly as non-destructive technique able to perform *in situ* measurements. In biosensing applications, EIS measures the changes of a complex electrical resistance (namely impedance) caused by the recognition of the analyte by means of the biological element immobilized on the electrode surface. However, EIS is often used as characterization technique for confirming the layer-by-layer construction of a biosensor.

In an EIS experiment, the impedance Z of a system is determined by applying an AC potential of small amplitude to an electrochemical

cell over a range of frequencies and by measuring the current that flows through the cell as a frequency-dependent parameter. Typically, a small amplitude of 5-10 mV is applied in order to guarantee that the cell's response is pseudo linear, which means that the current response to a sinusoidal potential will be a sinusoid at the same frequency but shifted in phase.

The applied potential, as a function of the time, can be defined as:

$$E_t = E_0 \sin(\omega t) \quad (4.10)$$

where E_t is the potential at the time t , E_0 is the amplitude of the potential and ω is the angular frequency ($\omega = 2\pi f$ where f is the frequency in Hertz). In a linear system, the output current I_t is also a sinusoid but is shifted in phase and can be expressed as:

$$I_t = I_0 \sin(\omega t + \varphi) \quad (4.11)$$

where I_0 is the amplitude of the current and φ is the phase shift. An expression similar to the Ohm's law enables the calculation of the impedance (Z) of the system as:

$$Z = \frac{E_t}{I_t} = \frac{E_0 \sin(\omega t)}{I_0 \sin(\omega t + \varphi)} = Z_0 \frac{\sin(\omega t)}{\sin(\omega t + \varphi)} \quad (4.12)$$

where the impedance Z is expressed in terms of a magnitude Z_0 and the phase φ . According to the Euler's relationships, the impedance can be expressed as a complex function. Considering that the potential (E_t) and the current (I_t) are described as:

$$E_t = E_0 e^{j\omega t} \quad (4.13)$$

$$I_t = I_0 e^{j\omega t - \varphi} \quad (4.14)$$

where $j = \sqrt{-1}$ is the imaginary unit, the impedance can be expressed as a complex number:

$$Z(\omega) = Z_0 e^{j\varphi} = Z_0 (\cos \varphi + j \sin \varphi) \quad (4.15)$$

The impedance values can be represented in two different ways. The Bode diagram where the impedance and the phase angle are plotted against the frequency and the Nyquist plot wherein the real and imaginary part of the impedance are plotted on X and Y axis, respectively. Although both these diagrams allow the characterization of the electrochemical system, such as surfaces, layers and diffusion processes, the Nyquist plot, also known as Cole-Cole plot, is commonly used in biosensing application because it allows the easily calculation of some parameters (**FIGURE 4.3**). The solution of the resistance (R_s) can be calculated by extrapolating the plot to x-axis at high frequencies, while the intercept at low frequencies is the sum of the solution resistance and the resistance to electrons transfer (R_{ct}). However, the diameter of the semicircle corresponds to the charge transfer resistance (R_{ct}) between the electrode and the electrolyte solution which is influenced by the surface modification. The double layer capacitance can be calculated from the frequency at the maximum of the semicircle ($\omega = 2\pi f = \frac{1}{R_{ct}C_{dl}}$). Note that in the Nyquist diagram the Y axis is negative and that each point on the graph is the impedance value at a given frequency. In addition, in a Nyquist plot the low frequency data are on the right side while the higher frequencies are on the left. A typical shape of the Nyquist plot (**FIGURE 4.3**) includes a semicircle region at high frequencies followed by a straight line at low frequencies.

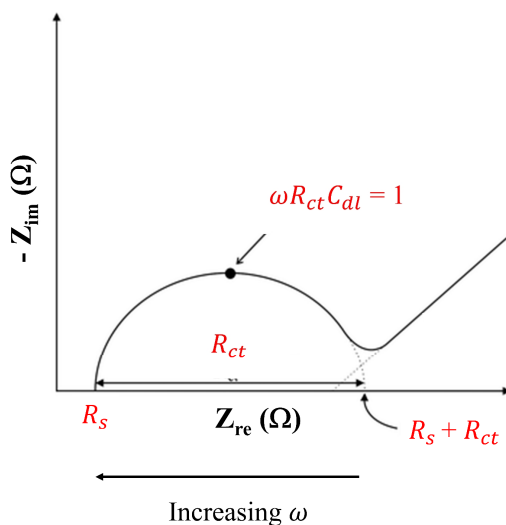


FIGURE 4.3. Example of a Nyquist plot showing the imaginary part of the impedance plotted as a function of the real part.

The linear part, with a slope of 45° , implies a diffusion-limited mass transfer process of the redox probe, whereas the semicircle portion entails a charge-transfer limited process.

In electrochemistry, EIS is commonly used due to the possibility of modelling the physical or chemical phenomena that take place in an electrochemical cell (i.e. charge transfer resistance, double layer formation, the diffusion process) with the elements of an equivalent circuit. (**FIGURE 4.4a**).

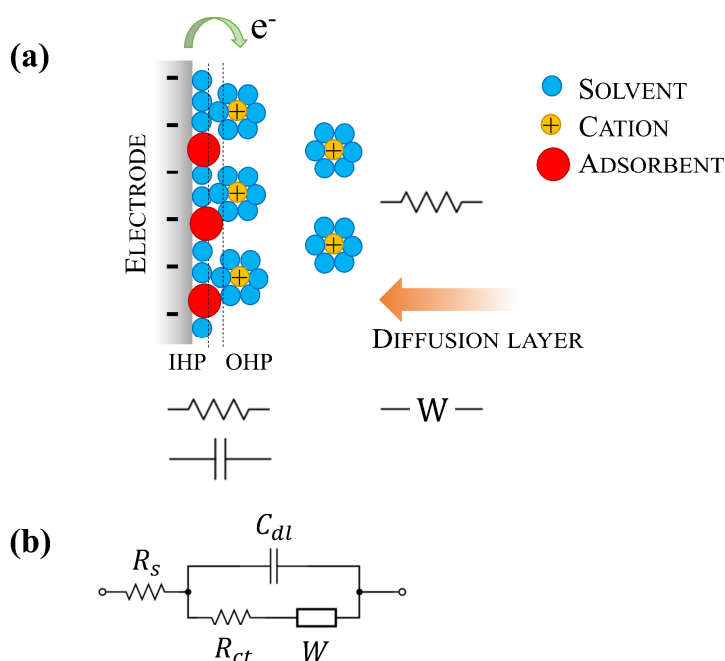


FIGURE 4.4. (a) Scheme of the electric double layer showing the arrangement of ions at the electrode-electrolyte interface.; (b) Randles circuit. R_s is the resistance of the solution, R_{ct} is the charge transfer resistance, W is the Warburg impedance and C_{dl} is the double layer capacitance. In biosensing application, C_{dl} is often replaced by CPE to account for inhomogeneity and defect areas.

The most common circuit is the *Randles circuit*, shown in **FIGURE 4.4b**. This circuit is composed by R_s , that is the resistance of the electrolyte solution, C_{dl} that represents the double-layer capacitance, R_{ct} that is the charge (or electron) transfer resistance and W that is the Warburg impedance. R_s and W represent the bulk properties of the electrolyte solution and diffusion features of the redox probe. These parameters are not influenced by modification on the electrode surface and are not

modified by the antibodies-analyte interaction. On the contrary, R_{ct} depends critically on the dielectric and insulating features at the electrode-electrolyte interface and can be used as sensing parameter since it is very sensitive to electrode modifications. A CPE (constant phase element) is frequently introduced in the equivalent circuit instead of an ideal capacitor C_{dl} to account for inhomogeneity and defect areas of the biological layer.¹¹⁸ This element can model the imperfect behaviour of the double layer capacitance due to the porosity or the roughness of the electrode area.

Upon applying the AC potential, the current flows through all components of the system and the impedance is the sum of the individual contributions. The individual circuit elements and the related contribution to the impedance are briefly described below.

The *electrolyte solution resistance* (R_s) depends on the ionic concentration, type of ions, temperature and geometry of the cell and can be defined as:

$$R_s = \rho \frac{l}{A} \quad (4.16)$$

where ρ is the solution resistivity, l is the distance between the two electrodes and A is the electrode area in contact with the electrolyte solution.

The *charge transfer resistance* R_{ct} is the resistance to the electron transfer between the redox probe and the electrode surface. It can be described as:

$$R_{ct} = \frac{RT}{\eta F i_0} \quad (4.17)$$

where η is the overpotential (i.e. the difference between the applied potential and the equilibrium potential) and i_0 is exchange current density.

In the frequency domain, a resistance contributes to the impedance only in the real part $Z_R(\omega) = R$ where $Z_{re}(\omega) = R$ and $Z_{im}(\omega) = 0$. In a Nyquist plot, a resistor is represented by a single point on the X axis, in correspondence of the value of R , regardless of the frequency used.

The *double layer capacitance* results from the interaction of the electrode surface and the surrounding electrolyte solution. At this interface, an electrical double layer exists as a result of the attraction of the ions in the solution to the charged surface electrode. These positive

and negative charges are separated by a small layer of insulating solvent molecules giving rise to a double layer capacitance. The double layer depends on many variable, including electrode potential, temperature, types of ions, ionic concentration, electrode roughness and adsorbed impurities. In the Nyquist plot, a capacitor is represented by a series of points on the ordinate axis. In such a case, the value of the imaginary part of Z_c depends on ω . Thus, for a given capacitor we will have a series of points on the ordinate axis, one for each value of ω , whose position, obviously, depends on the value of the capacity C . In the frequency domain, the C_{dl} merely contributes to the impedance in the part imaginary. The contribution of the capacity C to impedance is defined as:

$$Z_c(\omega) = \frac{1}{j\omega C} \quad (4.18)$$

A *constant phase element* (CPE) can be introduced in the equivalent circuit instead of a simple capacitor to account for the non-uniformity of the biological layer adsorbed on the surface electrode.¹¹⁸ This element can model such an imperfect behaviour of the double layer capacitance, mainly due to the porosity or the roughness of the electrode area, by adding the a coefficient. The CPE impedance contribution is:

$$Z_{CPE}(\omega) = \frac{1}{(j\omega)^a Y_0} \quad (4.19)$$

where Y_0 is a pre-factor of the CPE and a is the exponent coefficient whose value is between -1 and 1. The a coefficient can change the behaviour of the CPE from a resistor ($a = 0$) to a pure capacitor ($a = 1$).

The *Warburg impedance* (W) describes the diffusion process of the reactants toward or away from the electrode/electrolyte interface and how such a process can influence the resulting current or impedance. W depends on the concentration of the redox probe and, as the CPE, is dependent on the frequency. In the Nyquist plot, the Warburg impedance appears as a straight line with a slope of 45° at lower frequencies and it is defined as:

$$Z_W(\omega) = \frac{\sigma_W}{\sqrt{j\omega}} \quad (4.20)$$

where σ_W is the Warburg diffusion coefficient.

Since the Warburg element reflects the diffusion of the reactants, which is a slow rate process, it is predominant at low frequency. At higher frequencies, the reactants do not have enough time to diffuse. For analytical applications the equivalent circuit is often simplified by choosing a narrow frequency range where no 45° line is observed in the Nyquist plot.¹¹⁹

1.3 EIS APPLICATIONS IN BIOSENSING

Among different electrochemical techniques, electrochemical impedance spectroscopy (EIS) is very commonly used to investigate the recognition event at electrode/electrolyte interface.⁷⁹ Impedimetric immunosensors have gained particular popularity in the detection of different analytes, due to the low cost, miniaturization and the ability to carry out *in-situ* measurements. This technique can be categorized in two types depending on the presence or absence of redox probe in the electrolyte solution, namely faradaic and non-faradaic EIS.¹²⁰

Faradaic EIS

A typical EIS faradaic experiment requires the presence of an electrolyte solution containing a redox couple such as $[\text{Fe}(\text{CN})_6]^{3-/4-}$. The two forms (electron acceptor and electron donor) of the redox couple are alternately oxidized and reduced by the transfer of an electron to and from the metal electrode thus producing an electrical current. The experiment consists in analysing the variation of this current which is caused by the modification of the electrode surface. For instance, the immobilization of the bioreceptor (antibodies, aptamers, DNA, enzymes) and the bioreceptor-analyte interaction produce a decrease in the generated current. This phenomenon can be explained considering that when an insulating protein layer is adsorbed on the electrode, it acts as a barrier and the penetration of the redox probe towards the electrode is reduced. Accordingly, the current decreases and the charge transfer resistance (R_{ct}) increases. The further biorecognition event (antibody-analyte), that takes place on the modified electrode, gives rise to an additional barrier by further limiting the accessibility of the redox probe from the electrolyte solution to the electrode surface resulting, once again, in a further increase in the R_{ct} value. In particular, the impedance can increase due to the “blocking effect” of the barrier generated by the insulating layer on the electrode surface or as a consequence of the formation of a layer negatively charged which can inhibit the transfer of the redox couple. It is worth

highlighting that if the immobilized molecules or the recognized analytes have an opposite charge with respect to the redox couple, a decrease in impedance can be observed.¹²¹

Non-faradaic EIS

A typical non-faradaic EIS experiment does not demand the use of a redox couple. The parameters associated with the electron transfer such as charge transfer resistance (R_{ct}) and Warburg impedance are insignificant (by becoming infinite) and the double layer capacitance become the most important parameter. In such a case, the recognition event creates variations in the charge perturbation and, hence, the double layer capacitance is modified thus resulting in an impedance change. This approach is particularly interesting when the conductivity of the recognition layer changes as result of the specific binding event.

The choice of the most suitable EIS method relies mainly on the expected application, but it is important to underline that, by means of the current generated from the redox reactions that take place at the electrode/electrolyte interface, the faradaic EIS provides a higher sensitivity in comparison to the non-faradaic method.

In the last decade, due to the connection of impedance with biological recognition technology for the detection of pathogens, different impedimetric immunosensors have been developed for the detection of *E. coli* (some examples in **TABLE 4.1**). The lowest limit of detection (LOD) has been achieved by Barreiros dos Santos *et al.*,¹²² which reported a LOD as low as 2 CFU mL⁻¹ by immobilizing anti-*E. coli* antibodies onto gold electrodes via SAMs of mercaptohexadenoic acid (MHDA). Recently, Malvano and co-workers¹²³ reported an impedimetric immunosensor for the detection of *E. coli* O157:H7 comparing different protocols for anti-*E. coli* antibody immobilization onto gold electrodes. Each of these protocols allow to achieve a LOD in a range of 3-10³ CFU mL⁻¹ and the lowest (3 CFU mL⁻¹) was obtained by modifying the electrode surface with a cysteamine/ferrocene layer.¹²³ Lin *et al* compared the performances of a gold nanoparticles modified electrode with that of planar gold electrodes.¹²⁴ They used a functionalization method based on Protein G in order to immobilize the antibodies with a correct orientation. The gold nanoparticles-based immunosensor reached a LOD of 48 CFU mL⁻¹ which was lower than that obtained using a planar gold electrode (140 CFU mL⁻¹). Li and co-workers proposed an immunosensor with a limit of detection of 10² CFU mL⁻¹ based on screen-printed interdigitated microelectrode (SPIMs)

where biotinylated antibodies were immobilized on a gold electrode modified with 3-dithiobis-(sulfosuccinimidyl-propionate) (DTSP).¹²⁵ An impedimetric sensor for the detection of *Escherichia coli* O157:H7 based on antibodies covalently linked on a conducting polyaniline (PANI) film by using glutaraldehyde as cross-linker was described by Chowdhury *et al.*¹²⁶, who reported a LOD of 10^2 CFU mL⁻¹. Wan and co-workers¹²⁷ reported the development of a signal-off impedimetric biosensor based on gold nanoparticles for the sensitive detection of *Escherichia coli* O157:H7. Antibodies were covalently immobilized onto gold electrodes modified with mixed self-assembled monolayers of 11-mercaptopundecanoic acid (MUA) and 1-undecanethiol (UDT). After the detection of *E. coli* bacteria, the biosensor was modified with gold nanoparticles that acted as electron-transfer pathways leading to a LOD of 10^2 CFU mL⁻¹.

In addition, aptamers have been widely used as bioreceptor due to their high affinity and specificity.¹²⁸ Recently, Brosel-Oliu *et al.*¹²⁹ reported an aptasensor for detection and quantification of pathogenic *E. coli* O157:H7 with a low detection limit (10^2 CFU mL⁻¹), short detection time and good selectivity since no response was observed in the presence of other bacterial strains such as *Salmonella* Typhimurium. The covalent immobilization of the aptamers was performed via the mercaptosilane layer realized on a pre-treated electrode surface with (3-mercaptopropyl) trimethoxysilane (MPTES).

TABLE 4.1. Impedimetric immunosensors for *Escherichia coli* detection

Bioreceptor	Immobilization method	LOD (CFU mL ⁻¹)	Reference
Antibody	SAMs of MHDA	2	122
Antibody	Cys/Ferrocene	3	123
Antibody	Protein G	48	124
Biotinylated-Antibody	DTSP	10^2	125
Antibody	Glutaraldehyde	10^2	126
Antibody	SAMs of MUA - UDT	10^2	127
Aptamer	Mercaptosilane layer	10^2	129

SAMs: self-assembled monolayers; MHDA: 16-mercaptohexadecanoic acid; Cys: Cysteamine; DTSP: 3-dithiobis-(sulfosuccinimidyl-propionate); UDT: 1-undecanethiol; MUA: 11-mercaptopundecanoic acid.

1.4 SCREEN-PRINTED ELECTRODES

The use of screen-printed electrodes (SPEs) is one of the most promising approach when the development of a rapid and low-cost biosensor is required.¹³⁰ Examples of different SPEs are shown in **FIGURE 4.5**. Screen-printed electrodes can be produced in large amount at low cost and they are often used as disposable electrodes. Due to the main advantages such as sensitivity, selectivity, miniaturized size and the possibility to be connected to a portable instrumentation, these transducers can be successfully used for on-site and real-time detection of analytes in different areas including food industry, environmental monitoring and biomedical analysis. One of the main advantage associated to the miniaturization is the possibility to reduce the sample volumes to few microliters. Consequently, the whole device, in which the electrode is integrated, can be realized in smaller size thus reducing also the production cost. In addition, by using these low cost electrodes, it is possible to perform each measurement with a new electrode thus eliminating possible contaminations from previous experiments and tedious and time-consuming cleaning procedures. SPEs include the three electrodes (working, reference and counter) printed on the same substrate that is made of an inert material (glass, PVC, polycarbonate or ceramic). The first step during the production of a SPE is the realization of the substrate. Then, the deposition of inks upon the substrate is performed by means of a screen. The implementation of a variety of configuration (single working electrodes, arrays of working electrodes, 3-electrode configuration) with different electrode geometries and the wide range of materials that could be used are

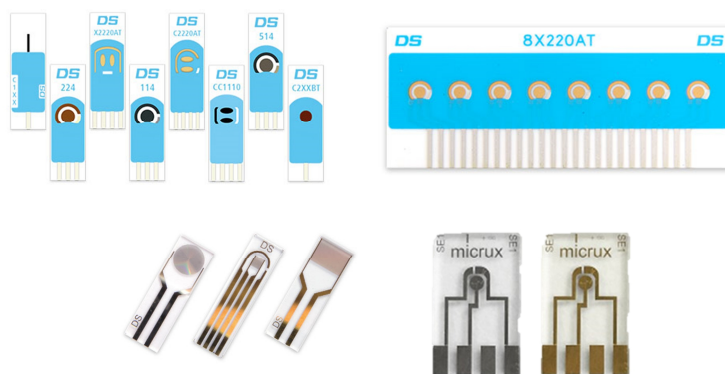


FIGURE 4.5. Different examples of screen-printed electrodes.

fundamental aspects of the screen printing technology, while the major challenge is the reproducibility of the fabricated SPEs. In fact, one of the main problems of SPEs is their batch to batch variation and the possible degradation of the surface when not stored in controlled environments. Various parameters are involved in the fabrication of the SPEs and it is essential to optimize them in order to guarantee a high reproducibility. Naturally, even the solvents used during the electrochemical experiment should be compatible with the inks used in the SPEs production. Some organics solvent, for instance, can cause the dissolution of the inks and can be responsible for the lack of sensitivity and reproducibility.

In this chapter, the development of a simple and low cost impedimetric immunosensor based on screen-printed gold electrodes for rapid detection of *E. coli* is reported. The immunosensor is fabricated by immobilizing anti-*E. coli* antibodies onto a gold surface in a covalent way by the photochemical immobilization techniques (PIT). The Nyquist plots can be modelled with a modified Randles equivalent circuit, identifying the charge transfer resistance R_{ct} as the relevant parameter after the immobilization of antibodies, the blocking with BSA and the binding of *E. coli* cells. The introduction of a standard amplification procedure leads to a significant enhancement of the impedance increase, which allows one to measure *E. coli* in drinking water with a limit of detection of 3×10^1 CFU mL⁻¹ while preserving the rapidity of the method which requires only 1 hour to provide a “yes/no” response.

2. MATERIALS AND METHODS

2.1 CHEMICALS

Gold screen printed electrodes (AuSPEs) were purchased from BVT Technologies (Strážek, Czech Republic). They include a gold disk-shaped ($d = 1$ mm) working electrode, a silver/silver chloride electrode and a gold counter electrode, all of them printed on a corundum ceramic base (0.7 cm × 2.5 cm). All potential values were referred to the silver/silver chloride reference electrode. Phosphate buffer saline (PBS) was prepared by dissolving PBS tablets (from GoldBio, St Louis, MO, USA) in Milli-Q water (each tablet prepares 100 mL of a 0.01 M PBS solution). Anti-*E. coli* polyclonal antibody (5.5 mg mL⁻¹) was obtained from Thermo Fisher Scientific (Rockford, IL, USA) and anti-*E. coli* solutions (25 µg mL⁻¹) were prepared in a 0.01 M PBS solution (pH 7.4). Bovine serum albumin (BSA), potassium hexacyanoferrate (II)

trihydrate ($\text{K}_4\text{Fe}(\text{CN})_6 \cdot 3\text{H}_2\text{O}$), potassium hexacyanoferrate (III) ($\text{K}_3\text{Fe}(\text{CN})_6$) and sulphuric acid (H_2SO_4 98%) were purchased from Sigma-Aldrich (Milano, Italy). The microfluidic setup involves a fluidic cell, silicon tubes and a continuous pump (HNP Mikrosysteme GmbH, Schwerin, Germany). The total volume of the circuit is about $100 \mu\text{L}$, the cell volume is about $10 \mu\text{L}$ and the flow rate is $6 \mu\text{L s}^{-1}$.

2.2 APPARATUS

Electrochemical impedance spectroscopy (EIS) and cyclic voltammetry (CV) measurements were carried out with a potentiostat and impedance analyser PALMSENS (Utrecht, The Netherlands) model PalmSens3 controlled by a computer through the PSTRACE version 5 software. Cyclic voltammetry (CV) and electrochemical impedance spectroscopy (EIS) were conducted in the presence of $\text{Fe}(\text{CN})_6^{3-}/\text{Fe}(\text{CN})_6^{4-}$ (1:1, 10 mM) as redox probe in 0.01 M PBS solution (pH = 7.4). In CVs, potential was cycled from -0.6 V to 0.6 V with a scan rate of 0.15 V s^{-1} in 10 mM $\text{Fe}(\text{CN})_6^{3-}/\text{Fe}(\text{CN})_6^{4-}$. EIS measurements were performed at the frequency range from 5 Hz to 10000 Hz at the formal potential of 0.16 V and using an amplitude perturbation of 10 mV. The impedance data were shown in the Nyquist plot and the EIS spectrum Analyzer software, supplied with the instrument, was used to fit EIS data to the electrical equivalent circuit in order to obtain the fit-component parameters values. A fluidic setup including a Plexiglas cell, silicon tubes and a continuous pump was used for the flowing of the different solutions (Abs, BSA and *E. coli*).

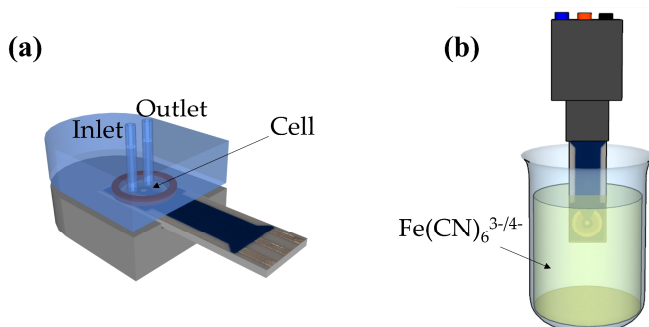


FIGURE 4.6. (a) Sketch of the fluidic cell used for an effective interaction of the solutions (Abs, BSA and *E. coli*) with the electrode and (b) scheme used for the electrochemical measurements: the AuSPE was dipped in a beaker containing 1.5 mL of $\text{Fe}(\text{CN})_6^{3-/4-}$ and it was connected to the potentiostat through a holder (in grey) for the impedance/current measurements.

A schematic representation of the cell is shown in **FIGURE 4.6a**. The main feature of the cell is its small volume that facilitates the interaction of the particles in the solutions (Abs, BSA, *E. coli*, etc.) with the electrode. Any solution was conveyed by a continuous pump at a flow rate of $6 \mu\text{L s}^{-1}$. Although effective for the interaction, such a cell was unsuitable for electrochemical measurements in view of the small amount of electrolytes involved. Thus, after each interaction we took the electrode out of the cell and dipped it into a 1.5 mL beaker containing $\text{Fe}(\text{CN})_6^{3-/4-}$ (**FIGURE 4.6b**), in which the electrochemical measurements were carried out at room temperature.

2.3 PREPARATION OF THE BIOLOGICAL SAMPLE

Bacterial strain *E. coli* ATCC 25922 was grown in Muller Hinton Broth (MHB, Becton Dickinson Difco, Franklin Lakes, NJ, USA) and on Tryptic Soy Agar (TSA; Oxoid Ltd., Hampshire, UK). In all the experiments, bacteria were inoculated and grown overnight in MHB at 37 °C. The next day, bacteria were centrifuged and solubilized in drinking water at the desired cell densities (10^1 – 10^6 CFU mL⁻¹). By colony counting assays, it was verified that bacterial growth was negligible in PBS 1X with respect to MHB through a time interval of 3 hours at room temperature, whereas bacterial death was not observed. Clinical isolated bacteria *Salmonella enteritidis* 706 RIVM¹³¹ and *Acinetobacter baumannii* (ATCC 17978) were grown in the same way and diluted drinking water in order to verify the specificity of the immunosensor towards *E. coli* in comparison with non-target bacteria.

2.4 GOLD SURFACE PREPARATION

Before the electrochemical measurements, the gold electrode was electrochemically cleaned with a 50 mM solution of sulphuric acid (H_2SO_4). Although, gold is commonly used as working electrode in electrochemical measurements because of its high chemical stability, it tends to adsorb ambient contaminants during the post-preparation, storage and transportation. This contamination will affect the quality of the gold electrode thus influencing its efficiency. The peak currents in cyclic voltammetry and the frequency response during electrochemical impedance spectroscopy will be dependent on the surface composition of the gold. It is for this reason that an effective pre-cleaning, performed immediately before the measurement, is an essential step prior the surface functionalization with antibodies. The AuSPE was electrochemically cleaned by cycling the potential between -0.4 V and

1.4 V at a scan rate of 0.1 V s⁻¹ in 0.05 M H₂SO₄ until the CV becomes stable (approximately 10 cycles). The electrode was then rinsed with a copious amount of Milli-Q water. Following cleaning, the gold electrode was characterized using cyclic voltammetry (CV) and electrochemical impedance spectroscopy (EIS) (**FIGURE 4.7**).

As it concerns the CV, the mean of the E_{pc} and E_{pa} values ($\frac{E_{pa} + E_{pc}}{2}$) and the potential difference ΔE_p ($\Delta E_p = E_{pa} - E_{pc}$) are used as a measure of the cleanliness of the surface electrode. Theoretically for a single-electron transfer reaction (as in the case of [Fe(CN)₆]^{3-/4-}) on a perfect clean gold surface ΔE_p should be 59mV and the ratio $\frac{E_{pa} + E_{pc}}{2}$ equal to the $E^{0'}$ (Formal Reduction Potential of the redox probe). In our case, $\frac{E_{pa} + E_{pc}}{2}$ matches with the $E^{0'}$ of the [Fe(CN)₆]^{3-/4-} couple (0.16V), while ΔE_p is slightly higher (**FIGURE 4.7a**). Considering that cycling the potential for a greater number of cycles (15-20 cycles) did not provide a reduction of ΔE_p , or even, caused the etching of the gold we interpreted this value to be caused by surface imperfections.

Moreover, the frequency response from the EIS measurements were fit to the Randles circuit, from which the charge transfer resistance (R_{ct}) was extracted. Since R_{ct} is a measure of the resistance encountered by the electron as it travels between the redox species and electrode surface, a lower R_{ct} indicates a cleaner and more electrochemically active surface (**FIGURE 4.7b**).

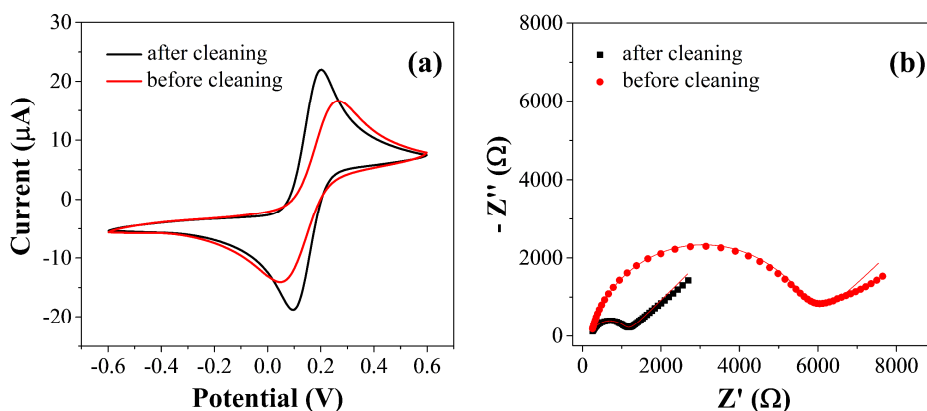


FIGURE 4.7. (a) CV and (b) EIS after and before the electrochemical cleaning of the gold electrode with H₂SO₄ showing that the cleaning gave rise to an increase in current (a) and a decrease of impedance (b).

2.5 EXPERIMENTAL PROCEDURE

The cleaned SPE was placed in the fluidic cell and the experimental procedure for impedance measurements consists in the flowing of different solutions onto the sensitive gold surface of the AuSPE. The different steps involved in the preparation of the immunosensor are schematically illustrate in **FIGURE 4.8**. Firstly, an anti-*E. coli* antibodies solution ($25 \mu\text{g mL}^{-1}$) was activated by the Photochemical Immobilization Technique. As described in details in Chapter 1, PIT is a functionalization method which allows the immobilization of antibodies onto gold surfaces in a correct orientation which means with their binding sites available for the binding of the analyte. In this experiment the PIT is accomplished by activating a solution of $25 \mu\text{g mL}^{-1}$ anti-*E. coli* pAbs for 30 secs by two low pressure mercury lamp (LP Hg lamp) emitting at 254 nm and manufactured by Procom Alta Tecnologia srl (Dicomano, FI, Italy). The two lamp (1.5 cm of diameter) are horseshoe-shaped and mounted in a stacked configuration so that its internal empty space fits with a quartz cuvette whose dimensions are 1 cm x 1 cm x 4 cm. The power of each lamp is 6 W and, by considering that the cuvette containing the anti-*E. coli* IgG solution is close to the lamps, the effective irradiation intensity used for the antibody activation is about 0.3 W/cm^2 . Then, the gold electrode was functionalized by conveying a solution of UV-activated anti-*E. coli* antibodies ($25 \mu\text{g mL}^{-1}$) onto the gold sensitive surface for 15 min by applying a constant flow rate of $6 \mu\text{L s}^{-1}$ (step I). Since the Ab activation only lasts approximately five minutes,³⁸ to saturate the gold electrode surface such a step was repeated 4 times with a fresh irradiated Abs solution. Subsequently, the electrode was rinsed for 1 h with 0.01 M PBS buffer to remove the unbound antibodies. After that, a BSA solution ($50 \mu\text{g mL}^{-1}$) flowed into the cell for 15 min filling the remaining free space on the gold surface (step II). This blocking step is crucial to avoid the possible non-specific interactions of the following molecules. A 1mL aliquot of drinking water incubated with different concentration of *E. coli* cells (from 10^1 to 10^8 CFU mL^{-1}) flowed into the circuit for 30 min at room temperature and the bacteria cells were captured by the immobilized antibodies (step III). The electrode was rinsed with 0.01 M PBS to remove non-specifically and weakly bound bacteria for 5 min. Each detection was repeated three times. The difference in impedance measured before and after *E. coli* incubation, normalized with the impedance value obtained after Abs immobilization, was taken as the signal produced by the binding between immobilized antibodies and

target bacterial cells. An aliquot of 1 mL of drinking water, without incubation of bacteria, was used as negative control.

2.6 ENHANCED SENSITIVITY PROTOCOL

In order to improve the signal, an amplification step has been included in the experimental procedure. The response enhancement has been achieved by conveying anti-*E. coli* (25 $\mu\text{g mL}^{-1}$) into the microfluidic cell for 30 min (step IV, **FIGURE 4.8**). This additional step, which leads to the formation of a sandwich complex, was used to amplify the slight impedance increment obtained after *E. coli* detection at low concentration. In such a case, the formation of a sandwich complex further hinders the electron-transfer process thus improving the electrochemical response. A final washing phase with 0.01 M PBS is used to remove unbound or weakly bonded molecules.

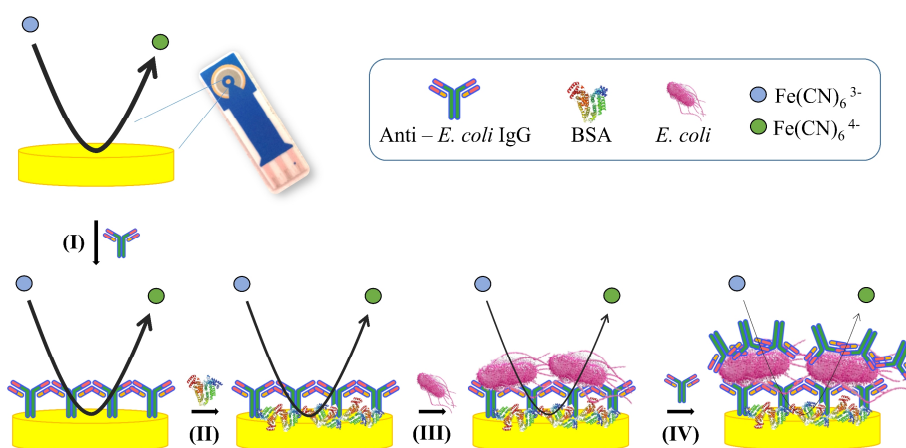


FIGURE 4.8. Schematic scheme (not in scale) of the stepwise functionalization and detection. The black line represents the intensity of the redox reaction, which is inhibited as the surface covering grows. The reduction of its thickness is associated to a decrease of the “effective” area available for the electrolyte current, which is measured as an increase of the charge transfer resistance.

3. RESULTS AND DISCUSSION

3.1 KINETIC OF THE FUNCTIONALIZATION

The kinetic of the functionalization was investigated to optimize the performance of the impedimetric immunosensor. A solution of anti-*E. coli* pAbs with a concentration of $25 \mu\text{L mL}^{-1}$ was fluxed in the cell and a study on the time the solution is fluxed was performed. The Abs are conveyed to the electrode after they have been irradiated by PIT. Since the activation of the Abs only lasts approximately 5 min,³⁸ it is necessary to optimize the time the solution is fluxed in the cell containing the working electrode ($10 \mu\text{L}$ volume). The results obtained with a flow rate of $6 \mu\text{L s}^{-1}$ are reported in **FIGURE 4.9a** (see **TABLE 4.2** for the data) that shows EIS spectra measured at intervals of 15 min, which are required to cover the whole surface. The resulting R_{ct} and its behaviour with the time is well fitted by an exponential function with a time constant of 13 ± 1 min. Thus, the whole functionalization procedure can be considered accomplished in one-hour time. Since no significant change of R_{ct} is observed after the blocking step, we can assess that the saturation of R_{ct} shown in **FIGURE 4.9b** corresponds to an electrode fully covered by antibodies. The errors of R_{ct} are within the thickness of the experimental points.

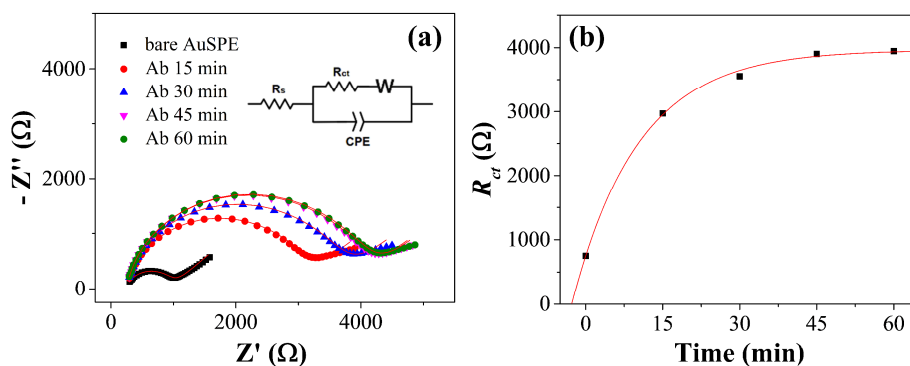


FIGURE 4.9. (a) EIS spectra measured at different times while the UV irradiated antibodies are conveyed to the interaction cell; (b) R_{ct} as a function of time showing that the surface saturation takes place within one-hour time.

TABLE 4.2. Results from the fitting of impedance data in **FIGURE 4.9**.

	R_s (Ω)	CPE		R_{ct} (Ω)	W ($k /s^{1/2}$)
		Q_1 $\mu(s^{n_1}/ cm^2)$	n_1		
Bare	253 ± 4	0.34 ± 0.02	0.898 ± 0.008	712 ± 7	3.53 ± 0.04
Ab 15 min	259 ± 3	0.203 ± 0.006	0.917 ± 0.004	2813 ± 14	4.57 ± 0.10
Ab 30 min	256 ± 2	0.192 ± 0.005	0.915 ± 0.003	3384 ± 13	4.69 ± 0.11
Ab 45 min	259 ± 2	0.170 ± 0.003	0.920 ± 0.002	3736 ± 15	4.61 ± 0.10
Ab 60 min	254 ± 2	0.171 ± 0.003	0.919 ± 0.002	3777 ± 13	4.62 ± 0.09

3.2 KINETIC OF THE DETECTION

The kinetic of *E. coli* detection was also studied to optimize the performance of the immunosensor. Drinking water samples incubated with a concentration of *E. coli* 10^5 CFU mL^{-1} was flowed over the antibody-modified electrode and the R_{ct} change was monitored at time intervals of 15 min. The results are reported in **FIGURE 4.10a**. The resulting ratio $\Delta R_{ct}/R_{ct(Ab)}$ as a function of the time is shown in **FIGURE 4.10b** with an exponential fit of the experimental data that provides a time constant of 14 ± 7 min (see **TABLE 4.3** for the data). Although with larger error, such a value is similar to that measured for surface functionalization by Abs suggesting that 30 min was a suitable incubation time to allow the completion of the analyte detection.

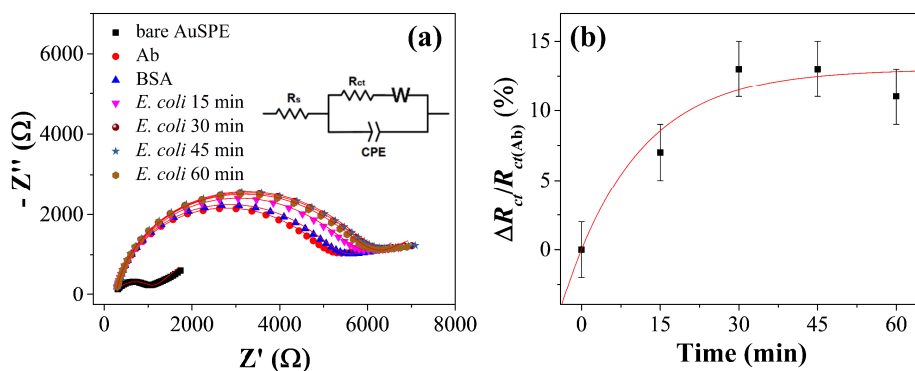


FIGURE 4.10. (a) EIS spectra measured at different times with *E. coli* at 10^5 CFU mL^{-1} ; (b) R_{ct} as a function of time showing an exponential kinetic with a constant time of 14 ± 7 min.

TABLE 4.3. Results from the fitting of impedance data in **FIGURE 4.10**.

	R_s (Ω)	Q_1 $\mu(s^{n_1}/\text{cm}^2)$	n_1	R_{ct} (Ω)	W ($\text{k}/\text{s}^{1/2}$)
Bare AuSPE	260 ± 7	0.58 ± 0.08	0.850 ± 0.016	787 ± 18	3.98 ± 0.09
Ab	267 ± 2	0.213 ± 0.005	0.919 ± 0.003	4730 ± 20	6.47 ± 0.16
BSA	268 ± 2	0.206 ± 0.004	0.922 ± 0.002	4817 ± 14	6.22 ± 0.16
<i>E. coli</i> 15 min	267 ± 2	0.217 ± 0.004	0.918 ± 0.001	5140 ± 20	6.39 ± 0.16
<i>E. coli</i> 30 min	269 ± 2	0.219 ± 0.004	0.916 ± 0.002	5440 ± 20	6.41 ± 0.16
<i>E. coli</i> 45 min	268 ± 2	0.216 ± 0.004	0.918 ± 0.002	5460 ± 20	6.63 ± 0.16
<i>E. coli</i> 60 min	267 ± 2	0.216 ± 0.004	0.917 ± 0.002	5350 ± 20	6.20 ± 0.15

We also measured the kinetics of the Ab binding to the *E. coli* from the top (sandwich configuration) by carrying out EIS as a function of time during the flow of a $25 \mu\text{g mL}^{-1}$ Ab solution into the cell. The Nyquist plots are reported in **FIGURE 4.11a** (see **TABLE 4.4** for the data) and the corresponding values for $\Delta R_{ct}/R_{ct(\text{Ab})}$ are shown in **FIGURE 4.11b** with an exponential fit of the data that provides a constant time of 13.5 ± 0.3 min. Once again, 30 min can be considered a recommended value that allows the accomplishment of the amplification step.

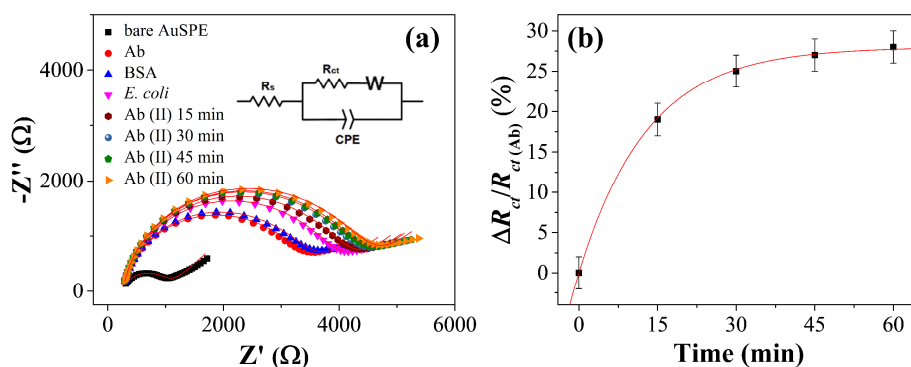


FIGURE 4.11. Kinetics of the secondary antibody. **(a)** EIS spectra measured at different times while a $25 \mu\text{g mL}^{-1}$ Ab solution is conveyed to the cell after the detection *E. coli* (10^5 CFU mL^{-1}); **(b)** R_{ct} as a function of time showing an exponential dynamic with a constant time of 13.5 ± 0.3 min.

TABLE 4.4. Results from the fitting of impedance data in FIGURE 4.11.

	R_s (Ω)	Q_1 $\mu(s^{n_1}/\text{cm}^2)$	n_1	R_{ct} (Ω)	W ($k /s^{1/2}$)
Bare AuSPE	259 ± 8	0.58 ± 0.09	0.844 ± 0.017	792 ± 18	3.88 ± 0.09
Ab	266 ± 3	0.224 ± 0.009	0.915 ± 0.004	3130 ± 20	5.49 ± 0.15
BSA	266 ± 3	0.223 ± 0.008	0.915 ± 0.002	3149 ± 16	5.64 ± 0.16
<i>E. coli</i>	267 ± 2	0.197 ± 0.005	0.925 ± 0.003	3565 ± 18	5.17 ± 0.12
Ab (II) 15 min	265 ± 2	0.202 ± 0.005	0.922 ± 0.003	3769 ± 19	5.29 ± 0.13
Ab (II) 30 min	265 ± 2	0.201 ± 0.005	0.922 ± 0.003	3939 ± 20	5.40 ± 0.13
Ab (II) 45 min	265 ± 2	0.204 ± 0.005	0.920 ± 0.003	3991 ± 20	5.47 ± 0.13
Ab (II) 60 min	265 ± 2	0.205 ± 0.005	0.919 ± 0.003	4044 ± 20	5.60 ± 0.13

3.3 BLOCKING WITH BSA

Experimental parameters including the concentration of BSA and the incubation time were also optimized. Firstly, a $50 \mu\text{g mL}^{-1}$ BSA solution was flowed over the antibody-modified electrode and the R_{ct} change was monitored at time intervals of 30 min. The corresponding Nyquist plots, reported in FIGURE 4.12a, show that a negligible increment of the R_{ct} value could be detected thereby proving that the gold surface is fully covered by the antibodies (see TABLE 4.5 for the R_{ct} values). In addition, the experiment was carried out by flowing a higher concentration of BSA ($100 \mu\text{g mL}^{-1}$, FIGURE 4.12b). Once again, a negligible increment of R_{ct} was observed after 30 min (see TABLE 4.6 for the R_{ct} values). Therefore, an incubation time of 30 min and a concentration of $50 \mu\text{g mL}^{-1}$ were chosen in the following experiments.

It is worth highlighting that the increment of R_{ct} after the antibody immobilization (and BSA blocking consequently) varies from one electrode to another. As FIGURES 4.9-4.12 show, in most cases, the R_{ct} value increases up to 3-4.5 K Ω but, occasionally, it reaches higher values such as 6-9 K Ω . This behaviour could be explained considering the inherent differences of any single AuSPEs, which are commercial cheap electrodes and used without any pre-treatment or surface modification. In order to take account of these differences, a normalized ΔR_{ct} (i.e. $\Delta R_{ct}/R_{ct(Ab)}$) is used as sensing parameter which enables us to build a successful dose-response curve (see paragraph 3.4).

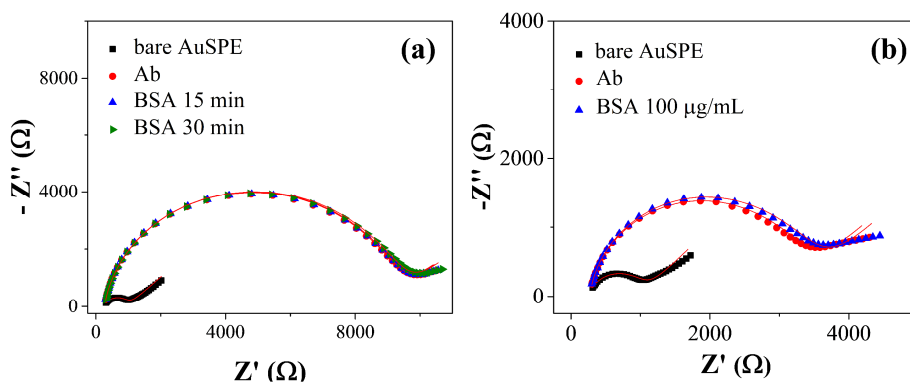


FIGURE 4.12. (a) EIS spectra measured at different times while a $50 \mu\text{g}\cdot\text{mL}^{-1}$ BSA solution is conveyed to the cell and (b) EIS spectra measured with $100 \mu\text{g}\cdot\text{mL}^{-1}$ BSA solution.

TABLE 4.5. Results from the fitting of impedance data in **FIGURE 4.12a**.

	R_s (Ω)	CPE		R_{ct} (Ω)	W ($\text{k} / \text{s}^{1/2}$)
		Q_1 $\mu(\text{s}^{n_1} / \text{cm}^2)$	n_1		
Bare	255 ± 6	0.57 ± 0.07	0.851 ± 0.014	736 ± 14	3.7 ± 0.1
Ab	266 ± 2	0.159 ± 0.002	0.921 ± 0.002	8820 ± 30	5.1 ± 0.2
BSA 15 min	265 ± 2	0.158 ± 0.002	0.921 ± 0.002	8850 ± 30	5.1 ± 0.2
BSA 30 min	266 ± 2	0.164 ± 0.003	0.918 ± 0.002	8920 ± 40	5.4 ± 0.2

TABLE 4.6. Results from the fitting of impedance data in **FIGURE 4.12b**.

	R_s (Ω)	CPE		R_{ct} (Ω)	W ($\text{k} / \text{s}^{1/2}$)
		Q_1 $\mu(\text{s}^{n_1} / \text{cm}^2)$	n_1		
Bare	250 ± 8	0.58 ± 0.09	0.844 ± 0.017	792 ± 18	3.88 ± 0.09
Ab	266 ± 3	0.224 ± 0.009	0.915 ± 0.004	3030 ± 20	5.49 ± 0.15
BSA $100 \mu\text{g}\cdot\text{mL}^{-1}$	266 ± 3	0.223 ± 0.009	0.915 ± 0.004	3150 ± 20	5.64 ± 0.16

3.4 DETECTION OF *ESCHERICHIA COLI*

Cyclic voltammetry (CV) and electrochemical impedance spectroscopy (EIS) measurements were carried out to investigate the layer by layer construction of the immunosensor and to verify the *E. coli* binding (**FIGURE 4.13**). Both characterization techniques investigate the electron transfer process and, specifically, the changes of charge transfer resistance caused by the adsorption of insulating molecules to the gold electrode. EIS plots of the step-by-step immunosensor fabrication are shown in **FIGURE 4.13a** utilizing 10 mM $\text{Fe}(\text{CN})_6^{3-}/\text{Fe}(\text{CN})_6^{4-}$ as redox probe in 0.01 M PBS buffer.

The potential applied for the EIS studies was set to 0.16 V (vs. Ag/AgCl) according to the CV result. The impedance data are represented as Nyquist plots and R_{ct} values were extracted by fitting the data with the Randles circuit (inset **FIGURE 4.13a**, see **TABLE 4.7** for the data) after each preparation step since the comparison of these values indicate the change of the redox probe kinetics at the electrode interface. The R_{ct} of the bare electrode was as small as 878 Ω . The surface was functionalized using previously activated antibodies which tether the surface providing a significantly resistance increase of approximately 5.4 k Ω , since the covalent immobilization of antibodies onto the electrode surface acts as an inert electron transfer blocking layer and the penetration of the redox probe. As reported in the previous paragraph, the blocking of the surface was carried out with BSA at 50 $\mu\text{g mL}^{-1}$ or 100 $\mu\text{g mL}^{-1}$ and in both cases a negligible increment of R_{ct} value could be detected thereby proving that the gold surface is fully covered by the antibodies. In the next step, the solution containing the *E. coli* cells (10^2 CFU mL^{-1}) flows in the circuit and the analyte is recognized by the Abs. However, with the further attachment of the *E. coli* cells (10^2 CFU mL^{-1}) to the modified electrode surface no significant increase of impedance is observed and a solution of anti-*E. coli* Abs is conveyed to the cell giving rise to a sandwich complex which produces an increase of the charge transfer resistance caused by the realization of a further barrier towards the access of the redox probe to the electrode. In such a case, the R_{ct} value increases by a 15% after the formation of antibody *E. coli* complex.

In addition, CV measurements were carried out to corroborate the EIS results. CV curves of the step-by-step modification are shown **FIGURE 4.13b**, using 10 mM $\text{Fe}(\text{CN})_6^{3-}/\text{Fe}(\text{CN})_6^{4-}$ as redox probe in 0.01 M PBS buffer. The bare gold electrode gave a well-defined anodic and cathodic peaks, due to the reversible interconversion of the redox probe $\text{Fe}(\text{CN})_6^{3-}/\text{Fe}(\text{CN})_6^{4-}$, with peak potential difference (ΔE_p) of 107 mV

and peak current (I_p) of 23.9 μA . After antibody immobilization, the ΔE_p increased to 192 mV and the I_p decreased to 19.1 μA confirming the attachment of charge transfer inhibiting molecules to the gold electrode. The surface blocking with BSA caused a negligible decrease of I_p (18.9 μA) confirming the complete saturation of the gold surface with antibodies. Finally, after the incubation with *E. coli* no significant decrease of current was observed and the resulting formation of antibody-*E. coli* complex lead to a further decrease of the peak current ($I_p = 17.2 \mu\text{A}$ and $\Delta E_p = 218 \text{ mV}$) which coincides with EIS results.

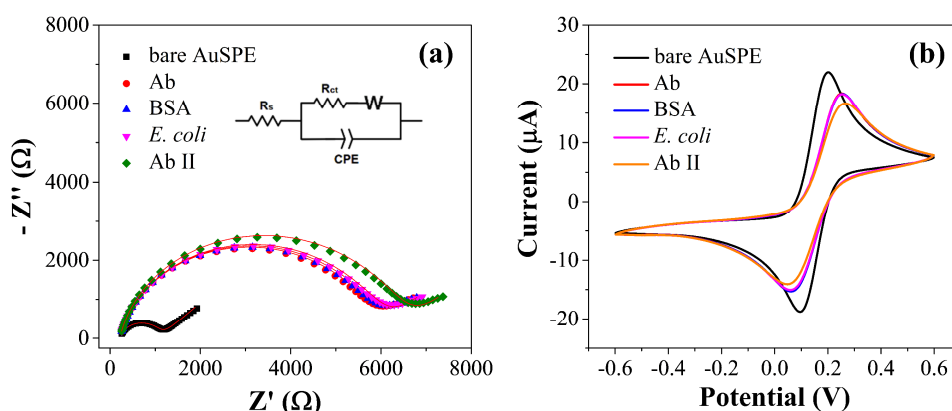


FIGURE 4.13. (a) EIS and (b) CV of the step-by-step immunosensor development and *E. coli* detection in 10 mM $\text{Fe}(\text{CN})_6^{3-}/\text{Fe}(\text{CN})_6^{4-}$ solution at pH 7.4.

TABLE 4.7. Results from the fitting of impedance data in **FIGURE 4.13**

	R_s (Ω)	CPE		R_{ct} (Ω)	W ($\text{k} / \text{s}^{1/2}$)
		Q_1 $\mu(\text{s}^{n_1} / \text{cm}^2)$	n_1		
Bare	224 ± 1	0.438 ± 0.010	0.892 ± 0.003	878 ± 3	2.84 ± 0.02
Ab	222 ± 1	0.302 ± 0.004	0.889 ± 0.001	5414 ± 16	3.84 ± 0.10
BSA	221 ± 1	0.304 ± 0.003	0.888 ± 0.001	5472 ± 16	3.83 ± 0.10
<i>E. coli</i>	221 ± 1	0.306 ± 0.003	0.887 ± 0.001	5540 ± 14	3.93 ± 0.10
Ab (II)	221 ± 1	0.291 ± 0.003	0.893 ± 0.001	6096 ± 18	3.92 ± 0.12

The performance of the immunosensor for the detection of *E. coli* was investigated in drinking water by EIS. Drinking water samples (1 mL) were incubated with *E. coli* at different concentration in the range of 10^1 – 10^8 CFU mL⁻¹. **FIGURE 4.14a** shows the dose response curves obtained with steps I-III (red curve, direct detection protocol without amplification or DDP) and steps I-IV (black curve, ballasting detection protocol with amplification or BDP). In the case of DDP, the sensing parameter is $\Delta R_{ct}/R_{ct(Ab)}$ where ΔR_{ct} is the change in the impedance brought about by *E. coli* [$\Delta R_{ct} = R_{ct(E. coli)} - R_{ct(BSA)}$], whereas $R_{ct(Ab)}$ is the impedance value measured after the functionalization. As **FIGURE 4.14a** (red curve) shows, a detection range of two decades (10^3 to 10^5 CFU mL⁻¹) is achieved before reaching a saturation at concentration higher than 10^5 CFU mL⁻¹. Each bacteria concentration and the negative control (1 mL of drinking water) have been tested three times in several days in different environmental conditions and using different electrodes. The standard deviation (σ) of the measurements is approximately 2% proving that the protocol shows good accuracy and reproducibility. According to the 3σ formula, it is necessary to achieve an impedance increase 6% in order to consider the variation as significant. As it shown in the dose-response curve, the limit *E. coli* concentration (LOD) producing such variation in impedance increase is 10^4 CFU mL⁻¹ (**FIGURE 4.14a**, red curve). The $\Delta R_{ct}/R_{ct(Ab)}$ measured for the negative sample (1 mL aliquot of drinking water) was less than 1% confirming the absence of interferences of the drinking water components (especially salts) with the biosensor surface.

In the DDP condition a LOD of approximately 10^4 CFU mL⁻¹ is obtained, which can be significantly improved by including the step IV that consists of addition of anti-*E. coli* Abs so that a sandwich configuration is realized (**FIGURE 4.14a**, black curve). In fact, the relative electron-transfer resistance difference in such a case is $\Delta R_{ct}/R_{ct(Ab)}$ where $\Delta R_{ct} = R_{ct(Ab II)} - R_{ct(BSA)}$. The black curve shows a remarkable increase in the slope as well as in the saturation level, which is achieved at lower concentration. With the same criteria used before (3σ formula with σ about 2%), the detection limit of this extended protocol (BDP) is estimated to be 3×10^1 CFU mL⁻¹ whereas the quantification range is 10^2 – 10^3 CFU mL⁻¹. It is worth noticing that a narrow quantification range is not a drawback when “on-off” biosensors are considered, as it is the case of the device proposed here.

The comparison of the two curves in **FIGURE 4.14a** suggests an enhancement of the signal whose factor depends on the *E. coli* concentration. In fact, by defining g as a gain factor, we have:

$$g([E - coli]) = \frac{\Delta R_{ct}^{(BDP)}([E - coli])}{\Delta R_{ct}^{(DDP)}([E - coli])}, \quad (4.21)$$

where the superscripts DDP and BDP refer to the three step and four step protocol, respectively.

The plot of g is reported in **FIGURE 4.14b** as a function of *E. coli* concentration together with the 95% confidence interval (grey area) obtained by propagating the error from the curves in **FIGURE 4.14a** into Equation (4.21). The enhancement factor is more than one order of magnitude ($10 < g < 33$) at lower concentration and decreases to an expected saturation value of approximately 1 at higher concentrations. Such a behavior may well be explained by considering that at higher concentration of *E. coli*, the surface has a higher degree of occupancy by the bacteria so that the binding of additional Ab II tethered to *E. coli*, gives rise to a smaller effect on R_{ct} when compared to the effect produced at lower concentration.

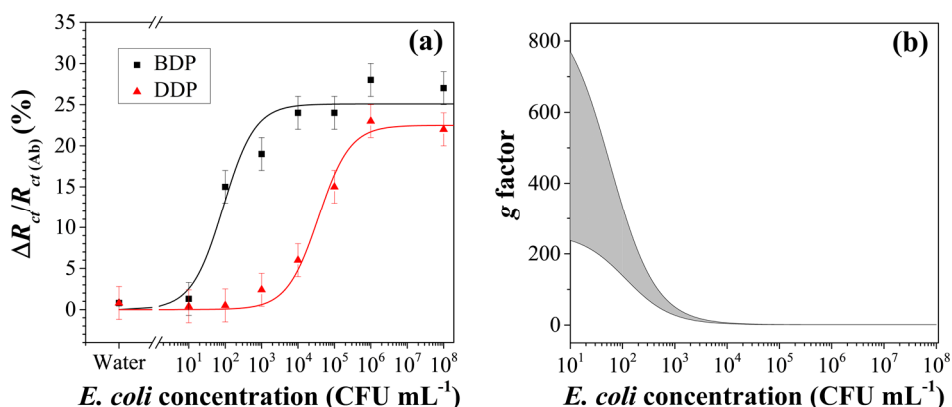


FIGURE 4.14. (a) Dose-response curve obtained using both protocols: DDP-direct detection protocol and BDP-ballasting detection protocol. (b) Gain factor g as a function of the *E. coli* concentration.

The analytical performances of the developed immunosensor have been compared with other recent impedimetric immunosensors for the detection of *E. coli* (**TABLE 4.8**). It is remarkable that all of them share a quite long functionalization time ranging from few hours to even twenty hours to immobilize antibodies on gold electrode surface. These immunosensors are based on immobilization procedures that include the formation of self-assembled monolayers, which usually require

particularly smooth gold electrode surfaces³⁰ and expert personnel for the setup of complex chemical procedures. In contrast, PIT is user-friendly nor is any previous modification of the surface required. Any single electrode (AuSPE) was used “as is” that is without any pretreatment (only a rapid cleaning in H₂SO₄) or surface modification, but, even more important, the inherent differences among them in terms of bare impedance did not prevent us from building the more than satisfactory dose-response curve shown in **FIGURE 4.14a**.

TABLE 4.8. Overview of the latest impedimetric biosensors for *E. coli* detection.

Functionalization scheme	Functionalization time (h)	LOD (CFU mL ⁻¹)	Reference
Au-MHDA-Ab	18 *	2	122
Au-Cys-Ferrocene-Ab	20 *	3	123
Au-PrG thiol-Ab	10	140	124
Au-AuNPs-PrG thiol-Ab	24 *	48	124
Au-PANI-Glu-Ab	>2	100	126
Au-MUA/UDT-Ab	20 *	100	127
Au-Ab (PIT activated)	1	30	This work

Ab: antibody; MHDA: 16-mercaptohexadecanoic acid; Cys: cysteamine; AuNPs: gold nanoparticles; PrG: Protein G; PANI: polyaniline; Glu: Glutaraldehyde; MUA: 11-mercaptoundecanoic acid; UDT: 1-undecanethiol.

* These times have been evaluated by considering overnight as 16 h.

3.5 SPECIFICITY TEST

In order to evaluate the specificity of the developed immunosensor for *E. coli*, we tested the response of the functionalized immunosensor by measuring $\Delta R_{ct}/R_{ct(Ab)}$ induced by some non-specific bacteria such as *Acinetobacter baumannii* and *Salmonella enteritidis* 706 RIVM. To this end a 1mL aliquot of drinking water incubated with *Salmonella enteritidis* 706 RIVM and *Acinetobacter baumannii* (10⁵ CFU mL⁻¹) flowed into the circuit for 30 min at room temperature, followed by a fresh solution of anti-*E. coli* Abs. **FIGURE 4.15** shows the electron transfer resistance changes for both protocols. According to the direct detection protocol (DDP), $\Delta R_{ct}/R_{ct(Ab)}$ increased by 2% and 7% when *Salmonella enteritidis* 706 RIVM and *Acinetobacter baumannii* were assayed, respectively, compared with an 15% increase achieved with *E. coli*. Actually, a greater increase with *Salmonella enteritidis* 706 RIVM would be expected in view of the stronger morphological

similarities with *E. coli* but, this unexpected behaviour can be likely ascribed to the different shape of *Acinetobacter baumannii*, which is a short, rod-shaped almost round bacterium which mostly hinder the electron-transfer process at the same concentration. With reference to the extended protocol (BDP), after the ballasting with a fresh solution of anti-*E. coli* Abs, $\Delta R_{ct}/R_{ct(Ab)}$ increased less than a 9% for both *Salmonella enteritidis* 706 RIVM and *Acinetobacter baumannii*, compared to the marked increase (24%) obtained with *E. coli* cells. This means that the amplification factor is about 1% for *Acinetobacter baumannii* and 4.5% for *Salmonella enteritidis* 706 RIVM, a difference likely due to the superior affinity between anti-*E. coli* pAbs and *Salmonella*, which share the same morphology of *E. coli*. Although a slight cross-reaction arises with other bacterial species, these results are more than satisfactory. In fact, the interference occurs with other bacteria, which, as for *E. coli*, should not be present in water. Thus, in view of an application of the biosensor for alert emergency such a limitation is not really a drawback of the device but it proves that the immunosensor is particularly suitable when an “on-off” approach is more advisable than a quantitative procedure.

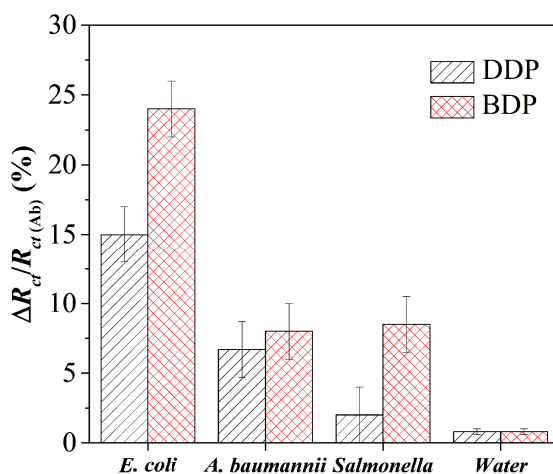


FIGURE 4.15. Specificity of the immunosensor in 10 mM $\text{Fe}(\text{CN})_6^{3-/4-}$ solution at pH 7.4. $\Delta R_{ct}/R_{ct(Ab)}$ induced by 10^5 CFU mL⁻¹ *E. coli* in comparison with the negative control (drinking water) and non-target bacteria (*Acinetobacter baumannii* and *Salmonella enteritidis* 706 RIVM).

3.6 DATA FITTING

To account for the dose-response curve, we propose a simple model that describes the change of the resistance R_{ct} due to the analyte recognition as a change of the “effective” electrode area. To start with, let’s consider that while R_{ct} in the bare electrode is in the range 500–900 Ω , its value increases up to tens of $k\Omega$ when the antibodies tether to the surface. Moreover, thanks to our functionalization procedure, no significant change of R_{ct} is observed after the blocking step (the surface is fully covered by antibodies), and, hence, the initial charge transfer resistance of the biosensor is due to the antibody layer and can be written:

$$R_{ct,0} = \frac{\rho d}{A_0} \quad (4.22)$$

where ρ is the resistivity of the antibody layer, d its thickness and A_0 the electrode area. Since the contact layer does not change during the detection procedure, both ρ and d are constant. On the contrary, the occurrence of the analyte detection reduces to some extent the effective area of the electrode, which in turn leads to an increase of the impedance, i.e.:

$$R_{ct}([C]) = \frac{\rho d}{A_0 - \alpha A([C])} \quad (4.23)$$

where $A([C])$ represents the area occupied by the analytes and α is a coefficient that accounts for their conducting properties ($\alpha = 0$, for a “conductive” analyte that does not affect the electrolyte current, whereas $\alpha = 1$ for a fully “insulator” analyte). The occupancy area can be described by the Langmuir isotherm:

$$A([C]) = A_0 \frac{[C]}{K + [C]} \quad (4.24)$$

where for convenience we used K as the inverse of the equilibrium constant. By combining Equations (4.23) and (4.24), we have:

$$R_{ct}([C]) = R_{ct,0} \frac{K + [C]}{K + (1 - \alpha)[C]} \quad (4.25)$$

Therefore, the sensing parameter becomes:

$$\frac{\Delta R_{ct}}{R_{ct(Ab)}} = \frac{R_{ct}([C]) - R_{ct,0}}{R_{ct,0}} = \frac{[C]}{\frac{K}{\alpha} + \frac{(1-\alpha)}{\alpha} [C]} \quad (4.26)$$

The best fit of the experimental data by the Langmuir-type Equation (4.26) is shown in **FIGURE 4.14a** whereas the fitting parameters are reported in **TABLE 4.9**.

TABLE 4.9. Fitting parameters α and K obtained for both protocols

	α	K (CFU mL ⁻¹)
DDP	0.185 ± 0.007	(3.0 ± 0.7) × 10 ⁴
BDP	0.20 ± 0.01	70 ± 30

As expected, the conductivity coefficient α , which measures the microscopic tendency of the analyte to inhibit the electrolyte current, is larger when antibodies are tied to the bacterium. The choice of $\Delta R_{ct}/R_{ct(Ab)}$ as sensing parameter not only allows one to measure the values for α reported in **TABLE 4.9**, but even more important from the practical point of view, introduces a high degree of robustness in the biosensors as demonstrated by the fact that each experimental point reported in **FIGURES 4.14a** was obtained with different electrode.

The increase of α observed when antibodies are bound to bacteria from the top is due to the high “opacity” of the antibodies, the latter property being deducible from the large increment of R_{ct} brought about by the surface functionalization (see **FIGURES 4.9–4.12**). By imaging that a bacterium fully covered by antibodies would have $\alpha = 1$, we can (under)estimate the fraction f of the bacterium area covered by the antibodies as:

$$f = \frac{\alpha_2 - \alpha_1}{1 - \alpha_1} \approx 0.024 \quad (4.27)$$

In Equation (4.27) α_2 and α_1 correspond to the value of α with and without amplification step, respectively. By considering that the area of *E. coli* is $A_{E-c} \approx 1 \mu\text{m}^2$ and that of an Ab is $A_{Ab} \approx 100 \text{nm}^2$, for the number N_{Ab} of Abs per bacterium, we have:

$$N_{Ab} = f \frac{A_{E-c}}{A_{Ab}} \approx 240 \quad (4.28)$$

Since this calculation is based on the assumption that an antibody is fully “opaque” to the electrolyte current, such a value has to be meant as an underestimation for the number of antibodies binding the bacterium from the top, which is likely to be larger than one thousand.

CONCLUSIONS

In this thesis, the Photochemical Immobilization Technique (PIT) has been coupled with two different types of transducers with the aim to realize efficient and reliable immunosensors for the detection of bacteria in real samples. Usually, antibodies (Abs) bind to a surface preferentially with Fab, assuming a bended conformation and exposing Fc region. This happens also in the case of non-treated Abs on gold surface, thus limiting the interaction of the same Abs with the antigens. On the contrary, a recent study evidences that, when Abs are irradiated prior their interaction with a surface - like gold -, they assume a preferential orientation with one Fab domain protruding and the other two portions of the Ab interacting with surface. Briefly, PIT is an alternative Abs immobilization technique based on the selective photoreduction of disulphide bridges produced by the UV activation of the trp/cys-cys by means of an UV lamp. This technique is a simple and fast procedure that allows the immobilization of the antibodies in a convenient orientation of the Fab region once immobilized onto gold and thiol-reactive surfaces thus representing a very important and innovative approach to improve biosensor sensitivity.

Using this immobilization procedure, we put forward an easy-to-use method for detecting *S. Typhimurium* in a real food matrix (chicken meat) based on a QCM functionalized with anti-*Salmonella* polyclonal antibodies. The QCM is a promising sensor technology that enables rapid response, real time monitoring, low cost analysis, portability and allows the direct label-free detection with high selectivity and specificity in several fields, from the food industry to the medical area. Moreover, the QCM measurement procedure does not require specialised personnel. The single analysis requires minimal sample treatment: pre-enrichment (2 h) at 37 °C, preparation steps (two centrifugations) and injection into the cell by five syringe draws, so that the whole measurement can be carried out in less than 4 hours. The LOD of proposed biosensor (less than 10^0 CFU mL⁻¹ of *S. Typhimurium* in chicken sample) and the minimum sample pre-enrichment step (2 h at 37 °C) required, make the biosensor suitable for food inspection when extremely low contamination levels need to be detected in chicken samples and, “rapidly” in test response “for all foodstuffs” respect to other diagnostic biosensors which, firstly, require a pre-enrichment step ranging from 6 up to 58 hours. The specificity of the whole system is more than satisfactory since no significant signal is detected when the *Salmonella* is replaced by *E. coli* while a signal is distinguished when both bacteria are present.

PIT has been also involved in the development of an electrochemical impedance immunosensor based on a screen printed gold electrode for the rapid detection of *E. coli* in drinking water. Nowadays, impedimetric biosensors are gaining particular attention in the development of new biosensors. The possibility of implementing label-free assays with affordable equipment make EIS one of the most promising electrochemical techniques for future low-cost devices. Firstly, the antibodies were immobilized on the gold surface of a screen-printed electrode using the PIT and the change in charge transfer resistance (R_{ct}) was monitored using faradaic EIS ($\text{Fe}(\text{CN})_6^{3-}/\text{Fe}(\text{CN})_6^{4-}$ as redox probe). The proposed immunosensor exhibits a limit of detection of $3 \times 10^1 \text{ CFU mL}^{-1}$ which was obtained by including in the measurement procedure a simple and rapid ballasting step, the latter consisting in the flowing of a fresh antibody solution onto the electrode surface so to realize a sandwich-complex. This is the first time PIT was used in biosensing by EIS and our results demonstrate that PIT is effective proved even on commercial cheap electrodes. This is a major achievement since in most situations careful surface treatments are required in order to get an effective sensor response.

In both cases, the whole measurement can be carried out in less than 6h, which means within a working day making our approach suitable for out-of-lab use when low bacteria concentration need to be detected for alert emergency and, hence, an “on-off” approach is more desirable than a time-consuming quantitative procedure. The application of these biosensors to detect other foodborne pathogens represents a new alternative method to monitor the food safety throughout the chain production so warranting the final quality of the products. These biosensors satisfy some of the technical parameters such as detection limit, time of analysis, validation of the method, sensitivity and specificity, and additional parameters like equipment, operation, and costs which should be considered before adapting a new rapid detection method. Therefore, in view of the results presented in this thesis, PIT has proven to be an effective and promising technology to couple biological sensitive elements with gold and thiol-reactive surfaces and can be considered a valid alternative to more complex and laborious surface functionalization procedures.

BIOBLIOGRAPHY

1. Turner, A. P. F., Karube, I., Wilson, G. S. & Worsfold, P. J. Biosensors: fundamentals and applications. *Anal. Chim. Acta* **201**, 363–364 (1987).
2. Clark, Jr., L. C. & Lyons, C. Electrode systems for continuous monitoring in cardiovascular surgery. *Ann. N. Y. Acad. Sci.* **102**, 29–45 (1962).
3. Mehrotra, P. Biosensors and their applications – A review. *J. Oral Biol. Craniofacial Res.* **6**, 153–159 (2016).
4. Patel, S., Nanda, R., Sahoo, S. & Mohapatra, E. Biosensors in Health Care: The Milestones Achieved in Their Development towards Lab-on-Chip-Analysis. *Biochem. Res. Int.* **2016**, 1–12 (2016).
5. Zhou, G., Wang, Y. & Cui, L. Biomedical Sensor, Device and Measurement Systems. in *Advances in Bioengineering* (InTech, 2015). doi:10.5772/59941
6. Oluwaseun, A. C., Phazang, P. & Sarin, N. B. Biosensing Technologies for the Detection of Pathogens - A Prospective Way for Rapid Analysis. in *Biosensing Technologies for the Detection of Pathogens - A Prospective Way for Rapid Analysis* (InTech, 2018). doi:10.5772/intechopen.74668
7. Zourob, M. *Recognition Receptors in Biosensors. Recognition Receptors in Biosensors* (Springer New York, 2010). doi:10.1007/978-1-4419-0919-0
8. Asal, M., Özen, Ö., ahinler, M. & Polato lu, . Recent Developments in Enzyme, DNA and Immuno-Based Biosensors. *Sensors* **18**, 1924 (2018).
9. Köhler, G. & Milstein, C. Continuous cultures of fused cells secreting antibody of predefined specificity. *Nature* **256**, 495–497 (1975).
10. Welch, N. G., Scoble, J. A., Muir, B. W. & Pigram, P. J. Orientation and characterization of immobilized antibodies for improved immunoassays (Review). *Biointerphases* **12**, 02D301 (2017).
11. van der Veen, M., Stuart, M. C. & Norde, W. Spreading of proteins and its effect on adsorption and desorption kinetics. *Colloids Surfaces B Biointerfaces* **54**, 136–142 (2007).

12. Rabe, M., Verdes, D. & Seeger, S. Understanding protein adsorption phenomena at solid surfaces. *Adv. Colloid Interface Sci.* **162**, 87–106 (2011).
13. Sharma, S., Byrne, H. & Kennedy, R. J. O. Antibodies and antibody-derived analytical biosensors. *Essays Biochem.* 9–18 (2016). doi:10.1042/EBC20150002
14. Um, H. *et al.* Electrochemically oriented immobilization of antibody on poly-(2-cyano-ethylpyrrole)-coated gold electrode using a cyclic voltammetry. *Talanta* **84**, 330–334 (2011).
15. Barton, A. C. *et al.* Labelless AC impedimetric antibody-based sensors with pg mL^{-1} sensitivities for point-of-care biomedical applications. *Biosens. Bioelectron.* **24**, 1090–1095 (2009).
16. Ouerghi, O. *et al.* Impedimetric immunosensor using avidin – biotin for antibody immobilization. *Bioelectrochemistry* **56**, 131–133 (2002).
17. Lee, J. E. *et al.* A comparative study on antibody immobilization strategies onto solid surface. *Korean J. Chem. Eng.* **30**, 1934–1938 (2013).
18. Inkpen, M. S. *et al.* Non-chemisorbed gold–sulfur binding prevails in self-assembled monolayers. *Nat. Chem.* **11**, 351–358 (2019).
19. Sharafeldin, M., McCaffrey, K. & Rusling, J. F. Influence of antibody immobilization strategy on carbon electrode immunoarrays. *Analyst* **144**, 5108–5116 (2019).
20. Fowler, J. M., Stuart, M. C. & Wong, D. K. Y. Self-Assembled Layer of Thiolated Protein G as an Immunosensor Scaffold. *Anal. Chem.* **79**, 350–354 (2007).
21. Icoz, K., Soylu, M. C., Canikara, Z. & Unal, E. Quartz-crystal Microbalance Measurements of CD19 Antibody Immobilization on Gold Surface and Capturing B Lymphoblast Cells: Effect of Surface Functionalization. *Electroanalysis* **30**, 834–841 (2018).
22. Mandler, D. & Kraus-Ophir, S. Self-assembled monolayers (SAMs) for electrochemical sensing. *J. Solid State Electrochem.* **15**, 1535–1558 (2011).
23. Chaki, N. K. & Vijayamohanan, K. Self-assembled monolayers as a tunable platform for biosensor applications. *Biosens. Bioelectron.* **17**, 1–12 (2002).
24. Sun, X., Du, S., Wang, X., Zhao, W. & Li, Q. A Label-Free

- Electrochemical Immunosensor for Carbofuran Detection Based on a Sol-Gel Entrapped Antibody. *Sensors* 9520–9531 (2011). doi:10.3390/s111009520
25. Bereli, N., Ertürk, G., A. M. & Denizli, A. Oriented immobilized anti-hlgG via Fc fragment-imprinted PHEMA cryogel for IgG purification. *Biomed. Chromatogr.* **2012**, 599–607 (2013).
 26. Moschallski, M., Evers, A., Brandstetter, T. & Rühle, J. Sensitivity of microarray based immunoassays using surface-attached hydrogels. *Anal. Chim. Acta* **781**, 72–79 (2013).
 27. Yamazoe, H. Antibody immobilization technique using protein film for high stability and orientation control of the immobilized antibody. *Mater. Sci. Eng. C* **100**, 209–214 (2019).
 28. Vericat, C., Vela, M. E., Benitez, G., Carro, P. & Salvarezza, R. C. Self-assembled monolayers of thiols and dithiols on gold: New challenges for a well-known system. *Chem. Soc. Rev.* **39**, 1805–1834 (2010).
 29. Lee, C. Y., Canavan, H. E., Gamble, L. J. & Castner, D. G. Evidence of impurities in thiolated single-stranded DNA oligomers and their effect on DNA self-assembly on gold. *Langmuir* **21**, 5134–5141 (2005).
 30. Butterworth, A. *et al.* SAM composition and electrode roughness affect performance of a DNA biosensor for antibiotic resistance. *Biosensors* **9**, 1–12 (2019).
 31. Reimers, J. R., Ford, M. J., Marcuccio, S. M., Ulstrup, J. & Hush, N. S. Competition of van der Waals and chemical forces on gold–sulfur surfaces and nanoparticles. *Nat. Rev. Chem.* **1**, 0017 (2017).
 32. Häkkinen, H. The gold-sulfur interface at the nanoscale. *Nat. Chem.* **4**, 443–455 (2012).
 33. Pensa, E. *et al.* The chemistry of the sulfur-gold interface: In search of a unified model. *Acc. Chem. Res.* **45**, 1183–1192 (2012).
 34. Della Ventura, B., Schiavo, L., Altucci, C., Esposito, R. & Velotta, R. Light assisted antibody immobilization for bio-sensing. *Biomed. Opt. Express* **2**, 3223 (2011).
 35. Della Ventura, B. *et al.* Biosensor surface functionalization by a simple photochemical immobilization of antibodies: An

- Experimental characterization by Mass Spectrometry and Surface Enhanced Raman Spectroscopy. *Anal.* (2019). doi:10.1039/c9an00443b
36. Funari, R. *et al.* Single Molecule Characterization of UV-Activated Antibodies on Gold by Atomic Force Microscopy. *Langmuir* **32**, 8084–8091 (2016).
 37. Neves-Petersen, M. T. *et al.* High probability of disrupting a disulphide bridge mediated by an endogenous excited tryptophan residue. *Protein Sci.* **11**, 588–600 (2009).
 38. Della Ventura, B. *et al.* Biosensor surface functionalization by a simple photochemical immobilization of antibodies: experimental characterization by mass spectrometry and surface enhanced Raman spectroscopy. *Analyst* **144**, 6871–6880 (2019).
 39. Ellman, G. L. Tissue Sulfyd Groups. *Arch. Biochem. Biophys.* 70–77 (1959).
 40. Funari, R. *et al.* Detection of parathion and patulin by quartz-crystal microbalance functionalized by the photonics immobilization technique. *Biosens. Bioelectron.* **67**, 224–229 (2015).
 41. Funari, R. *et al.* Detection of parathion pesticide by quartz crystal microbalance functionalized with UV-activated antibodies. *Anal. Chem.* **85**, 6392–6397 (2013).
 42. Della Ventura, B., Saka , N., Funari, R. & Velotta, R. Flexible immunosensor for the detection of salivary -amylase in body fluids. *Talanta* **174**, 52–58 (2017).
 43. Funari, R. *et al.* Label-Free Detection of Gliadin in Food by Quartz Crystal Microbalance-Based Immunosensor. *J. Agric. Food Chem.* **65**, 1281–1289 (2017).
 44. Iarossi, M. *et al.* Colorimetric Immunosensor by Aggregation of Photochemically Functionalized Gold Nanoparticles. *ACS Omega* **3**, 3805–3812 (2018).
 45. Dzi bowska, K., Czaczyk, E. & Nidzworski, D. Application of Electrochemical Methods in Biosensing Technologies. in *Biosensing Technologies for the Detection of Pathogens - A Prospective Way for Rapid Analysis* (InTech, 2018). doi:10.5772/intechopen.72175
 46. Grieshaber, D., MacKenzie, R., Vörös, J. & Reimhult, E.

- Electrochemical Biosensors - Sensor Principles and Architectures. *Sensors* **8**, 1400–1458 (2008).
47. Montagut, Y. *et al.* QCM Technology in Biosensors. in *Biosensors - Emerging Materials and Applications* (InTech, 2011). doi:10.5772/17991
 48. Pohanka, M. Overview of Piezoelectric Biosensors, Immunosensors and DNA Sensors and Their Applications. *Materials (Basel)*. **11**, 448 (2018).
 49. Vashist, S. K. & Luong, J. H. T. Quartz Crystal Microbalance–Based Sensors. in *Handbook of Immunoassay Technologies* 333–357 (Elsevier, 2018). doi:10.1016/B978-0-12-811762-0.00013-X
 50. Ronkainen, N. J., Halsall, H. B. & Heineman, W. R. Electrochemical biosensors. *Chem. Soc. Rev.* **39**, 1747 (2010).
 51. Wang, J. *Analytical Electrochemistry*. (John Wiley & Sons, Inc., 2006). doi:10.1002/0471790303
 52. Arslan, F., Ustaba, S. & Arslan, H. An Amperometric Biosensor for Glucose Determination Prepared from Glucose Oxidase Immobilized in Polyaniline-Polyvinylsulfonate Film. *Sensors* **11**, 8152–8163 (2011).
 53. Hammond, J. L., Formisano, N., Estrela, P., Carrara, S. & Tkac, J. Electrochemical biosensors and nanobiosensors. *Essays Biochem.* **60**, 69–80 (2016).
 54. Dzyadevych, S. & Jaffrezic-Renault, N. Conductometric biosensors. in *Biological Identification* 153–193 (Elsevier, 2014). doi:10.1533/9780857099167.2.153
 55. Grunert, K. G. Food quality and safety: consumer perception and demand. *Eur. Rev. Agric. Econ.* **32**, 369–391 (2005).
 56. Wu, M. Y.-C. *et al.* Point-of-Care Detection Devices for Food Safety Monitoring: Proactive Disease Prevention. *Trends Biotechnol.* **35**, 288–300 (2017).
 57. World Health Organization. Drinking-Water. Available online: <https://www.who.int/news-room/fact-sheets/detail/drinking-water>.
 58. Kaittanis, C., Santra, S. & Perez, J. M. Emerging nanotechnology-based strategies for the identification of microbial pathogenesis. *Adv. Drug Deliv. Rev.* **62**, 408–423

- (2010).
59. Grimont, P. & Weill, F. X. Antigenic formulae of the *Salmonella* serovars. in *WHO Collab. Cent. Ref. Res. Salmonella* 1–167 (2007).
 60. Fabrega, A. & Vila, J. *Salmonella enterica* Serovar Typhimurium Skills To Succeed in the Host: Virulence and Regulation. *Clin. Microbiol. Rev.* **26**, 308–341 (2013).
 61. The European Union summary report on trends and sources of zoonoses, zoonotic agents and food-borne outbreaks in 2015. *EFSA J.* **14**, (2016).
 62. Mrema, N., Mpuchane, S. & Gashe, B. A. Prevalence of *Salmonella* in raw minced meat, raw fresh sausages and raw burger patties from retail outlets in Gaborone, Botswana. *Food Control* **17**, 207–212 (2006).
 63. Hanning, I. B., Nutt, J. D. & Ricke, S. C. Salmonellosis Outbreaks in the United States Due to Fresh Produce: Sources and Potential Intervention Measures. *Foodborne Pathog. Dis.* **6**, 635–648 (2009).
 64. Kaper, J. B., Nataro, J. P. & Mobley, H. L. T. Pathogenic *Escherichia coli*. *Nat. Rev. Microbiol.* **2**, 123–140 (2004).
 65. Odonkor, S. T. & Ampofo, J. K. *Escherichia coli* as an indicator of bacteriological quality of water: an overview. *Microbiol. Res. (Pavia)*. **4**, 2 (2013).
 66. Microbiology of the food chain - Horizontal method for the detection, enumeration and serotyping of *Salmonella*. Part 1: Detection of *Salmonella* spp. *International Organization for Standardization, Geneva* (2017).
 67. Velusamy, V., Arshak, K., Korostynska, O., Oliwa, K. & Adley, C. An overview of foodborne pathogen detection: In the perspective of biosensors. *Biotechnol. Adv.* **28**, 232–254 (2010).
 68. Evers, E. G. Predicted quantitative effect of logistic slaughter on microbial prevalence. *Prev. Vet. Med.* **65**, 31–46 (2004).
 69. Delibato, E. *et al.* Validation of a 1-Day Analytical Diagnostic Real-Time PCR for the Detection of *Salmonella* in Different Food Meat Categories. *Food Anal. Methods* **6**, 996–1003 (2013).
 70. Lee, K., Runyon, M., Herrman, T. J., Phillips, R. & Hsieh, J. Review of *Salmonella* detection and identification methods:

- Aspects of rapid emergency response and food safety. *Food Control* **47**, 264–276 (2015).
71. Eijkelkamp, J. M. & Aarts, H J M and van der Fels-Klerx, H. J. Suitability of Rapid Detection Methods for *Salmonella* in Poultry Slaughterhouses. **2**, 1–13 (2009).
 72. Bai, Y., Huang, W. C. & Yang, S. T. Enzyme-linked immunosorbent assay of *Escherichia coli* O157:H7 in surface enhanced poly(methyl methacrylate) microchannels. *Biotechnol. Bioeng.* **98**, 328–339 (2007).
 73. Shah, K. & Maghsoudlou, P. Enzyme-linked immunosorbent assay (ELISA): the basics. *Br. J. Hosp. Med.* **77**, C98–C101 (2016).
 74. Hill, W. E. & Wachsmuth, K. The polymerase chain reaction: Applications for the detection of foodborne pathogens. *Crit. Rev. Food Sci. Nutr.* **36**, 123–173 (1996).
 75. Holland, J. L., Louie, L., Simor, A. E. & Louie, M. PCR detection of *Escherichia coli* O157:H7 directly from stools: Evaluation of commercial extraction methods for purifying fecal DNA. *J. Clin. Microbiol.* **38**, 4108–4113 (2000).
 76. Guan, J. & Levin, R. E. Quantitative detection of *Escherichia coli* O157:H7 in ground beef by the polymerase chain reaction. *Food Microbiol.* **19**, 159–165 (2002).
 77. Deisingh, A. K. & Thompson, M. Detection of infectious and toxigenic bacteria. *Analyst* **127**, 567–581 (2002).
 78. Váradi, L. *et al.* Methods for the detection and identification of pathogenic bacteria: Past, present, and future. *Chem. Soc. Rev.* **46**, 4818–4832 (2017).
 79. Furst, A. L. & Francis, M. B. Impedance-Based Detection of Bacteria. *Chem. Rev.* **119**, 700–726 (2019).
 80. Mortari, A. & Lorenzelli, L. Recent sensing technologies for pathogen detection in milk: A review. *Biosens. Bioelectron.* **60**, 8–21 (2014).
 81. Nayak, M., Kotian, A., Marathe, S. & Chakravorty, D. Detection of microorganisms using biosensors-A smarter way towards detection techniques. *Biosens. Bioelectron.* **25**, 661–667 (2009).
 82. Thakur, M. S. & Ragavan, K. V. Biosensors in food processing. *J. Food Sci. Technol.* **50**, 625–641 (2013).

83. Walker, J. M. *Biosensors and Biodetection*. *Biosensors* **504**, (Humana Press, 2009).
84. Leonard, P. *et al.* Advances in biosensors for detection of pathogens in food and water. *Enzym. Microbiological Technol.* **32**, 3–13 (2003).
85. Ricci, F., Volpe, G., Micheli, L. & Palleschi, G. A review on novel developments and applications of immunosensors in food analysis. *Anal. Chim. Acta* **605**, 111–129 (2007).
86. Dudak, F. C. & Boyaci, I. H. Development of an immunosensor based on surface plasmon resonance for enumeration of *Escherichia coli* in water samples. *Food Res. Int.* **40**, 803–807 (2007).
87. Leahy, S. & Lai, Y. A cantilever biosensor based on a gap method for detecting *E. coli* in real time. *Sensors Actuators, B Chem.* **246**, 1011–1016 (2017).
88. Shu, J. & Tang, D. Current Advances in Quantum-Dots-Based Photoelectrochemical Immunoassays. *Chem. - An Asian J.* **12**, 2780–2789 (2017).
89. Guo, X., Lin, C. S., Chen, S. H., Ye, R. & Wu, V. C. H. A piezoelectric immunosensor for specific capture and enrichment of viable pathogens by quartz crystal microbalance sensor, followed by detection with antibody-functionalized gold nanoparticles. *Biosens. Bioelectron.* **38**, 177–183 (2012).
90. Wang, L. *et al.* QCM-based aptamer selection and detection of *Salmonella Typhimurium*. *Food Chem.* **221**, 776–782 (2017).
91. Fei, J., Dou, W. & Zhao, G. A sandwich electrochemical immunosensor for *Salmonella pullorum* and *Salmonella gallinarum* based on a screen-printed carbon electrode modified with an ionic liquid and electrodeposited gold nanoparticles. *Microchim. Acta* **182**, 2267–2275 (2015).
92. Xiang, C. *et al.* Sensitive electrochemical detection of *Salmonella* with chitosan–gold nanoparticles composite film. *Talanta* **140**, 122–127 (2015).
93. Xu, M., Wang, R. & Li, Y. Electrochemical biosensors for rapid detection of *Escherichia coli* O157:H7. *Talanta* **162**, 511–522 (2017).
94. Alexandre, D. L. *et al.* A Rapid and Specific Biosensor for

- Salmonella* Typhimurium Detection in Milk. *Food Bioprocess Technol.* **11**, 748–756 (2018).
95. Pérez-López, B. & Merkoçi, A. Nanomaterials based biosensors for food analysis applications. *Trends Food Sci. Technol.* **22**, 625–639 (2011).
 96. Hayat, A., Yang, C., Rhouati, A. & Marty, J. Recent Advances and Achievements in Nanomaterial-Based, and Structure Switchable Aptasensing Platforms for Ochratoxin A Detection. *Sensors* **13**, 15187–15208 (2013).
 97. Thanh Ngo, V. K. *et al.* Quartz crystal microbalance (QCM) as biosensor for the detecting of *Escherichia coli* O157:H7. *Adv. Nat. Sci. Nanosci. Nanotechnol.* **5**, 045004 (2014).
 98. Felix, F. S. & Angnes, L. Electrochemical immunosensors – A powerful tool for analytical applications. *Biosens. Bioelectron.* **102**, 470–478 (2018).
 99. Mollarasouli, F., Kurbanoglu, S. & Ozkan, S. A. The Role of Electrochemical Immunosensors in Clinical Analysis. 1–20 (2019). doi:10.3390/bios9030086
 100. Zhang, Z., Zhou, J. & Du, X. Electrochemical Biosensors for Detection of Foodborne Pathogens. *Micromachines* (2019).
 101. Vashist, S. K. & Vashist, P. Recent Advances in Quartz Crystal Microbalance-Based Sensors. *J. Sensors* **2011**, 1–13 (2011).
 102. Becker, B. & Cooper, M. A. A survey of the 2006-2009 quartz crystal microbalance biosensor literature. *J. Mol. Recognit.* **24**, 754–787 (2011).
 103. Sauerbrey, G. Verwendung von Schwingquarzen zur Wägung dünner Schichten und zur Mikrowägung. *Zeitschrift für Phys.* **155**, 206–222 (1959).
 104. Kanazawa, K. K. & Gordon, J. G. Frequency of a Quartz Microbalance in Contact with Liquid. *Anal. Chem.* **57**, 1770–1771 (1985).
 105. Shons, A., Dorman, F. & Najarian, J. An immunospecific microbalance. *J. Biomed. Mater. Res.* **6**, 565–570 (1972).
 106. Pathirana, S. . *et al.* Rapid and sensitive biosensor for *Salmonella*. *Biosens. Bioelectron.* **15**, 135–141 (2000).
 107. Su, X.-L. & Li, Y. A QCM immunosensor for *Salmonella* detection

- with simultaneous measurements of resonant frequency and motional resistance. *Biosens. Bioelectron.* **21**, 840–848 (2005).
108. Salam, F., Uludag, Y. & Tothill, I. E. Real-time and sensitive detection of *Salmonella* Typhimurium using an automated quartz crystal microbalance (QCM) instrument with nanoparticles amplification. *Talanta* **115**, 761–767 (2013).
 109. Ozalp, V. C., Bayramoglu, G., Erdem, Z. & Arica, M. Y. Pathogen detection in complex samples by quartz crystal microbalance sensor coupled to aptamer functionalized core-shell type magnetic separation. *Anal. Chim. Acta* **853**, 533–540 (2015).
 110. Muller-Loennies, S., Brade, L. & Brade, H. Neutralizing and cross-reactive antibodies against enterobacterial lipopolysaccharide. *Int. J. Med. Microbiol.* **297**, 321–340 (2007).
 111. Singh, S. P., Upshaw, Y., Abdullah, T., Singh, S. R. & Klebba, P. E. Structural relatedness of enteric bacterial porins assessed with monoclonal antibodies to *Salmonella* Typhimurium OmpD and OmpC. *J. Bacteriol.* **174**, 1965–1973 (1992).
 112. Keasey, S. L. *et al.* Extensive Antibody Cross-reactivity among Infectious Gram-negative Bacteria Revealed by Proteome Microarray Analysis. *Mol. Cell. Proteomics* **8**, 924–935 (2009).
 113. Rolfe, M. D. *et al.* Lag phase is a distinct growth phase that prepares bacteria for exponential growth and involves transient metal accumulation. *J. Bacteriol.* **194**, 686–701 (2012).
 114. Stern, O. Zur Theorie der Elektrolytischen Doppelschicht. *Zeitschrift fur Elektrochemie* **30**, 508–516 (1924).
 115. Dai, H., Jiang, B. & Wei, X. Impedance Characterization and Modeling of Lithium-Ion Batteries Considering the Internal Temperature Gradient. *Energies* **11**, 220 (2018).
 116. Encinas-Sánchez, V., de Miguel, M. T., Lasanta, M. I., García-Martín, G. & Pérez, F. J. Electrochemical impedance spectroscopy (EIS): An efficient technique for monitoring corrosion processes in molten salt environments in CSP applications. *Sol. Energy Mater. Sol. Cells* **191**, 157–163 (2019).
 117. Maalouf, R. *et al.* Label-free detection of bacteria by electrochemical impedance spectroscopy: Comparison to surface plasmon resonance. *Anal. Chem.* **79**, 4879–4886 (2007).
 118. Daniels, J. S. & Pourmand, N. Label-Free Impedance

- Biosensors: Opportunities and Challenges. *Electroanalysis* **19**, 1239–1257 (2007).
119. Lisdat, F. & Schäfer, D. The use of electrochemical impedance spectroscopy for biosensing. *Anal. Bioanal. Chem.* **391**, 1555–1567 (2008).
 120. Dorledo de Faria, R. A., Dias Heneine, L. G., Matencio, T. & Messaddeq, Y. Faradaic and non-faradaic electrochemical impedance spectroscopy as transduction techniques for sensing applications. *Int. J. Biosens. Bioelectron.* **5**, 29–31 (2019).
 121. Figueroa-Miranda, G. *et al.* Aptamer-based electrochemical biosensor for highly sensitive and selective malaria detection with adjustable dynamic response range and reusability. *Sensors Actuators, B Chem.* **255**, 235–243 (2018).
 122. Barreiros dos Santos, M. *et al.* Highly sensitive detection of pathogen *Escherichia coli* O157: H7 by electrochemical impedance spectroscopy. *Biosens. Bioelectron.* **45**, 174–180 (2013).
 123. Malvano, F., Pilloton, R. & Albanese, D. Sensitive detection of *Escherichia coli* O157:H7 in food products by impedimetric immunosensors. *Sensors* **18**, 1–11 (2018).
 124. Lin, D., Pillai, R. G., Lee, W. E. & Jemere, A. B. An impedimetric biosensor for *E. coli* O157:H7 based on the use of self-assembled gold nanoparticles and protein G. *Microchim. Acta* **186**, 1–9 (2019).
 125. Li, Z., Fu, Y., Fang, W. & Li, Y. Electrochemical impedance immunosensor based on self-assembled monolayers for rapid detection of *Escherichia coli* O157:H7 with signal amplification using lectin. *Sensors (Switzerland)* **15**, 19212–19224 (2015).
 126. Chowdhury, A. D., De, A., Chaudhuri, C. R., Bandyopadhyay, K. & Sen, P. Label free polyaniline based impedimetric biosensor for detection of *E. coli* O157:H7 Bacteria. *Sensors Actuators, B Chem.* **171–172**, 916–923 (2012).
 127. Wan, J. *et al.* Signal-off impedimetric immunosensor for the detection of *Escherichia coli* O157:H7. *Sci. Rep.* **6**, 2–7 (2016).
 128. Zhao, Y.-W., Wang, H.-X., Jia, G.-C. & Li, Z. Application of Aptamer-Based Biosensor for Rapid Detection of Pathogenic *Escherichia coli*. *Sensors* **18**, 2518 (2018).

129. Brosel-Oliu, S. *et al.* Novel impedimetric aptasensor for label-free detection of *Escherichia coli* O157:H7. *Sensors Actuators, B Chem.* **255**, 2988–2995 (2018).
130. Taleat, Z., Khoshroo, A. & Mazloun-Ardakani, M. Screen-printed electrodes for biosensing: a review (2008–2013). *Microchim. Acta* **181**, 865–891 (2014).
131. Gaglione, R. *et al.* Novel human bioactive peptides identified in Apolipoprotein B: Evaluation of their therapeutic potential. *Biochem. Pharmacol.* **130**, 34–50 (2017).

APPENDIX

A1. INTERNATIONAL VISITING EXPERIENCE

Supervisor: Dr Dirk Mayer

Institute: Forschungszentrum Juelich GmbH

Institute of Complex Systems– Bioelectronics (ICS-8)

Wilhelm-Johnen Straße, 52428, Juelich, Germany

from 9th November 2017 to 20th December 2018

A2. LIST OF PUBLICATIONS

A. Fulgione, M. Cimafronte, B. Della Ventura, M. Iannaccone, C. Ambrosino, F. Capuano, Y.T.R. Proroga, R. Velotta, R. Capparelli

QCM-based immunosensor for rapid detection of Salmonella in Typhimurium in food

Scientific Reports **2018**, 8:16137; doi:10.1038/s41598-018-34285-y

M. Cimafronte, A. Fulgione, R. Gaglione, M. Pappaianni, R. Capparelli, A. Arciello, S. Bolletti Censi, G. Borriello, R. Velotta, B. Della Ventura
Screen Printed Based Impedimetric Immunosensor for Rapid Detection of Escherichia coli in Drinking Water

Sensors **2020**, 20, 274; doi:10.3390/s20010274

A3. ORAL PRESENTATION

M. Cimafronte, A. Fulgione, B. Della Ventura, A. Arciello, R. Capparelli, R. Velotta

Electrochemical impedance based immunosensor for rapid detection of Escherichia coli

17th International Conference on Electroanalysis (ESEAC 2018), Rhodes, 3-7 June 2018

A4. POSTER PRESENTATIONS

M. Cimafronte, B. Della Ventura, A. Fulgione, R. Gaglione, A. Arciello, R. Capparelli, R. Velotta

Impedimetric immunosensor based on screen printed gold electrode for rapid Escherichia coli detection

MATRAFURED 2019, International Meeting on Chemical Sensor, Visegrad, 16-21 June 2019

M. Cimafonte, A. Fulgione, B. Della Ventura, A. Arciello, R. Gaglione, R. Capparelli, R. Velotta, D. Mayer

Development of an electrochemical impedance immunosensor for *Escherichia coli* detection

11th International Workshop on Impedance Spectroscopy (IWIS 2018), Chemnitz, 25-28 September 2018

SCIENTIFIC REPORTS



OPEN

QCM-based immunosensor for rapid detection of *Salmonella* Typhimurium in food

Andrea Fulgione^{1,2}, Martina Cimafonte³, Bartolomeo Della Ventura³, Marco Iannaccone¹, Concetta Ambrosino², Federico Capuano⁴, Yolande Thérèse Rose Proroga⁴, Raffaele Velotta³ ³ & Rosanna Capparelli¹

Salmonella Typhimurium is one of the main causes of outbreaks and sporadic cases of human gastroenteritis. At present, the rapid detection of this pathogen is a major goal of biosensing technology applied to food safety. In fact, ISO standardized culture method takes up to ten days to provide a reliable response. In this paper, we describe a relatively simple protocol for detecting *Salmonella* Typhimurium in chicken meat based on a Quartz-Crystal Microbalance (QCM), which leads to a limit of detection (LOD) less than of 10⁶ CFU/mL and requires a pre-enrichment step lasting only 2 h at 37 °C. The reliability of the proposed immunosensor has been demonstrated through the validation of the experimental results with ISO standardized culture method. The cost-effectiveness of the procedure and the rapidity of the QCM-based biosensor in providing the qualitative response make the analytical method described here suitable for applications in food inspection laboratory and throughout the chain production of food industry.

Salmonella species are facultative anaerobic Gram-negative bacteria¹. Worldwide, they are foodborne pathogens and second only to *Campylobacter* spp. for causing gastrointestinal human infections². In the EU member states 6.2 million cases of human salmonellosis occur each year³. In particular, *Salmonella* Typhimurium (*S.* Typhimurium) represents one of the main pathogens responsible for provoked human gastroenteritis⁴, which is caused mainly by the consumption of raw or uncooked eggs, poultry meat vegetables, fruits and foodstuff of animal origin^{5–8}. Infection symptoms such as fever, nausea, vomiting, diarrhea, dehydration, weakness, and loss of appetite usually appear 12–72 h after ingestion of contaminated products. Several studies focused on the control of *Salmonella* contaminations by the use of new natural antimicrobial molecules for controlling bacteria contaminations^{9,10}, but the crucial step represented by the rapid detection of pathogen in the food still remains.

The official food safety agencies - such as US Food and Drug Administration (FDA) and International Organization of Standardization (ISO)¹¹ - recommend the conventional culture method as the reference test for food analyses. The ISO method includes pre-enrichment steps followed by selective enrichment, isolation on selective agars, biochemical characterization of probable colonies, and their final serological confirmation. Inevitably, the positive time response with this procedure, ranges from five to about ten days. This method is very sensitive and cheap; however, it is labor-intensive, time-consuming and unsuitable for testing a large number of samples. While waiting for test results without shipping the foodstuffs could have a strong negative impact on the business profitably, the alternative of missing possible positive result for pathogenic contamination, obviously, implicates costly recalls of goods, human suffering and loss of reputation¹².

In this context, the development of rapid, cost-effective, and automated methods for the identification and, eventually, quantification of bacteria such as *S.* Typhimurium is urgent. These methods, - integrated with preventive strategies such as Hazard Analysis Critical Control Points (HACCP) - could significantly improve the safety of the food chain, from raw to processed foods¹³. Such an issue has been addressed by adopting a number of strategies¹⁴, but the goal is far from being accomplished since the current regulation for food analysis requires that

¹Department of Agriculture, University of Naples "Federico II", Portici (Naples), 80055, Italy. ²Department of Science and Technology, University of Sannio, Benevento, 82100, Italy. ³Department of Physics "Ettore Pancini", University of Naples "Federico II", Naples, 80126, Italy. ⁴Department of Food Inspection, Istituto Zooprofilattico Sperimentale del Mezzogiorno, Portici (Naples), 80055, Italy. Andrea Fulgione and Martina Cimafonte contributed equally. Correspondence and requests for materials should be addressed to B.D.V. (email: dellaventura@fisica.unina.it) or R.C. (email: capparel@unina.it)

alternative methods, should have sensitivity and specificity of at least 99%, be rapid and not requiring specialized personnel to carry out the analysis¹⁵. These techniques can be grouped as immunology-based assays (ELISA), nucleic acid-based (PCR) assays, and biosensors. The first two groups have specificity and sensitivity almost comparable to the conventional methods^{14,16}, but cannot be considered easy-to-use techniques. Moreover, they share with other tests for *Salmonella* spp. some drawbacks such as the need for a long pre-enrichment step to recover stressed cells, possible cross-reactions with related antigens, sensitivity and antigen modification depending on the sample matrix, and high cost for automation and industrial application. Furthermore, the result provided by these methods is easily influenced by intrinsic characteristics of the food such as background microbiota, sample matrix and inhibitory substances (heavy metals, proteins, fats, carbohydrates, antibiotics and organic compounds)¹⁷. In addition, though PCR is very sensitive, thereby allowing shorter enrichment times, it is prone to detect also dead bacteria.

In contrast to complex and lengthy methods, biosensors offer accurate and rapid detection method for pathogens in foodstuffs so to be applicable on a wider scale as, for instance, in selecting the correct direction for finished products: sale at retail market or industrial treatments to eliminate *Salmonella* bacteria¹⁵. Currently, considerable attention is given to rapid and sensitive biosensor devices based on surface plasmon resonance (SPR)^{18–20} and photoelectrochemical immunoassay (PEC)^{21–24}. Together with enzyme controlled colorimetric sensor²⁵, all these devices are able to detect very low concentrations of different molecules and proteins with an acceptable specificity and reproducibility, but it is worth to highlight that these classes of sensors still requires specialized personnel in view of the complexity of the surface functionalization procedure²⁶. Electrochemical-based biosensors exploit the biological recognition of compounds like enzymes, antibodies, DNA and aptamers. This class of biosensors can reach wide linear ranges (10^{-10} – 10^5 CFU/mL) and good LOD (5 CFU/mL), although their application to food samples is limited by cross-reactivity^{27,28}. Rapid detection is also provided by QCM-based immunosensors that can be considered user-friendly, but they currently lack the required sensitivity unless ballasting procedures by antibodies or even by functionalized nanoparticles are carried out^{29–33}. The application of such a procedure to bacteria has led to LODs of 10^2 CFU/mL using ballasting procedure or QCM-based aptasensor and 10^1 CFU/mL with gold nanoparticles^{34,35}.

Here, we describe a simple, reliable, fast, sensitive and specific QCM-based immunosensor, which is able to detect concentration less than 10^0 CFU/mL of *S. Typhimurium* in chicken meat after 2 hours of pre-enrichment step at 37 °C, in compliance with ISO standardized culture method. The method we propose exploits an effective surface functionalization (PIT, photochemical immobilization technique) that is able to tether upright antibodies on gold surfaces, thereby enhancing the sensitivity of the device. We also show that the presence of food constituents does not prevent bacteria from being recognized by antibodies making our approach extendable to further applications.

Results

QCM detection of *S. Typhimurium*. QCM provides a frequency change proportional to the mass deposited on the surface^{36,37} and, a typical sensorgram is shown in Fig. 1a. The spikes in the plot are due to the syringe draws and do not affect the measurement of the frequency shift. The sensorgram refers to a chicken sample – initially contaminated with 10^9 CFU/mL of *S. Typhimurium* – after 2 h of pre-enrichment step at 37 °C, a time leading to approximately 10^2 multiplication factor by assuming a replication time of 20 min³⁸. The initial concentration was checked in three independent experiments by spotting 10 μ L of the samples analysed by QCM at different dilutions. One of these cases is shown in Fig. 1b where the top left section (dilution 1:10) contains three spots each containing 5 CFU/10 μ L. After the stabilization of the resonance frequency by PBS 1X solution (step 1 in Fig. 1a), the surface was functionalized (step 2) by conveying to the QCM, a solution containing UV activated anti-*Salmonella* polyclonal antibodies (anti-*Salmonella* pAbs; 50 μ g/mL), which brings about a frequency drop of about 130 Hz. The subsequent washing step with PBS 1X (step 3) was carried out to remove possible anti-*Salmonella* pAbs not tethered onto gold surface, whereas blocking with BSA (step 4) was carried out to prevent non-specific signal from the uncovered gold surface. The lack of significant frequency change during the last step demonstrates that the whole electrode was covered with anti-*Salmonella* p-Abs. Eventually, step 5 and 6 correspond to the sample injection after 2 hours of pre-enrichment (10^0 CFU/mL initial concentration) and the final washing, respectively.

In order to evaluate the performance of the QCM sensor, we measured the dose-response curve that is reported in Fig. 2, in which the values on *x*-axis refer to the initial *Salmonella* concentration selected for the contamination of chicken sample. The samples were analysed after 1 and 2 hours of pre-enrichment, but with 1 h pre-enrichment step, the immunosensor was able to detect *Salmonella* only in the range 10^2 – 10^5 CFU/mL (data not shown), whereas 2 hours pre-enrichment allowed us to decrease the lower limit down to 10^0 CFU/mL (see Fig. 2).

With the longer pre-enrichment it was possible to observe a frequency shift induced by the step (5) of the protocol for all the samples infected, whereas no significant frequency shift could be detected with uncontaminated chicken sample (negative control). The subsequent washing (step 6) did not lead to any frequency change; thus, the lack of detachment from the surface underscores once again the stability of the interaction between bacteria and UV photoactivated anti-*Salmonella* pAbs and, hence, demonstrates the effectiveness of PIT as a gold surface functionalization procedure. Each point of the dose-response curve (Fig. 2) represents the mean triplicates of measurements carried out in several days, in different environmental conditions, and using different electrodes. The curve displays a linearity range of three decades from 10^0 to 10^3 CFU/mL before reaching a saturation profile at the highest concentrations, whereas the frequency shift measured for the negative sample was 7.5 ± 4.0 Hz and is may well be due to non-specific interaction of the food constituents with the biosensor surface. Such a value for the blank does not prevent us from estimating a very low limit of detection of our biosensing procedure. In fact, the concentration that provides a signal corresponding to 3 SD of the background noise

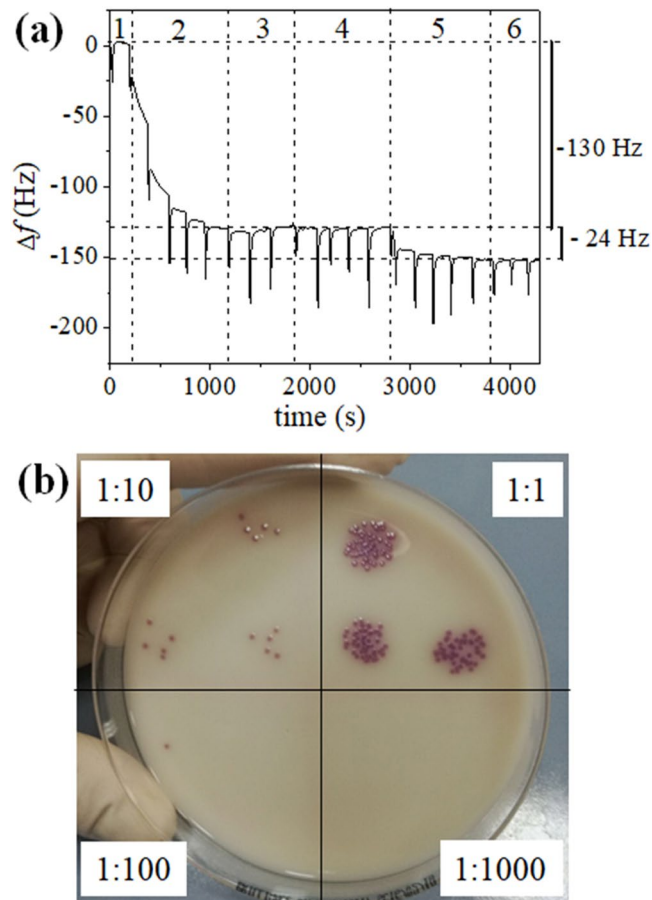


Figure 1. QCM sensorgram and microbiological detection of *S. Typhimurium*. Food sample contaminated with *Salmonella Typhimurium* (10^0 CFU/mL). (a) QCM sensorgram after pre-enrichment step (2 h at 37°C); (b) Spot dilutions of the sample before the pre-enrichment step on *Salmonella Chromogenic Agar Base* after overnight incubation. Each section shows the dilution factor.

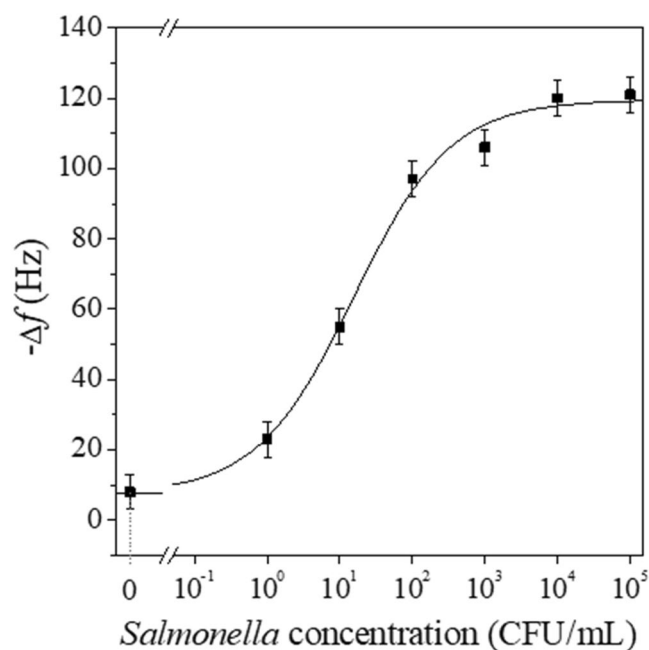


Figure 2. Dose-response curves of the QCM-based biosensor referred to samples of chicken meat contaminated with different concentrations of *Salmonella Typhimurium*. The curve is the best fits of the experimental values obtained by a logistic function.

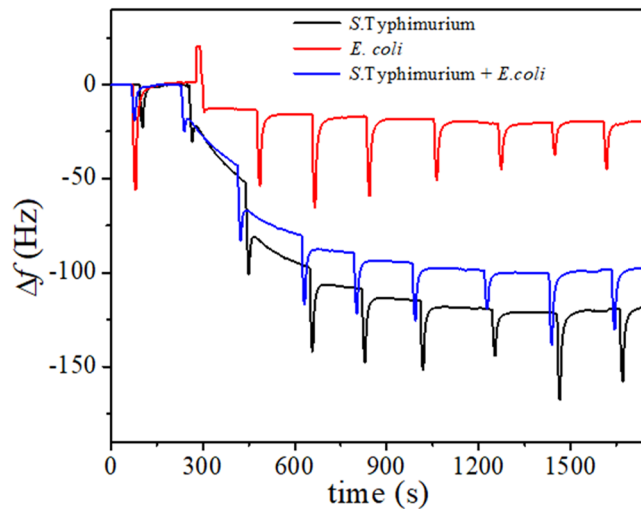


Figure 3. QCM biosensor specificity. Sensorgrams of *Salmonella* Typhimurium (black curve), *Escherichia coli* (red curve) and both bacteria (blue curve) contaminated chicken meat samples, after the pre-enrichment step (2 h at 37 °C). Each bacterial concentration was at 10^4 CFU/mL before the pre-enrichment step.

($7.5 \text{ Hz} + 3 \times 4.0 \text{ Hz} \approx 20 \text{ Hz}$) is lower than 10^0 CFU/mL (Fig. 2), a concentration that can be safely considered the LOD of the proposed biosensor.

Specificity test. The specificity tests have been carried by considering the possible cross-interference provided by *Escherichia coli* (*E. coli*), which is among the most spread bacteria in food. Figure 3 shows the sensorgrams measured when chicken meat samples were contaminated by *S. Typhimurium*, *E. coli* and a mixture of them. In all the cases, the initial concentration of each bacteria was 10^4 CFU/mL and the pre-enrichment step lasted 2 hours at 37 °C. It was observed a significant frequency variation only when *Salmonella* bacteria were present (Fig. 3; black or blue lines), whereas no significant variation was observed when the sample was contaminated with only *E. coli* (Fig. 3; red line). In particular, the frequency detected in the case of *Salmonella* chicken meat sample (115 Hz; black line) was comparable to that reported on dose response curve. Instead, the drop frequency evaluated in samples infected with both *S. Typhimurium* and *E. coli* was lower respect to that of only *Salmonella* infected sample (95 Hz (blue line) vs 115 Hz (black line)). This last result can be ascribed to the competition - between the two bacteria during the enrichment step, when both are present in food matrix. The initial bacterial concentration selected for the test were also supported by microbial count carried out on the same sample and highlight once again the high specificity of the anti-*Salmonella* pAbs produced against *Salmonella* respect to *E. coli* even when they are photoactivated, demonstrating, by this way, the effectiveness of the proposed QCM sensor in detecting *Salmonella* in a real food matrix as chicken meat.

Discussion and Conclusion

In summary, we put forward an easy-to-use method for detecting *S. Typhimurium* in a real food matrix (chicken meat) based on a QCM functionalized with anti-*Salmonella* polyclonal antibodies UV activated by PIT. This last technique represents a very important and innovative approach to improve biosensor sensitivity. Usually, Abs bind to a surface preferentially with Fab, assuming a bended conformation and exposing Fc region. This happened also in the case of no treated Abs on gold surface, thus limiting the interaction of the same Abs with the antigens. On the contrary, a recent study evidenced that, when Abs are irradiated prior their interaction with a surface - like gold -, they assumed a preferential orientation with one Fab domain protruding and the other two portions of the Ab interacting with surface³⁹.

The QCM measurement procedure does not require specialised personnel, and it is rapid, low-cost, and suitable for out-of-lab use. The single analysis requires minimal sample treatment: pre-enrichment (2 h) at 37 °C, preparation steps (two centrifugations) and injection into the cell by five syringe draws, so that the whole measurement can be carried out in less than 4 hours. Although not suitable for accurate quantitative analysis, the QCM sensor proposed here lends itself as a very attractive device for “on-off” qualitative analysis of food contaminated. The LOD of proposed biosensor (less than 10^0 CFU/mL of *S. Typhimurium* in chicken sample) and the minimum sample pre-enrichment step (2 h at 37 °C) required, make the biosensor suitable for food inspection when extremely low contamination levels need to be detected in chicken samples and, “rapidly” in test response “for all foodstuffs” respect to other diagnostic biosensors which, firstly, require a pre-enrichment step ranging from 6 up to 58 hours¹⁵.

The specificity of the whole system is more than satisfactory since no significant signal is detected when the *Salmonella* is replaced by *E. coli* while a signal is distinguished when both bacteria are present. The application of this biosensor to detect other foodborne pathogens represents a new alternative method to monitor the food safety throughout the chain production so warranting the final quality of the products. Furthermore, this biosensor satisfies some of the technical parameters such as detection limit, time of analysis, validation of the method,

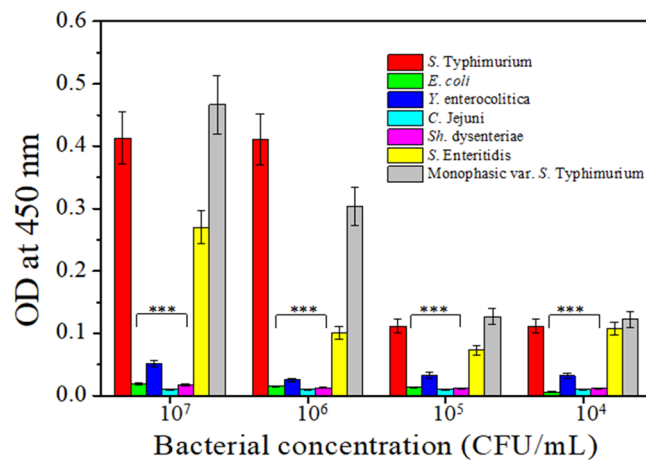


Figure 4. Anti-*Salmonella* pAbs specificity against different foodborne pathogens. Cross-reactivity between anti-*Salmonella* pAbs and selected foodborne pathogens: *Escherichia coli*, *Yersinia enterocolitica*, *Campylobacter jejuni*, *Shigella dysenteriae*, *Salmonella Enteritidis*, *Salmonella* Typhimurium and the monophasic variant of *Salmonella* Typhimurium. Results are presented as mean value \pm S.D and are representative of three independent experiments, each performed in triplicate. ***p value < 0.001.

sensitivity and specificity, and additional parameters like equipment, operation, and costs which should be considered before adapting a new rapid detection method^{15,40,41}.

Methods

Bacteria. *Salmonella enterica* subsp. *enterica* serovar Typhimurium ATCC 13311 (*S. Typhimurium*) and *E. coli* ATCC 25922 were used to carry out the chicken meat samples infection.

Antibodies production and purification. Antibodies were produced in Fischer 344 rats (Harlan, Italy). Each animal received two intraperitoneal injections—at two weeks interval—of heat killed *S. Typhimurium* bacteria at 10⁷ CFU/mL in 0,9% NaCl (300 μ L), emulsified with an equal volume of incomplete Freund's adjuvant (Sigma-Aldrich, Italy). After 1 week from the last injection, animals were sacrificed, and peripheral blood was collected. Serum was separated by centrifugation at 5000 rpm for 5 min. IgG purification was carried out by using NAb™ Protein G Spin Kit (Thermo Fisher Scientific, USA). Anti-*Salmonella* pAbs level was determined by NanoDrop 2000 spectrophotometer (Thermo Fisher Scientific, USA). All procedures were approved by Italian Minister of Health (authorization n° 891/2015-PR) and were performed in accordance with relevant guidelines and regulations.

Salmonella antibodies titer and immunoadsorption. In order to evaluate the cross-reactivity of anti-*Salmonella* pAbs against major foodborne pathogens, the antibodies titer was measured by ELISA. Briefly, 100 μ L of *S. Typhimurium* (10⁵ CFU/mL) in pure PBS were seeded in a 96-well plate. After incubation overnight at room temperature, wells were washed 3 times with 0.05% Tween 20 (Sigma-Aldrich, Italy) (v/v) in pure PBS; quenched with 100 μ L of 1% Bovine Serum Albumin (BSA; Sigma-Aldrich, Italy) (v/v) in pure PBS and incubated at room temperature for 1 h. Then, 100 μ L of anti-*Salmonella* pAbs at different dilutions (1:20; 1:50; 1:60; 1:80; 1:100; 1:150) were added to the wells and the plate was incubated at room temperature for 3 h using a constant shaking (100 rpm). Subsequently the wells were rinsed 3 times with 0.05% Tween 20 (v/v) in pure PBS and incubated 1 h at room temperature with 100 μ L of Goat Anti-Rat HRP (Abcam, UK) diluted 1:5000. Then, wells were washed 3 times with 0.05% Tween 20 (v/v) in pure PBS and was added 3,3',5,5'-Tetramethylbenzidine (TMB; 50 μ L; Sigma-Aldrich, Italy). The plate was incubated again, in the dark, at room temperature for 20 min. The reaction was stopped by the addition of 0.16 M H₂SO₄ (100 μ L) to all wells and the titer was determined through the measurement of the optical absorbance at 450 nm (Biorad microplate reader model 680, USA).

Subsequently, an immunoadsorption protocol was carried out to avoid any possible cross-reaction of anti-*Salmonella* pAbs with *E. coli* bacteria. Briefly, in 1.5 mL eppendorf tube, quenched with 2% skimmed milk powder (Sigma-Aldrich, Italy), 50 μ L of pure PBS containing *E. coli* at the concentration of 10⁸ CFU/mL were mixed with 1 mL of anti-*Salmonella* pAbs diluted 1:50. The eppendorf was incubated at room temperature overnight, under constant shaking (100 rpm) and later centrifuged at 13400 rpm for 5 min. The supernatant, containing the antibodies which have not interacted with *E. coli*, was collected and the anti-*Salmonella* pAbs level was determined by NanoDrop 2000 spectrophotometer (Thermo Fisher Scientific, USA)^{42–44}. The same titer above mentioned was also adopted to evaluate the cross-reactivity of anti-*Salmonella* pAbs with other foodborne pathogens such as *Yersinia enterocolitica*, *Campylobacter jejuni*, *Shigella dysenteriae*, *Escherichia coli*, *Salmonella enteritidis*, and the monophasic variant of *S. Typhimurium* (serotype 1,4,[5],12:i:-). The results (Fig. 4) evidence the high reactivity of anti-*Salmonella* pAbs against three different *Salmonella* strains compared to non-*Salmonella* strains ($p < 0.001$). Rather than a drawback, the significant reactivity with other *Salmonella* strains is a strength feature of our pAbs since both the monophasic variant of *S. Typhimurium* and *S. Enteritidis* are hazardous for

human health, so that possible positive response of the biosensor coming from the presence of these two strains would be beneficial for food analysis in practical use.

QCM immunosensor and measurement. The quartz oscillators (AT10-14-6-UP-01) were from Novaetech S.r.l. (Naples, Italy). They were AT-CUT quartz with a fundamental frequency of 10 MHz. The crystal and gold electrode diameters are 1.37 cm and 0.68 cm, respectively. The gold surfaces were cleaned by immersing the oscillators for 1 min in a glass beaker containing Piranha solution (3:1 ratio between concentrated sulfuric acid and 40% hydrogen peroxide solution); then, the quartzes were washed with milli-Q water. The whole cleaning procedure, strong enough to remove any organic residue from the gold surface, was performed in the hood and can be repeated 3–4 times before the quartz is exhausted and has to be changed. The piranha treatment requires new functionalization, a step which is cheap and quick when carried out by PIT. The gold-quartz wafer was placed on the electronic console and the resonance frequency of the oscillator was monitored by producer-released software. The QCM was integrated into a microfluidic circuit consisting of the cell which contains the oscillator, Tygon tubes, and a syringe. The volume of the circuit was about 200 μ L and the syringe was used to suck a similar volume repeatedly. The syringe draws conveyed fresh solution to the cell and were separated each other by a time interval of 3 min that showed to be long enough to reach a temporary frequency stabilization. No further frequency change was observed after 5 syringe draws so that 1 mL was the volume to be changed for reaching the equilibrium (frequency stabilization); since it was changed by sucking 200 μ L every 3 min the whole step took 15 min to be completed.

Device functionalization with UV activated antibodies. The gold electrode of quartz crystal was functionalized with the above anti-*Salmonella* pAbs, UV activated by Photochemical Immobilization Technique (PIT). This is a quick reproducible technique which allows the immobilization of antibodies onto gold surfaces - in an upright orientation with their binding sites exposed to the environment³⁹ - thanks to the UV activation of the triad cysteine-cysteine/tryptophan⁴⁵ (typical structural characteristic of the antibodies)⁴⁶. Briefly, the UV photon is absorbed by the tryptophan and this phenom generates solvated electrons, which are captured by electrophilic molecules such as cysteine, causing the cleavage of the disulphide bridge. The free thiol (SH) groups - generated by this last reaction - can easily interact with thiol reactive surfaces like gold electrodes through covalent bond. The increasing number of the free SH groups allows a new structural conformation of the immobilized immunoglobulin which are characterized by a good exposure of the antigen binding sites, thus significantly improving sensor sensitivity³⁹.

In this experiment the PIT was carried out by irradiating a solution of 50 μ g/mL anti-*Salmonella* pAbs for 1 min by a HERAEUS amalgam type NNI 40/20 lamp emitting at 254 nm with a power average of 40 W. The lamp was approximately 20 cm long and had a diameter of 1 cm, so the effective irradiation intensity for the antibodies activation was about 0.7 W/cm². It is worth mentioning that PIT does not affect the ability of antibodies to capture the antigen, as reported by Funari *et al.*⁴⁷.

Detection of *Salmonella* in chicken meat samples. Chicken meat samples were purchased from a local supermarket and tested to confirm *Salmonella* absence, according to ISO 6579-1: 2017. Later, a test portion (25 g) was contaminated or not with *S. Typhimurium* at different concentrations ranging from 10⁰ CFU/mL to 10⁵ CFU/mL and were placed in sterile stomacher bag containing 225 mL of buffered peptone water (BPW; A.E.S. Laboratoire Groupe, France). Samples bag were then placed into a stomacher device for 90 sec. and incubated for 1 or 2 hours at 37 °C (pre-enrichment step). After the incubation, 15 mL of each sample were collected and centrifuged at 2000 rpm for 15 min to remove part of food debris. 1 mL of supernatant, containing bacterial cells, was centrifuged at 13400 rpm for 5 min at room temperature. The bacterial pellet was suspended in pure PBS and used for QCM analysis.

The measurements have been carried out by following the steps listed below (see Fig. 1a).

- (1) Stabilization with PBS 1X solution to stabilize the frequency of the device;
- (2) Functionalization with anti-*Salmonella* pAbs (50 μ g/mL), previously UV photoactivated, to functionalize the gold surface;
- (3) Washing with PBS 1X to remove the antibodies no tethered on gold surface, so checking for the efficiency of the functionalization;
- (4) Blocking with BSA (50 μ g/mL) to hold non-specific sites and avoiding free spaces onto gold surface;
- (5) Sample analysis of chicken meat infected or not with *S. Typhimurium* or *E. coli* or both, for testing the biosensor response;
- (6) Washing with PBS 1X to remove all the elements which have no interacted with the antibodies or with gold surface.

Each of the steps entailed the change of 1 mL volume and was carried out in 15 min.

At each chicken sample flowed into circuit corresponds a variation of the resonance frequency and this correlation has been explained by Sauerbrey equation³⁷. This equation states that the decrease in frequency is linearly proportional to the increase in surface mass loading of QCM. Data collected were fitted to obtain a dose-response curve.

Before the pre-enrichment step, the samples contaminated or not were diluted and then spotted on *Salmonella* Chromogenic Agar Base (CM1007, Oxoid, Thermo Fisher, UK) or Tryptone Bile X-Gluc (TBX Agar, CM0945, Oxoid, Thermo Fisher, UK) for *S. Typhimurium* or *E. coli* isolation, respectively. The plates were then incubated at 37 °C (*S. Typhimurium*) or 44 °C (*E. coli*) for 24 h. This procedure allowed us to validate the presence and the concentration of the bacteria in food samples.

Method specificity. In order to evaluate the method specificity, the chicken meat samples were infected with *E. coli* (10^4 CFU/mL) alone or in combination with *S. Typhimurium* (both bacteria at 10^4 CFU/mL). All the sample infected were pre-enriched for 2 hours at 37 °C and later, analysed at QCM immunosensor.

Statistics. Specificity of anti-*Salmonella* pAbs was assessed using ANOVA Test (GraphPad Software, La Jolla, CA, USA) and only differences with p-value < 0.05 were considered significant.

References

- Grimont, P. & Weill, F.-X. Antigenic Formulae of the Salmonella Servovars. *WHO Collab. Cent. Ref. Res. Salmonella*, 1–167 (2008).
- Food, E. & Authority, S. The European Union Summary Report on Trends and Sources of Zoonoses, Zoonotic Agents and Foodborne Outbreaks in 2015. *EFSA J.* **14** (12) (2016).
- Havelaar, A. H. *et al.* Disease Burden of Foodborne Pathogens in the Netherlands, 2009. *Int. J. Food Microbiol.* **156**(3), 231–238 (2012).
- Jurado-Tarifa, E. *et al.* Genetic Diversity and Antimicrobial Resistance of Campylobacter and Salmonella Strains Isolated from Decoys and Raptors. *Comp. Immunol. Microbiol. Infect. Dis.* **48**, 14–21 (2016).
- Hanning, I. B., Nutt, J. D. & Ricke, S. C. Salmonellosis Outbreaks in the United States due to Fresh Produce: Sources and Potential Intervention Measures. *Foodborne Pathog. Dis.* **6**(6), 635–648 (2009).
- Sivapalasingam, S., Friedman, C. R., Cohen, L. & Tauxe, R. V. Fresh Produce: A Growing Cause of Outbreaks of Foodborne Illness in the United States, 1973 through 1997. *J. Food Prot.* **67**(10), 2342–2353 (2004).
- Mrema, N., Mpuchane, S. & Gashe, B. A. Prevalence of Salmonella in Raw Minced Meat, Raw Fresh Sausages and Raw Burger Patties from Retail Outlets in Gaborone, Botswana. *Food Control* **17**(3), 207–212 (2006).
- Crum-Cianflone, N. F. Salmonellosis and the Gastrointestinal Tract: More than Just Peanut Butter. *Curr. Gastroenterol. Rep.* **10**(4), 424–431 (2008).
- Rai, M., Pandit, R., Gaikwad, S. & Kövics, G. Antimicrobial Peptides as Natural Bio-Preservative to Enhance the Shelf-Life of Food. *J. Food Sci. Technol.* **53**(9), 3381–3394 (2016).
- Capparelli, R. *et al.* New Perspectives for Natural Antimicrobial Peptides: Application as Anti-inflammatory Drugs in a Murine Model. *BMC Immunol.* **13** (2012).
- ISO. ISO 11290-1:1996 Microbiology of Food and Animal Feeding Stuffs - Horizontal Method for the Detection and Enumeration of Listeria Monocytogenes - Part 1: Detection Method. *International Organization for Standardization, Geneva.*, p 16 (1996).
- Evers, E. G. Predicted Quantitative Effect of Logistic Slaughter on Microbial Prevalence. *Prev. Vet. Med.* **65**(1–2), 31–46 (2004).
- Delibato, E. *et al.* Validation of a 1-Day Analytical Diagnostic Real-Time PCR for the Detection of Salmonella in Different Food Meat Categories. *Food Anal. Methods* **6**(4), 996–1003 (2013).
- Lee, K. M., Runyon, M., Herrman, T. J., Phillips, R. & Hsieh, J. Review of Salmonella Detection and Identification Methods: Aspects of Rapid Emergency Response and Food Safety. *Food Control.*, pp 264–276 (2015).
- Eijkkamp, J. M., Aarts, H. J. M. & Van Der Fels-Klerx, H. J. Suitability of Rapid Detection Methods for Salmonella in Poultry Slaughterhouses. *Food Anal. Methods* **2**(1), 1–13 (2009).
- López-Campos, G., Martínez-Suárez, J. V., Aguado-Urda, M. & López-Alonso, V. Microarray Detection and Characterization of Bacterial Foodborne Pathogens. *Food, Heal. Nutr.* 13–33 (2012).
- Mortari, A. & Lorenzelli, L. Recent Sensing Technologies for Pathogen Detection in Milk: A Review. *Biosensors and Bioelectronics.*, pp 8–21 (2014).
- Leonard, P. *et al.* Advances in Biosensors for Detection of Pathogens in Food and Water. *Enzyme and Microbial Technology.*, pp 3–13 (2003).
- Park, M.-K. & Oh, J.-H. Rapid Detection of *E. Coli* O157:H7 on Turnip Greens Using a Modified Gold Biosensor Combined with Light Microscopic Imaging System. *J. Food Sci.* **77**(2), M127–34 (2012).
- Ricci, F., Volpe, G., Micheli, L. & Pallechi, G. A Review on Novel Developments and Applications of Immunosensors in Food Analysis. *Analytica Chimica Acta.*, pp 111–129 (2007).
- Shu, J. & Tang, D. Current Advances in Quantum-Dots-Based Photoelectrochemical Immunoassays. *Chemistry - An Asian Journal.* pp 2780–2789 (2017).
- Zhang, K., Lv, S., Lin, Z. & Tang, D. Cds:Mn Quantum Dot-Functionalized G-C3N4nanohybrids as Signal-Generation Tags for Photoelectrochemical Immunoassay of Prostate Specific Antigen Coupling DNAzyme Concatamer with Enzymatic Biocatalytic Precipitation. *Biosens. Bioelectron.* **95**, 34–40 (2017).
- Zhang, K., Lv, S., Lin, Z., Li, M. & Tang, D. Bio-Bar-Code-Based Photoelectrochemical Immunoassay for Sensitive Detection of Prostate-Specific Antigen Using Rolling Circle Amplification and Enzymatic Biocatalytic Precipitation. *Biosens. Bioelectron.* **101**, 159–166 (2018).
- Lin, Y., Zhou, Q., Tang, D., Niessner, R. & Knopp, D. Signal-On Photoelectrochemical Immunoassay for Aflatoxin B 1 Based on Enzymatic Product-Etching MnO₂ Nanosheets for Dissociation of Carbon Dots. *Anal. Chem.* **89**(10), 5637–5645 (2017).
- Lai, W., Wei, Q., Xu, M., Zhuang, J. & Tang, D. Enzyme-Controlled Dissolution of MnO₂nanoflakes with Enzyme Cascade Amplification for Colorimetric Immunoassay. *Biosens. Bioelectron.* **89**, 645–651 (2017).
- Mazumdar, S. D., Barlen, B., Kämpfer, P. & Keusgen, M. Surface Plasmon Resonance (SPR) as a Rapid Tool for Serotyping of Salmonella. *Biosens. Bioelectron.* **25**(5), 967–971 (2010).
- Xiang, C. *et al.* Sensitive Electrochemical Detection of Salmonella with Chitosan-Gold Nanoparticles Composite Film. *Talanta* **140**, 122–127 (2015).
- Fei, J., Dou, W. & Zhao, G. A Sandwich Electrochemical Immunosensor for Salmonella Pullorum and Salmonella Gallinarum Based on a Screen-Printed Carbon Electrode Modified with an Ionic Liquid and Electrodeposited Gold Nanoparticles. *Microchim. Acta* **182**(13–14), 2267–2275 (2015).
- Funari, R. *et al.* Detection of Parathion and Patulin by Quartz-Crystal Microbalance Functionalized by the Photonics Immobilization Technique. *Biosens. Bioelectron.* **67** (2015).
- Della Ventura, B. *et al.* Effective Antibodies Immobilization and Functionalized Nanoparticles in a Quartz-Crystal Microbalance-Based Immunosensor for the Detection of Parathion. *PLoS One* **12**(2), e0171754 (2017).
- Waijijit, U. *et al.* Biosensor for Salmonella Typhimurium Detection. In *2012 IEEE International Conference on Electron Devices and Solid State Circuit, EDSSC 2012* (2012).
- Su, X. L. & Li, Y. A. QCM Immunosensor for Salmonella Detection with Simultaneous Measurements of Resonant Frequency and Motional Resistance. *Biosens. Bioelectron.* **21**(6), 840–848 (2005).
- Kim, G., Moon, J. H., Moh, C. Y. & Lim, J. g. A Microfluidic Nano-Biosensor for the Detection of Pathogenic Salmonella. *Biosens. Bioelectron.* **67**, 243–247 (2015).
- Salam, F., Uludag, Y. & Tothill, I. E. Real-Time and Sensitive Detection of Salmonella Typhimurium Using an Automated Quartz Crystal Microbalance (QCM) Instrument with Nanoparticles Amplification. *Talanta* **115**, 761–767 (2013).
- Wang, L. *et al.* QCM-Based Aptamer Selection and Detection of Salmonella Typhimurium. *Food Chem.* **221**, 776–782 (2017).
- Kanazawa, K. K. & Gordon, J. G. Frequency of a Quartz Microbalance in Contact with Liquid. *Anal. Chem.* **57**(8), 1770–1771 (1985).

37. Sauerbrey, G. V. von Schwingquarzen Zur Wägung Dünner Schichten Und Zur Mikrowägung. *Zeitschrift für Phys.* **155**(2), 206–222 (1959).
38. Rolfe, M. D. *et al.* Lag Phase Is a Distinct Growth Phase That Prepares Bacteria for Exponential Growth and Involves Transient Metal Accumulation. *J. Bacteriol.* **194**(3), 686–701 (2012).
39. Funari, R. *et al.* Single Molecule Characterization of UV-Activated Antibodies on Gold by Atomic Force Microscopy. *Langmuir* **32**(32), 8084–8091 (2016).
40. de Boer, E. & Beumer, R. R. Methodology for Detection and Typing of Foodborne Microorganisms. *Int. J. Food Microbiol.* **50**(1–2), 119–130 (1999).
41. Ivnitski, D., Abdel-Hamid, I., Atanasov, P., Wilkins, E. & Stricker, S. Application of Electrochemical Biosensors for Detection of Food Pathogenic Bacteria. *Electroanalysis* **12**(5), 317–325 (2000).
42. Müller-Loennies, S., Brade, L. & Brade, H. Neutralizing and Cross-Reactive Antibodies against Enterobacterial Lipopolysaccharide. *International Journal of Medical Microbiology*. pp 321–340 (2007).
43. Singh, S. P., Upshaw, Y., Abdullah, T., Singh, S. R. & Klebba, P. E. Structural Relatedness of Enteric Bacterial Porins Assessed with Monoclonal Antibodies to Salmonella Typhimurium OmpD and OmpC. *J. Bacteriol.* **174**(6), 1965–1973 (1992).
44. Keasey, S. L. *et al.* Extensive Antibody Cross-Reactivity among Infectious Gram-Negative Bacteria Revealed by Proteome Microarray Analysis. *Mol. Cell. Proteomics* **8**(5), 924–935 (2009).
45. Neves-Petersen, M. T. *et al.* High Probability of Disrupting a Disulphide Bridge Mediated by an Endogenous Excited Tryptophan Residue. *Protein Sci.* **11**(3), 588–600 (2002).
46. Joerger, T. R., Du, C. & Linthicum, D. S. Conservation of Cys-Cys Trp Structural Triads and Their Geometry in the Protein Domains of Immunoglobulin Superfamily Members. *Mol. Immunol.* **36**(6), 373–386 (1999).
47. Funari, R. *et al.* Detection of Parathion Pesticide by Quartz Crystal Microbalance Functionalized with UV-Activated Antibodies. *Anal. Chem.* **85**(13), 6392–6397 (2013).

Acknowledgements

All the authors wish to thank Vincenzo Morelli, Lucia Mauro, Maria Chiara Albanese and Rugiada Salvio for technical assistance and prof. D. Iannelli for very fruitful discussion about the manuscript. A. Fulgione acknowledges the financial support of the project “Sensor Regione Campania (grant n. 23)”. B.B. Della Ventura and R. Velotta acknowledge the contribution of “Fondazione con il Sud” (project Nr. 2011-PDR-18, “Biosensori piezoelettrici a risposta in tempo reale per applicazioni ambientali e agro-alimentari”). Martina Cimafonte acknowledges the financial support of the Programma Operativo Nazionale (PON) Ricerca e Innovazione 2014–2020 “Dottorati innovativi con caratterizzazione industriale”.

Author Contributions

R.V., R.C. conceived the experiments. A.F., M.C., B.D.V., M.I. performed the experiments. R.V., R.C., A.F., B.D.V., M.I. analyzed the results. F.C., Y.T.R.P., C.A. contributed reagents/materials. R.V., R.C., A.F., B.D.V. wrote the paper. All authors reviewed the manuscript.

Additional Information

Competing Interests: The authors declare no competing interests.

Publisher’s note: Springer Nature remains neutral with regard to jurisdictional claims in published maps and institutional affiliations.







Open Access This article is licensed under a Creative Commons Attribution 4.0 International License, which permits use, sharing, adaptation, distribution and reproduction in any medium or format, as long as you give appropriate credit to the original author(s) and the source, provide a link to the Creative Commons license, and indicate if changes were made. The images or other third party material in this article are included in the article’s Creative Commons license, unless indicated otherwise in a credit line to the material. If material is not included in the article’s Creative Commons license and your intended use is not permitted by statutory regulation or exceeds the permitted use, you will need to obtain permission directly from the copyright holder. To view a copy of this license, visit <http://creativecommons.org/licenses/by/4.0/>.

© The Author(s) 2018

Article

Screen Printed Based Impedimetric Immunosensor for Rapid Detection of *Escherichia coli* in Drinking Water

Martina Cimafronte ¹, Andrea Fulgione ^{2,3} , Rosa Gaglione ⁴, Marina Papaiani ³ ,
Rosanna Capparelli ³, Angela Arciello ⁴, Sergio Bolletti Censi ⁵, Giorgia Borriello ² ,
Raffaele Velotta ¹  and Bartolomeo Della Ventura ^{6,*}

¹ Department of Physics “Ettore Pancini”, University of Naples “Federico II”, Via Cinthia, 26, 80126 Naples, Italy; martina.cimafronte@unina.it (M.C.); rvelotta@unina.it (R.V.)

² Istituto Zooprofilattico Sperimentale del Mezzogiorno, Via Salute, 2, 80055 Portici Naples, Italy; andrea.fulgione@unina.it (A.F.); giorgia.borriello@cert.izsmportici.it (G.B.)

³ Department of Agriculture, University of Naples “Federico II”, Via Università, 133, 80055 Portici Naples, Italy; marina.papaiani@unina.it (M.P.); capparel@unina.it (R.C.)

⁴ Department of Chemical Sciences, University of Naples “Federico II”, Via Cinthia, 26, 80126 Naples, Italy; rosa.gaglione@unina.it (R.G.); angela.arciello@unina.it (A.A.)

⁵ Cosvitech Società Consortile a Responsabilità Limitata, 80142 Naples, Italy; sergiobolletti@cosvitech.eu

⁶ Department of Physics, Politecnico di Milano, Piazza Leonardo da Vinci, 32, 20133 Milano, Italy

* Correspondence: dellaventura@fisica.unina.it

Received: 29 November 2019; Accepted: 30 December 2019; Published: 3 January 2020



Abstract: The development of a simple and low cost electrochemical impedance immunosensor based on screen printed gold electrode for rapid detection of *Escherichia coli* in water is reported. The immunosensor is fabricated by immobilizing anti-*E. coli* antibodies onto a gold surface in a covalent way by the photochemical immobilization technique, a simple procedure able to bind antibodies upright onto gold surfaces. Impedance spectra are recorded in 0.01 M phosphate buffer solution (PBS) containing 10 mM $\text{Fe}(\text{CN})_6^{3-}/\text{Fe}(\text{CN})_6^{4-}$ as redox probe. The Nyquist plots can be modelled with a modified Randles circuit, identifying the charge transfer resistance R_{ct} as the relevant parameter after the immobilization of antibodies, the blocking with BSA and the binding of *E. coli*. The introduction of a standard amplification procedure leads to a significant enhancement of the impedance increase, which allows one to measure *E. coli* in drinking water with a limit of detection of 3×10^1 CFU mL⁻¹ while preserving the rapidity of the method that requires only 1 h to provide a “yes/no” response. Additionally, by applying the Langmuir adsorption model, we are able to describe the change of R_{ct} in terms of the “effective” electrode, which is modified by the detection of the analyte whose microscopic conducting properties can be quantified.

Keywords: *Escherichia coli*; immunosensor; electrochemical impedance spectroscopy; antibodies; photochemical immobilization technique; cyclic voltammetry

1. Introduction

Water is a natural resource, essential for the life sustainment and significant for health in both developing and developed countries worldwide. In the recent years, the inappropriate handling of urban, industrial and agricultural wastewater has affected the quality of the drinking water which turns out to be alarmingly contaminated and chemically polluted [1]. Contaminated water causes a serious impact on the population as it induces a large number of diseases caused by microorganisms [2]. According to the World Health Organization (WHO), water-related diseases are a worldwide problem

and each year 3.4 million people, mostly children below the age five, suffer from waterborne diseases and die [3]. Pathogenic bacteria in water are mainly responsible for human infection diseases and one of the most common bacteria associated with the sanitary risk of water is the species *Escherichia coli*.

Escherichia coli is a gram-negative bacterium of the genus *Escherichia* identified for the first time in 1885 by the German paediatrician and bacteriologist Theodor Escherich. *E. coli* is a rod-shaped gut bacterium, natural inhabitant in the intestinal tracts of humans and warm-blooded animals. It is considered one of the most dangerous pathogens because some strains can cause serious illness, including severe diarrhoea, urinary tracts infections, inflammations and peritonitis. As a consequence, the presence of *E. coli* in drinking water is considered as a possible indicator of the microbiological water quality deterioration and the presence of *E. coli* in processed food products can indicate faecal contamination [1]. In fact, according to WHO and the European Union [4] no *E. coli* should be detected in 100 mL of water. Such a limit can only be reached by time-consuming measurements carried out in equipped laboratories; therefore, nowadays one of the challenges in food industry and environmental monitoring is the development of methods for the rapid detection of low levels of *E. coli*

Conventional methods for the detection of *E. coli* include multiple-tube fermentation, membrane filter and plate counting. Although, these culture-based methods are accurate, reliable and have low detection limits, they are typically labor-intensive and time-consuming since they require 2–3 days to yield initial results and up to 7–10 for the confirmation [5]. Other detection methods, such as ELISA [6] and PCR [7,8] are less time consuming but they require expensive equipment and initial sample pre-treatment which make the application of these methods limited only to the laboratory environment [9–11]. Thus, the research for new strategies that could be promising alternatives to the conventional techniques to be used in industrial applications is very timely.

Detection techniques based on biosensors are widely recognized as powerful tools for the detection of bacteria due to their several advantages such as fast response, robustness, low cost, sensitivity, specificity and real time detection [12]. Among them, biosensors based on antibody-antigen interaction (the so-called immunosensors) are broadly investigated, and, in fact, immunosensors using electrochemical [13], surface plasmon resonance (SPR) [14], piezoelectric [15] and cantilever [16] based transducers have been applied for *E. coli* detection. Electrochemical biosensors are considered powerful instruments overcoming the limitations of the conventional methods due to their multiple advantages such as low cost, high sensitivity, fast response, robustness and simple operation [17–19]. Among different electrochemical techniques, electrochemical impedance spectroscopy (EIS) is very commonly used to investigate the recognition events at electrode/electrolyte interface [11,20] and EIS based biosensors are particularly attractive since they allow antigen detection with high sensitivity. In the last decade, different impedimetric immunosensors for the detection of *E. coli* have already been developed [21–24].

The immobilization of antibodies (Abs) is a crucial step in the realization of an immunosensor because its analytical performance strongly depends both on the orientation of the antibodies and their density on the surface. Thus, it would highly desirable to rely on a surface functionalization procedure that would overcome such an issue [25,26]. Generally, antibodies can be immobilized via physical or chemical adsorption involving electrostatic or ionic bonds, hydrophobic interactions and van der Waals forces [27,28], via covalent attachment [29–32], by using the biotin–avidin approach [33,34] or immobilizing intermediate binding proteins, such as protein A or G [35–38] and through entrapment into a polymer matrix [39–42]. These approaches, particularly protein A and G method, are time-consuming, but even more important, require a surface modification or pre-treatment for an effective protein A/G binding [43] that can affect the robustness and reproducibility of the protocol.

Among all the possible strategies, self-assembled monolayers (SAMs) is currently one of the most widespread methods for electrode functionalization aiming at detecting *E. coli* by electrochemical approaches. For instance, an oriented anti-*E. coli* immobilization on gold electrode surfaces could be achieved by exploiting SAMs of thiolated carboxylic acid [44–46] or by immobilizing anti-*E. coli* on electrochemically deposited cysteamine layers [45]. The use of thiolated scaffolds such as protein

G [45,47] and cross-linkers as glutaraldehyde [48], the latter allowing the immobilization of anti-*E. coli* onto electrochemically synthesized polyaniline substrate, have also been reported with promising results for the immobilization of anti-*E. coli*.

Thus, SAMs are broadly used as linkers for the immobilization of antibodies onto gold electrode surfaces, but in spite of the many advantages they offer in many applications, there are several issues that should be considered in order to find out and control their physical and chemistry properties [49–51]. SAMs on gold surfaces are usually represented as perfect monolayers, with molecules in a closed packed configuration. Nevertheless, this concept is far from reality and the control of the quality of SAMs is a key point in many applications. The realization of a well-assembled monolayer strongly relies on the purity of the solutions used and the presence of even a low amount of contaminants, as for instance thiolated precursor molecules that are the typical impurities in thiol compounds, can lead to a non-uniform and, hence, non-ideal monolayer [52]. In addition, the electrode surface plays an important role in the realization of SAMs. EIS analysis of electrode surfaces with different roughness showed that the rougher substrate exhibited small and variable response as a result of a non-ideal SAM formation, while the smoother surface produces higher and more reproducible response due to the increase of the SAM homogeneity [53]. Moreover, over the years several studies have worked to clarify the true nature of the interaction gold-thiols SAMs [36,54–56]. Considering these issues, it is worth developing alternative methods to covalent bind antibodies on gold electrode surfaces in an easier, more rapid and reliable way.

In this paper, we propose a simple and low-cost EIS immunosensor based on screen printed gold electrodes (AuSPEs) for the detection of *Escherichia coli*. The anti-*E. coli* antibodies were immobilized on the gold electrode surface using the Photochemical Immobilization Technique (PIT) a simple procedure able to steer antibodies in a convenient orientation of the Fab region once immobilized onto gold surface [57,58]. In this work, PIT has been used for the first time in the functionalization of commercial gold electrodes in order to develop an “on-off” electrochemical immunosensor based on impedance spectroscopy (EIS) using $\text{Fe}(\text{CN})_6^{3-}/\text{Fe}(\text{CN})_6^{4-}$ as redox probe. The effectiveness of our approach is demonstrated by detecting *E. coli* ATCC 25922 in drinking water. Our immunosensor exhibits a limit of detection (LOD) of 3×10^1 CFU mL⁻¹, with no need for pre-concentration and pre-enrichment steps. The selectivity against other bacteria was evaluated and the immunosensor was applied to the analysis of inoculated drinking water samples.

2. Materials and Methods

2.1. Chemicals and Materials

Gold screen printed electrodes (AuSPEs) were purchased from BVT Technologies (Strážek, Czech Republic). They include a gold disk-shaped ($d = 1$ mm) working electrode, a silver/silver chloride electrode and a gold counter electrode, all of them printed on a corundum ceramic base (0.7 cm × 2.5 cm). All potential values were referred to the silver/silver chloride reference electrode. Phosphate buffer solution (PBS) was prepared by dissolving PBS tablets (from GoldBio, St Louis, MO, USA) in Milli-Q water (each tablet prepares 100 mL of a 0.01 M PBS solution). Anti-*E. coli* polyclonal antibody (5.5 mg mL⁻¹) was obtained from Thermo Fisher Scientific (Rockford, IL, USA) and anti-*E. coli* solutions (25 µg mL⁻¹) were prepared in a 0.01 M PBS solution (pH 7.4). Bovine serum albumin (BSA), potassium hexacyanoferrate (II) trihydrate ($\text{K}_4\text{Fe}(\text{CN})_6 \cdot 3\text{H}_2\text{O}$), potassium hexacyanoferrate (III) ($\text{K}_3\text{Fe}(\text{CN})_6$) and sulphuric acid (H_2SO_4 98%) were purchased from Sigma-Aldrich (Milano, Italy). The microfluidic setup involves a fluidic cell, silicon tubes and a continuous pump (HNP Mikrosysteme GmbH, Schwerin, Germany). The total volume of the circuit is about 100 µL, the cell volume is about 10 µL and the flow rate is 6 µL s⁻¹.

2.2. Apparatus

Electrochemical impedance spectroscopy (EIS) and cyclic voltammetry (CV) measurements were carried out with a potentiostat/galvanostat and impedance analyzer PALMSENS (Utrecht, The Netherlands) model PalmSens3 controlled by a computer through the PSTRACE version 5 software. Cyclic voltammetry (CV) and electrochemical impedance spectroscopy (EIS) were conducted in the presence of $\text{Fe}(\text{CN})_6^{3-}/\text{Fe}(\text{CN})_6^{4-}$ (1:1, 10 mM) as redox probe in 0.01 M PBS solution (pH = 7.4). In CVs, potential was cycled from -0.6 V to 0.6 V with a scan rate of 0.15 V s^{-1} in 10 mM $\text{Fe}(\text{CN})_6^{3-}/\text{Fe}(\text{CN})_6^{4-}$. EIS measurements were performed at the frequency range from 5 Hz to 10000 Hz at the formal potential of 0.16 V and using an amplitude perturbation of 10 mV. The impedance data were shown in the Nyquist plot and the EIS spectrum Analyzer software, supplied with the instrument, was used to fit EIS data to the electrical equivalent circuit in order to obtain the fit-component parameters values.

A fluidic setup including a Plexiglas cell, silicon tubes and a continuous pump was used for the flowing of the different solutions (Abs, BSA and *E. coli*). A schematic representation of the cell is shown in Figure 1a. The main feature of the cell is its small volume that facilitate the interaction of the particles in the solutions (Abs, BSA, *E. coli*, etc.) with the electrode. Any solution was conveyed by a continuous pump at a flow rate of 6 $\mu\text{L s}^{-1}$. Although effective for the interaction, such a cell was unsuitable for electrochemical measurements in view of the small amount of electrolytes involved. Thus, after each interaction (i.e., each steps shown in Scheme 1), we took the electrode out of the cell and dipped it into a 1.5 mL beaker containing $\text{Fe}(\text{CN})_6^{3-}/\text{Fe}(\text{CN})_6^{4-}$ (Figure 1b), in which the electrochemical measurements were carried out at room temperature.

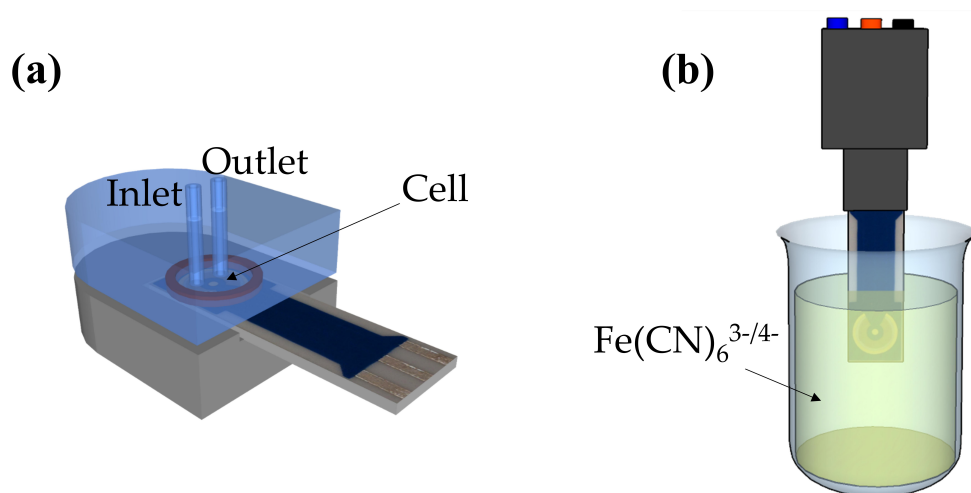


Figure 1. (a) Sketch of the fluidic cell used for an effective interaction of the solutions (Abs, BSA and *E. coli*) with the electrode and (b) scheme used for the electrochemical measurements: the AuSPE was dipped in a beaker containing 1.5 mL of $\text{Fe}(\text{CN})_6^{3-/4-}$ and it was connected to the potentiostat through a holder (in grey) for the impedance/current measurements.

2.3. Preparation of the Biological Sample

Bacterial strain *E. coli* ATCC 25922 was grown in Muller Hinton Broth (MHB, Becton Dickinson Difco, Franklin Lakes, NJ, USA) and on Tryptic Soy Agar (TSA; Oxoid Ltd., Hampshire, UK). In all the experiments, bacteria were inoculated and grown overnight in MHB at 37 °C. The next day, bacteria were centrifuged and solubilized in drinking water at the desired cell densities (10^1 – 10^6 CFU mL^{-1}). By colony counting assays, it was verified that bacterial growth was negligible in PBS 1X with respect to MHB through a time interval of 3 hrs at room temperature, whereas bacterial death was not observed. Clinical isolated bacteria *Salmonella enteritidis* 706 RIVM [59] and *Acinetobacter baumannii* (ATCC 17978) were grown in the same way and diluted drinking water in order to verify the specificity of the immunosensor towards *E. coli* in comparison with non-target bacteria.

2.4. UV Activation of Antibody Solution

The gold SPE was functionalized with anti-*E. coli* antibodies, previously activated by the Photochemical Immobilization Technique (PIT) [57,58]. PIT is a functionalization method able to tether antibodies (Abs) upright on metal (gold or silver) surfaces with their binding sites well exposed to the environment [60], based upon the selective photochemical reduction of disulphide bridges in immunoglobulins (IgGs) produced by UV activation of near aromatic amino acid [61]. Briefly, a selective photoreduction of disulphide bridges produced by the UV activation of the trp/cys-cys triad occurs. This triad is a typical structural feature of IgGs and basically, the UV photon energy is adsorbed by tryptophan and transferred to near electrophilic species like the close cys-cys. The result is the cleavage of the disulphide bridges and the formation of new thiol (SH) groups able to bind, through a covalent bond, thiol reactive surfaces like gold ones (Figure 2b). Every IgGs have twelve triads but, it has recently been demonstrated [57] that only two of them are involved in this process. These triads are located in the constant variable region and allow the attack of the antibody to the surface with one of the two Fab regions exposed to the solution (Figure 2c) [57]. Considering that the triad of residues trp/cys-cys can be found in every IgGs, the PIT is applicable in a wide range of fields. PIT is accomplished by activating 300 μL of antibody samples ($25 \mu\text{g mL}^{-1}$) in a quartz cuvette by two low pressure mercury lamp (LP Hg lamp) emitting at 254 nm and manufactured by Procom Alta Tecnologia s.r.l. (Dicomano, FI, Italy) (Figure 2a). The two lamps (1.5 cm of diameter) are horseshoe-shaped and mounted in a stacked configuration so that its internal empty space fits with a (quartz) cuvette whose dimensions are $1 \text{ cm} \times 1 \text{ cm} \times 4 \text{ cm}$. The power of each lamp is 6 W and by considering that the cuvette containing the anti-*E. coli* IgG solution is close to the lamps, the effective irradiation intensity used for the antibody activation is about 0.3 W/cm^2 . The samples are irradiated for 30 s. This time is the result of an optimized protocol that, as confirmed by the Ellman's assay [62], produces an high concentration of activated Abs while guaranteeing no denaturation of antibodies as evidenced by their efficiency in antigen binding in the developed biosensors.

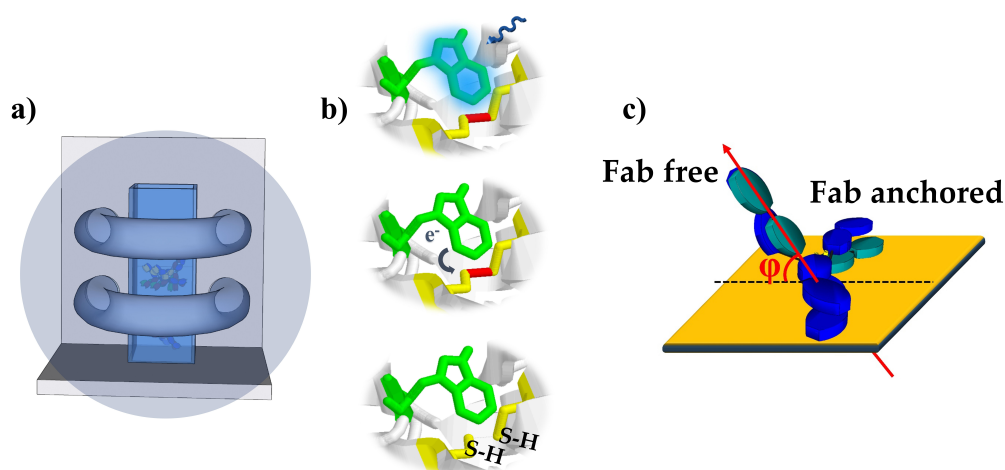


Figure 2. (a) UV lamp used for the UV activation of the antibodies. Emitting wavelength: 254 nm, diameter of each lamp: 1.5 cm, dimensions internal: space $1 \text{ cm} \times 1 \text{ cm} \times 4 \text{ cm}$, power of each lamp 6 W, irradiation intensity 0.3 W/cm^2 ; (b) Description of the reaction involved in PIT: the UV photon energy is adsorbed by tryptophan and transferred to near cys-cys. The result is the cleavage of the disulphide bridges and the formation of new thiol (SH) groups; (c) Antibody is immobilized onto the surface so that the angle ϕ is 45° on average thereby providing one Fab free and well-exposed to the environment.

After the activation, the Abs solution was conveyed to the electrode surface by means of a fluidic circuit. In previous works, this method has been used in a number of experiments to develop sensitive and selective QCM-based immunosensors [63–67] as well as colorimetric biosensors [68].

2.5. Immunosensor Development and *E. coli* Detection

Before the functionalization, the AuSPE was electrochemically cleaned by applying 10 cycles between -0.4 V and 1.4 V at a scan rate of 0.1 V s^{-1} in 0.1 M H_2SO_4 . The electrode was rinsed with a copious amount of Milli-Q water and it was ready to use. The cleaned SPE was placed in the fluidic cell and the experimental procedure for impedance measurements consists in the flowing of different solutions onto the sensitive gold surface of the AuSPE. First, a solution of UV-activated anti-*E. coli* antibodies (25 μg mL^{-1}) was conveyed onto the gold sensitive surface for 15 min by applying a constant flow rate (6 μL s^{-1}). Since the Ab activation only lasts approximately five minutes [57], to saturate the gold electrode surface, such a step was repeated 4 times with a fresh irradiated Abs solution. Subsequently, the electrode was rinsed for 1 h with 0.01 M PBS buffer to remove the unbound antibodies. After that, a BSA solution (50 μg mL^{-1}) flowed into the cell for 15 min filling the remaining free space on the gold surface. This blocking step is crucial because, by filling the free remaining spaces on the gold electrode surface, the possible non-specific interactions of the following molecules are avoided. A 1 mL aliquot of drinking water incubated with different concentration of *E. coli* cells (from 10^1 to 10^8 CFU mL^{-1}) flowed into the circuit for 30 min at room temperature and the bacteria cells were captured by the immobilized antibodies. The electrode was rinsed with 0.01 M phosphate buffer to remove non-specifically and weakly bound bacteria for 5 min. Each detection was repeated three times. The difference in impedance measured before and after *E. coli* incubation, normalized with the impedance value obtained after Abs immobilization, was taken as the signal produced by the binding between immobilized antibodies and target bacterial cells. An aliquot of 1 mL of drinking water, without incubation of bacteria, was used as negative control.

2.6. Enhanced Sensitivity Protocol

In order to improve the signal, an amplification step has been included in the experimental procedure. The response enhancement has been achieved by conveying anti-*E. coli* (25 μg mL^{-1}) into the microfluidic cell for 30 min. This additional step, which leads to the formation of a sandwich complex, was used to amplify the slight impedance increment obtained after *E. coli* detection at low concentration. In such a case, the formation of a sandwich complex further hinders the electron-transfer process thus improving the electrochemical response. A final washing phase with 0.01 M PBS is used to remove unbound or weakly bonded molecules.

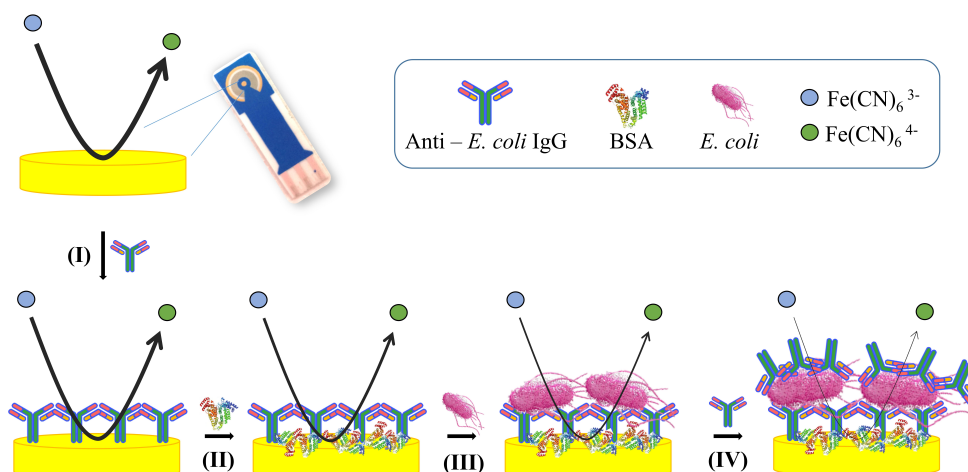
3. Results and Discussion

3.1. Principle of the Impedimetric Biosensor

The different steps involved in the preparation of our immunosensor are schematically illustrated in Scheme 1 (not to scale). After cleaning the AuSPE with H_2SO_4 , the surface is functionalized (step I) with previously activated antibodies using the LP Hg lamp above described. Then, bovine serum albumin (BSA) is used as blocking reagent to fill the free remaining spaces on the gold electrode (step II). In the next step (step III) a specific binding event occurs between the immobilized antibodies and the *E. coli* cells. Finally, in order to improve the sensitivity, a sandwich complex is realized by conveying a fresh anti-*E. coli* Abs solution to the circuit. Consecutive steps of the immunosensor development as well as the *E. coli* detection are described in detail in the Materials and Methods section above.

EIS is characterization techniques to study the electron transfer process and, specifically, the changes of charge transfer resistance caused by the adsorption of isolating molecules to the gold electrode. The impedance data are represented as Nyquist plots (see Figures 3–6), where the real and the imaginary components of impedance are plotted in the X and Y axes, respectively. The Nyquist plots consist of two portions: the semicircle portion at high frequencies indicates the electron-transfer process while the linear part at lower frequencies represents the diffusion-limited mass transfer process of the redox probe. A modified Randles circuit (shown as inset in Figures 3–6) was used to fit the experimental data over the whole frequency range. In this equivalent circuit, R_s stands for the resistance of the solution,

CPE is the constant phase element, R_{ct} is the charge transfer resistance and W the Warburg impedance. R_s and W represent bulk properties of the electrolyte solution and diffusion features of the redox probe in the solution. These parameters are not influenced by modification of the electrode surface and are not modified by the antibodies-bacteria interaction. On the contrary, R_{ct} depends critically on the dielectric and insulating features at the electrode-electrolyte interface and can be used as sensing parameter since it is very sensitive to electrode modifications. The CPE is introduced in the equivalent circuit instead of a simple capacitor to account for inhomogeneity and defect areas of the layer [69].



Scheme 1. Schematic diagram (not in scale) of the stepwise functionalization and detection. The black line represents the intensity of the redox reaction, which is inhibited as the surface covering grows. The reduction of its thickness is associated to a decrease of the “effective” area available for the electrolyte current, which is measured as an increase of the charge transfer resistance.

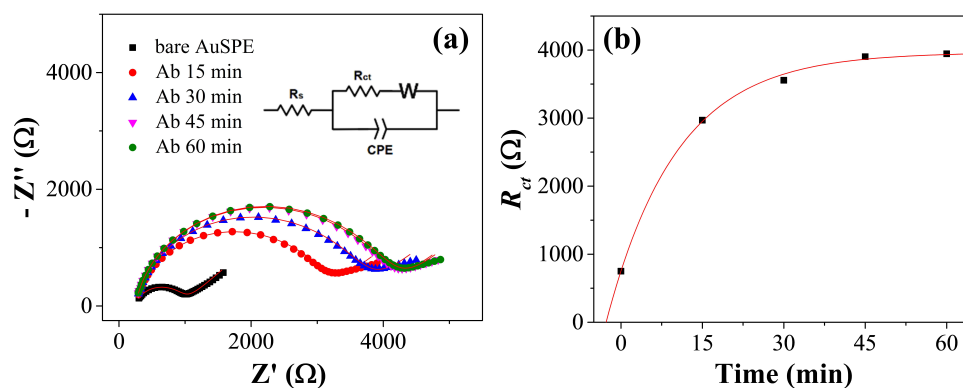


Figure 3. (a) EIS spectrum measured at different times while the UV irradiated antibodies are conveyed to the interaction cell; (b) R_{ct} as a function of time showing that the surface saturation takes place within one-hour time. The errors of R_{ct} are within the thickness of the experimental points.

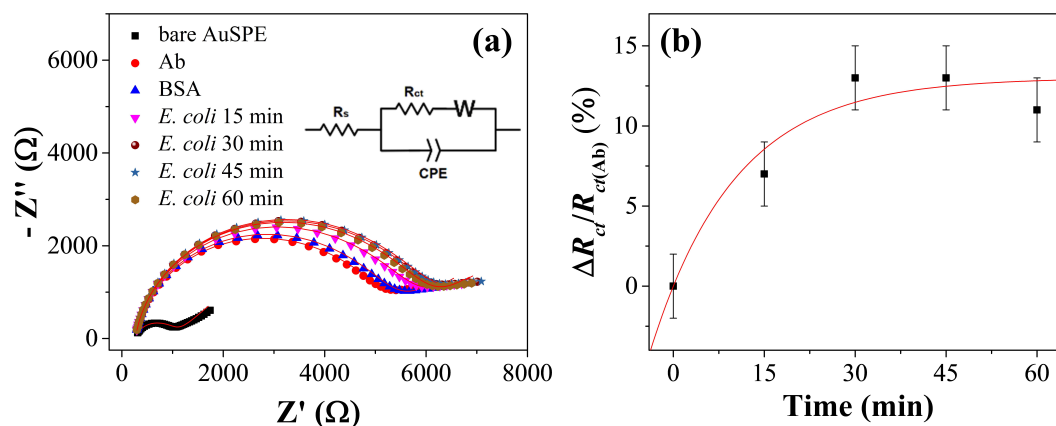


Figure 4. (a) EIS spectrum measured at different times with *E. coli* at 10^5 CFU mL⁻¹; (b) R_{ct} as a function of time showing an exponential kinetic with a constant time of 14 ± 7 min.

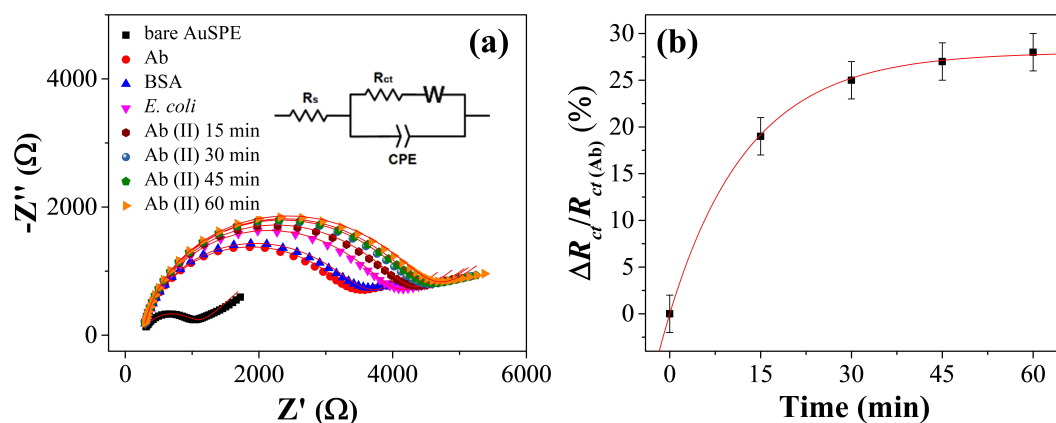


Figure 5. Kinetics of the secondary antibody. (a) EIS spectrum measured at different times while a $25 \mu\text{g mL}^{-1}$ Ab solution is conveyed to the cell after the detection *E. coli* (10^5 CFU mL⁻¹); (b) R_{ct} as a function of time showing an exponential dynamic with a constant time of 13.5 ± 0.3 min.

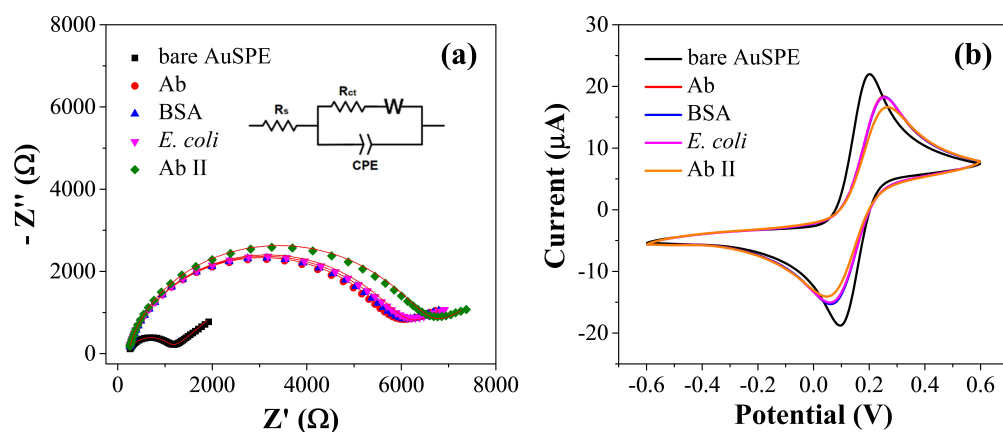


Figure 6. (a) EIS and (b) CV of the step-by-step immunosensor development and *E. coli* detection in 10 mM $\text{Fe}(\text{CN})_6^{3-}/\text{Fe}(\text{CN})_6^{4-}$ solution at pH 7.4.

3.2. Kinetics of the Functionalization and Detection

In the photochemical immobilization technique, the Abs are conveyed to the electrode after they have been irradiated by the UV lamp. Since the activation of the Abs only lasts approximately 5 min [57], it is necessary to optimize the time the solution is fluxed in the cell containing the working electrode (10 μL volume). The results obtained with a flow rate of $6 \mu\text{L s}^{-1}$ are reported in Figure 3a

(see Table S1 for the data), that shows EIS spectra measured at intervals of 15 min, which are required to cover the whole surface. The resulting R_{ct} is shown in Figure 3b and its behavior with the time is well fitted by an exponential function with time constant of 13 ± 1 min. Thus, the whole functionalization procedure can be considered accomplished in one-hour time. Since no significant change of R_{ct} is observed after the blocking step, we can assess that the saturation of R_{ct} shown in Figure 3b corresponds to an electrode fully covered by antibodies.

The kinetic of *E. coli* detection was studied to optimize the performance of the immunosensor. Drinking water samples incubated with a concentration on *E. coli* 10^5 CFU mL⁻¹ was flowed over the antibody-modified electrode and the R_{ct} change was monitored at time intervals of 15 min. The results are reported in Figure 4a (Nyquist plot) and 4b (normalized R_{ct}) with an exponential fit of the experimental data that provides a time constant of 14 ± 7 min (see Table S2 for the data). Although with larger error, such a value is similar to that measured for surface functionalization by Abs suggesting that 30 min was a suitable incubation time to allow the completion of the analyte detection.

We also measured the kinetics of the Ab binding to the *E. coli* from the top (sandwich configuration) by carrying out EIS as a function of time during the flow of a $25 \mu\text{g mL}^{-1}$ Ab solution into the cell. The Nyquist plots are reported in Figure 5a and the corresponding values for R_{ct} are shown in Figure 5b (see Table S3 for the data) with an exponential fit of the data that provides a constant time of 13.5 ± 0.3 min. Once again, 30 min can be considered a recommended value that allows the accomplishment of the amplification step.

3.3. Electrochemical Characterization of the Immunosensor Preparation

Cyclic voltammetry (CV) and electrochemical impedance spectroscopy (EIS) measurements were carried out to investigate the layer by layer construction of the immunosensor and to verify the *E. coli* binding (Figure 6). Both characterization techniques investigate the electron transfer process and, specifically, the changes of charge transfer resistance caused by the adsorption of isolating molecules to the gold electrode. EIS plots of the step-by-step immunosensor fabrication are shown in Figure 6a, utilizing $10 \text{ mM Fe(CN)}_6^{3-}/\text{Fe(CN)}_6^{4-}$ as redox probe in 0.01 M PBS buffer.

The potential applied for the EIS studies was set to 0.16 V (vs. Ag/AgCl) according to the CV result. The impedance data are represented as Nyquist plots and R_{ct} values were extracted by fitting the data with the Randles circuit (inset Figure 6a, see Table S4 for the data,) after each preparation step since the comparison of these values indicate the change of the redox probe kinetics at the electrode interface. The R_{ct} of the bare electrode was as small as 878 Ω . The surface is functionalized using previously activated antibodies which tether the surface providing a significantly resistance increase of approximately 5.4 k Ω , since the covalent immobilization of antibodies onto the electrode surface acts as an inert electron transfer blocking layer and the penetration of the redox probe. The blocking of the surface was carried out with BSA at $50 \mu\text{g mL}^{-1}$ as well as at $100 \mu\text{g mL}^{-1}$ and in both cases a negligible increment of R_{ct} value could be detected thereby proving that the gold surface is fully covered by the antibodies (Figure S1, see Tables S5 and S6 for the data). In the next step, the solution containing the *E. coli* cells (10^2 CFU mL⁻¹) flows in the circuit and the analyte is recognized by the Abs. However, with the further attachment of the *E. coli* cells (10^2 CFU mL⁻¹) to the modified electrode surface no significant increase of impedance is observed and a solution of anti-*E. coli* Abs is conveyed to the cell giving rise to a sandwich complex which produces an increase of the charge transfer resistance caused by the realization of a further barrier towards the access of the redox probe to the electrode. In such a case, the R_{ct} value increases by a 15% after the formation of antibody *E. coli* complex.

In addition, CV measurements were carried out to corroborate the EIS results. CV curves of the step-by-step modification are shown in Figure 6b, using $10 \text{ mM Fe(CN)}_6^{3-}/\text{Fe(CN)}_6^{4-}$ as redox probe in 0.01 M PBS buffer. The bare gold electrode gave a well-defined anodic and cathodic peaks, due to the reversible interconversion of the redox probe $\text{Fe(CN)}_6^{3-}/\text{Fe(CN)}_6^{4-}$, with peak potential difference (ΔE_p) of 107 mV and peak current (I_p) of 23.9 μA . After antibodies immobilization, the ΔE_p increased to 192 mV and the I_p decreased to 19.1 μA confirming the attachment of charge transfer inhibiting

molecules to the gold electrode. The surface blocking with BSA caused a negligible decrease of I_p (18.9) confirming the complete saturation of the gold surface with antibodies. Finally, after the incubation with *E. coli* no significant decrease of current is observed and the resulting formation of antibody-*E. coli* complex lead to a further decrease of the peak current ($I_p = 17.2$ and $\Delta E_p = 218$) which coincides with EIS results.

3.4. Immunosensor Analytical Performance

The performance of the immunosensor for the detection of *E. coli* was investigated in drinking water by EIS. Drinking water samples (1 mL) were incubated with *E. coli* at different concentration in the range of 10^1 – 10^8 CFU mL⁻¹. Figure 7a shows the dose response curves obtained with steps I-III (red curve, direct detection protocol without amplification or DDP) and I-IV (black curve, ballasting detection protocol with amplification or BDP). The sensing parameter is $\Delta R_{ct}/R_{ct(Ab)}$ where ΔR_{ct} is the change in the impedance brought about by *E. coli* [in case of DDP $\Delta R_{ct} = R_{ct(E. coli)} - R_{ct(BSA)}$], whereas $R_{ct(Ab)}$ is the impedance value measured after the functionalization. As Figure 7a (red curve) shows, a detection range of two decades (10^3 to 10^5 CFU mL⁻¹) is achieved before reaching a saturation at concentration higher than 10^5 CFU mL⁻¹.

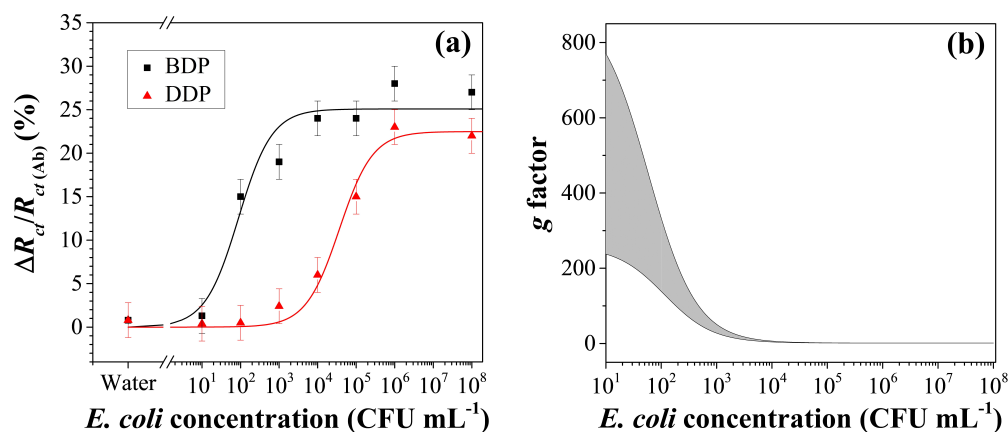


Figure 7. (a) Dose-response curve obtained using both protocols: DDP–direct detection protocol and BDP–ballasting detection protocol. The experimental data are fitted by Equation (6); (b) Gain factor g as a function of the *E. coli* concentration.

Each concentration has been tested three times in several days in different environmental conditions and using different electrode. The standard deviation (σ) of the measurements is approximately 2% proving that the protocol shows good accuracy and reproducibility. According to the 3σ formula, it is necessary to achieve an impedance increase $\geq 6\%$ in order to consider the variation as significant. As it shown in the dose-response curve, the limit *E. coli* concentration (LOD) producing such variation in impedance increase is 10^4 CFU mL⁻¹ (Figure 7a, red curve). The $\Delta R_{ct}/R_{ct(Ab)}$ measured for the negative sample (1 mL aliquot of drinking water) was less than 1% confirming the absence of interferences of the drinking water components (especially salts) with the biosensor surface.

In the DDP condition a LOD of approximately 10^4 CFU mL⁻¹ is obtained, which can be significantly improved by including the step IV that consists of addition of anti-*E. coli* Abs so that a sandwich configuration is realized as shown in Scheme 1 (step IV with Ab II). In fact, the relative electron-transfer resistance difference in such a case is $\Delta R_{ct}/R_{ct(Ab)}$ where $\Delta R_{ct} = R_{ct(AbII)} - R_{ct(BSA)}$ (Figure 7a, black curve). The black curve shows a remarkable increase in the slope as well as in the saturation level, which is achieved at lower concentration. With the same criteria used before (3σ formula with σ about 2%), the detection limit of this extended protocol (BDP) is estimated to be 3×10^1 CFU mL⁻¹ whereas the quantification range is 10^2 – 10^3 CFU mL⁻¹. It is worth noticing that a narrow quantification range is not a drawback when “on-off” biosensors are considered, as it is the case of the device proposed here.

The comparison of the two curves in Figure 7a suggests an enhancement of the signal whose factor depends on the *E. coli* concentration. In fact, by defining g as a gain factor, we have:

$$g([E - coli]) = \frac{\Delta R_{ct}^{(BDP)}([E - coli])}{\Delta R_{ct}^{(DDP)}([E - coli])}, \quad (1)$$

where the superscripts DDP and BDP refer to the three step and four step protocol, respectively. The plot of g is reported in Figure 7b as a function of *E. coli* concentration together with the 95% confidence interval (grey area) obtained by propagating the error from the curves in Figure 7a into Equation (1). The enhancement factor is more than one order of magnitude ($10 < g < 33$) at lower concentration and decreases to an expected saturation value of approximately 1 at higher concentrations. Such a behavior may well be explained by considering that at higher concentration of *E. coli*, the surface has a higher degree of occupancy by the bacteria so that the binding of additional Ab II tethered to *E. coli*, gives rise to a smaller effect on R_{ct} when compared to the effect produced at lower concentration.

The analytical performances of the developed immunosensor have been compared with other recent impedimetric immunosensors for the detection of *E. coli* (Table 1). It is remarkable that all of them share a quite long functionalization time ranging from few hours to even twenty hours to immobilize antibodies on gold electrode surface.

Table 1. Overview of the latest impedimetric biosensors for *Escherichia coli* detection.

Functionalization Scheme	Functionalization Time (h)	LOD (CFU mL ⁻¹)	Reference
Au-MHDA-Ab	18 *	2	[44]
Au-Cys-Ferrocene-Ab	20 *	3	[45]
Au-MUA/UDT-Ab	20 *	100	[46]
Au-PrG thiol-Ab	10	140	[47]
Au-AuNPs-PrG thiol-Ab	24 *	48	[47]
Au-PANI-Glu-Ab	>2	100	[48]
Au-Ab (PIT activated)	1	30	This work

Ab: antibody; MHDA: 16-mercaptohexadecanoic acid; Cys: Cysteamine; AuNPs: gold nanoparticles; PrG: Protein G; PANI: polyaniline; Glu: Glutaraldehyde; MUA: 11-mercaptoundecanoic acid; UDT: 1-undecanethiol. * These times have been evaluated by considering overnight as 16 h.

The immunosensors reported in Table 1 are based on immobilization procedures that include the formation of self-assembled monolayers, which usually require particularly smooth gold electrode surfaces [53] and expert personnel for the setup of complex chemical procedures. In contrast, PIT is user-friendly nor is any previous modification of the surface required. Any single electrode (AuSPE) was used “as is” that is without any pretreatment (only a rapid cleaning in H₂SO₄) or surface modification, but, even more important, the inherent differences among them in terms of bare impedance did not prevent us from building the more than satisfactory dose-response curve shown in Figure 7a.

3.5. Data Fitting

To account for the dose-response curve, we propose a simple model that describes the change of the resistance R_{ct} due to the analyte recognition as a change of the “effective” electrode area. To start with, let’s consider that while R_{ct} in the bare electrode is in the range 500–900 Ω , its value increases up to tens of k Ω when the antibodies tether to the surface. Moreover, thanks to our functionalization procedure, no significant change of R_{ct} is observed after the blocking step (the surface is fully covered by antibodies), and, hence, the initial charge transfer resistance of the biosensor is due to the antibody layer and can be written:

$$R_{ct,0} = \frac{\rho d}{A_0} \quad (2)$$

In Equation (2) ρ is the resistivity of the antibody layer, d its thickness and A_0 the electrode area. Since the contact layer does not change during the detection procedure, both ρ and d are constant. On the contrary, the occurrence of the analyte detection reduces to some extent the effective area of the electrode, which in turn leads to an increase of the impedance, i.e.:

$$R_{ct}([C]) = \frac{\rho d}{A_0 - \alpha A([C])} \quad (3)$$

where $A([C])$ represents the area occupied by the analytes and α is a coefficient that accounts for their conducting properties ($\alpha = 0$, for a “conductive” analyte that does not affect the electrolyte current, whereas $\alpha = 1$ for a fully “insulator” analyte). The occupancy area can be described by the Langmuir isotherm:

$$A([C]) = A_0 \frac{[C]}{K + [C]} \quad (4)$$

where for convenience we used K as the inverse of the equilibrium constant. By combining Equations (3) and (4), we have:

$$R_{ct}([C]) = R_{ct,0} \frac{K + [C]}{K + (1 - \alpha)[C]} \quad (5)$$

and the sensing parameter becomes:

$$\frac{\Delta R_{ct}}{R_{ct(Ab)}} = \frac{R_{ct}([C]) - R_{ct,0}}{R_{ct,0}} = \frac{[C]}{\frac{K}{\alpha} + \frac{(1-\alpha)}{\alpha}[C]} \quad (6)$$

The best fit of the experimental data by the Langmuir-type Equation (6) is shown in Figure 7a, whereas the fitting parameters are reported in Table 2.

Table 2. Fitting parameters α and K obtained for both protocols DDP and BDP.

	α	K
DDP	0.185 ± 0.007	$(3.0 \pm 0.7) \times 10^4$
BDP	0.20 ± 0.01	70 ± 26

As expected, the conductivity coefficient α , which measures the microscopic tendency of the analyte to inhibit the electrolyte current, is larger when antibodies are tied to the bacterium. The choice of $\Delta R_{ct}/R_{ct(Ab)}$ as sensing parameter not only allows one to measure the values for α reported in Table 2, but even more important from the practical point of view, introduces a high degree of robustness in the biosensors as demonstrated by the fact that each experimental point reported in Figure 7a was obtained with different electrode.

The increase of α observed when antibodies are bound to bacteria from the top is due to the high “opacity” of the antibodies, the latter property being deducible from the large increment of R_{ct} brought about by the surface functionalization (see Figures 3–6). By imagining that a bacterium fully covered by antibodies would have $\alpha = 1$, we can (under)estimate the fraction f of the bacterium area covered by the antibodies as:

$$f = \frac{\alpha_2 - \alpha_1}{1 - \alpha_1} \approx 0.024 \quad (7)$$

In Equation (7) α_2 and α_1 correspond to the value of α with and without amplification step, respectively. By considering that the area of *E. coli* is $A_{E-c} \approx 1 \mu\text{m}^2$ and that of an Ab is $A_{Ab} \approx 100 \text{nm}^2$, for the number N_{Ab} of Abs per bacterium, we have:

$$N_{Ab} = f \frac{A_{E-c}}{A_{Ab}} \approx 240 \quad (8)$$

Since this calculation is based on the assumption that an antibody is fully “opaque” to the electrolyte current, such a value has to be meant as an underestimation for the number of antibodies binding the bacterium from the top, which is likely to be larger than one thousand.

3.6. Immunosensor Specificity

In order to evaluate the specificity of the developed immunosensor for *E. coli*, we tested the response of the functionalized immunosensor by measuring $\Delta R_{ct}/R_{ct(Ab)}$ induced by some non-specific bacteria such as *Acinetobacter baumannii* and *Salmonella enteritidis* 706 RIVM. To this end a 1mL aliquot of drinking water incubated with *Salmonella enteritidis* 706 RIVM and *Acinetobacter baumannii* (10^5 CFU mL⁻¹) flowed into the circuit for 30 min at room temperature, followed by a fresh solution of anti-*E. coli* Abs. Figure 8 shows the electron transfer resistance changes for both protocols. According to the direct detection protocol (DDP), $\Delta R_{ct}/R_{ct(Ab)}$ increased by 2% and 7% when *Salmonella enteritidis* 706 RIVM and *Acinetobacter baumannii* were assayed, respectively, compared with an 15% increase achieved with *E. coli*. Actually, a greater increase with *Salmonella enteritidis* 706 RIVM would be expected in view of the stronger morphological similarities with *E. coli* but, this unexpected behaviour can be likely ascribed to the different shape of *Acinetobacter baumannii*, which is a short, rod-shaped almost round bacterium which mostly hinder at the same concentration. With reference to the extended protocol (BDP), after the ballasting with a fresh solution of anti-*E. coli* Abs, $\Delta R_{ct}/R_{ct(Ab)}$ increased less than a 9% for both *Salmonella enteritidis* 706 RIVM and *Acinetobacter baumannii*, compared to the marked increase (24%) obtained with *E. coli* cells. This means that the amplification factor is about 1% for *Acinetobacter baumannii* and 4.5% for *Salmonella enteritidis* 706 RIVM, a difference likely due to the superior affinity between anti-*E. coli* pAbs and *Salmonella*, which share the same morphology. These results are more than satisfactory since only a slight cross-reaction arises with other bacterial species.

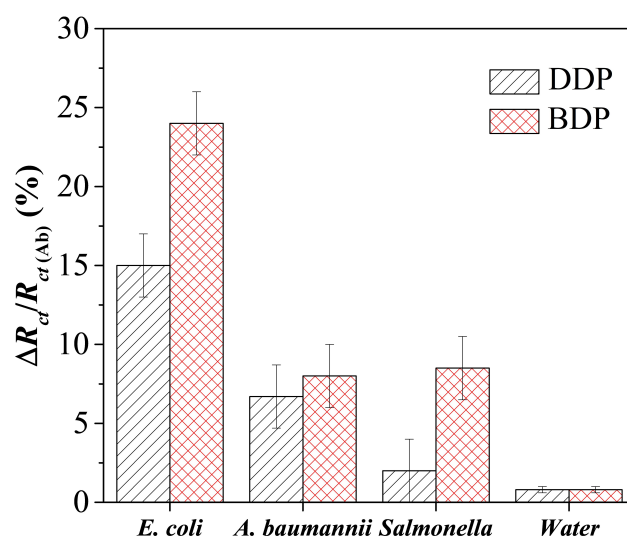


Figure 8. Specificity of the immunosensor in 10 mM $\text{Fe}(\text{CN})_6^{3-/4-}$ solution at pH 7.4. $\Delta R_{ct}/R_{ct(Ab)}$ induced by 10^5 CFU mL⁻¹ *E. coli* in comparison with the negative control (drinking water) and non-target bacteria (*Acinetobacter baumannii* and *Salmonella enteritidis* 706 RIVM).

4. Conclusions

An electrochemical impedance immunosensor based on a screen printed gold electrode for the rapid detection of *E. coli* in drinking water is proposed. Firstly, the antibodies were immobilized on the gold electrode surface in a covalent way using the Photochemical Immobilization Technique and the change in charge transfer resistance was monitored in the redox probe $\text{Fe}(\text{CN})_6^{3-}/\text{Fe}(\text{CN})_6^{4-}$ using the EIS. The proposed immunosensor exhibits a limit of detection of 3×10^1 CFU mL⁻¹ which was obtained

by including in the measurement procedure a simple and rapid ballasting step, the latter consisting in the flowing of a fresh antibody solution onto the electrode surface so to realize a sandwich-complex.

PIT is an alternative method to bind antibodies onto gold surfaces and this is the first time it was used in biosensing by EIS. Our results demonstrate that PIT is effective proved even on commercial cheap electrodes. This is a major achievement since in most situations careful surface treatments are required in order to get an effective sensor response. In addition, PIT is a really a quick functionalization method since only 30 s are required for the antibodies activation and 1 h for the whole functionalization procedure (solution flowing on the electrode surface). Thus, the whole measurement can be carried out in less than 6 h (which means within a working day) since the total analysis time is 3 h and 30 min including washing and sensing processes making our approach suitable for out-of-lab use when low contamination levels need to be detected for alert emergency and, hence, an “on-off” approach is more desirable than a time-consuming quantitative procedure.

Supplementary Materials: The following are available online at <http://www.mdpi.com/1424-8220/20/1/274/s1>, Figure S1: (a) EIS spectrum measured with 100 $\mu\text{g mL}^{-1}$ BSA solution. (b) EIS spectrum measured at different times while a 50 $\mu\text{g mL}^{-1}$ BSA solution is conveyed to the cell, Table S1: Results from the fitting of impedance data (Figure 3) to the Randles circuit, Table S2: Results from the fitting of impedance data (Figure 4) to the Randles circuit, Table S3: Results from the fitting of impedance data (Figure 5) to the Randles circuit, Table S4: Results from the fitting of impedance data (Figure 6) to the Randles circuit, Table S5: Results from the fitting of impedance data (Figure S1a) to the Randles circuit, Table S6: Results from the fitting of impedance data (Figure S1b) to the Randles circuit.

Author Contributions: Conceptualization, M.C., B.D.V. and A.F.; methodology, M.C., R.G., A.F., R.C. and A.A.; validation, G.B., M.C., A.F., M.P. and R.G.; formal analysis, B.D.V., R.C., A.A. and R.V.; investigation, M.C., A.F., M.P. and R.G.; resources, A.A., A.F., R.C., R.V., R.G. and S.B.C.; data curation, M.C., A.F., A.A. and M.P.; writing—original draft preparation, M.C., A.F. and M.P.; writing—review and editing, M.C., B.D.V. and R.V.; visualization, G.B., M.C., A.F. and R.G.; supervision, B.D.V.; funding acquisition, S.B.C. and R.V. All authors have read and agreed to the published version of the manuscript.

Funding: This research was funded by Programma Operativo Nazionale (PON) Ricerca e Innovazione 2014–2020 “Dottorati innovativi con caratterizzazione industriale” and by Progetto “MultiPath-Multiplex nanostructured platform for label-free detection of foodborne pathogens and carcinogenic pesticides” - POR FESR CAMPANIA 2014/2020-O.S. 1.1–Avviso pubblico progetti di trasferimento tecnologico e di prima industrializzazione per le imprese innovative ad alto potenziale per la lotta alle patologie oncologiche.

Conflicts of Interest: The authors declare no conflict of interest.

References

- Odonkor, S.T.; Ampofo, J.K. *Escherichia coli* as an indicator of bacteriological quality of water: An overview. *Microbiol. Res.* **2013**, *4*, e2. [[CrossRef](#)]
- Cabral, J.P.S. Water microbiology. Bacterial pathogens and water. *Int. J. Environ. Res. Public Health* **2010**, *7*, 3657–3703. [[CrossRef](#)] [[PubMed](#)]
- World Health Organization. Drinking-Water. Available online: <https://www.who.int/news-room/fact-sheets/detail/drinking-water> (accessed on 17 September 2019).
- Price, R.G.; Wildeboer, D. *E. coli* as an Indicator of Contamination and Health Risk in Environmental Waters. In *Escherichia coli—Recent Advances on Physiology, Pathogenesis and Biotechnological Applications*; InTech: London, UK, 2017.
- Velusamy, V.; Arshak, K.; Korostynska, O.; Oliwa, K.; Adley, C. An overview of foodborne pathogen detection: In the perspective of biosensors. *Biotechnol. Adv.* **2010**, *28*, 232–254. [[CrossRef](#)]
- Bai, Y.; Huang, W.C.; Yang, S.T. Enzyme-linked immunosorbent assay of *Escherichia coli* O157:H7 in surface enhanced poly(methyl methacrylate) microchannels. *Biotechnol. Bioeng.* **2007**, *98*, 328–339. [[CrossRef](#)]
- Holland, J.L.; Louie, L.; Simor, A.E.; Louie, M. PCR detection of *Escherichia coli* O157:H7 directly from stools: Evaluation of commercial extraction methods for purifying fecal DNA. *J. Clin. Microbiol.* **2000**, *38*, 4108–4113. [[CrossRef](#)]
- Guan, J.; Levin, R.E. Quantitative detection of *Escherichia coli* O157:H7 in ground beef by the polymerase chain reaction. *Food Microbiol.* **2002**, *19*, 159–165. [[CrossRef](#)]

9. Deisingh, A.K.; Thompson, M. Detection of infectious and toxigenic bacteria. *Analyst* **2002**, *127*, 567–581. [[CrossRef](#)]
10. Váradi, L.; Luo, J.L.; Hibbs, D.E.; Perry, J.D.; Anderson, R.J.; Orenga, S.; Groundwater, P.W. Methods for the detection and identification of pathogenic bacteria: Past, present, and future. *Chem. Soc. Rev.* **2017**, *46*, 4818–4832. [[CrossRef](#)]
11. Furst, A.L.; Francis, M.B. Impedance-Based Detection of Bacteria. *Chem. Rev.* **2019**, *119*, 700–726. [[CrossRef](#)]
12. Nayak, M.; Kotian, A.; Marathe, S.; Chakravorty, D. Detection of microorganisms using biosensors—A smarter way towards detection techniques. *Biosens. Bioelectron.* **2009**, *25*, 661–667. [[CrossRef](#)]
13. Xu, M.; Wang, R.; Li, Y. Electrochemical biosensors for rapid detection of *Escherichia coli* O157:H7. *Talanta* **2017**, *162*, 511–522. [[CrossRef](#)] [[PubMed](#)]
14. Dudak, F.C.; Boyaci, I.H. Development of an immunosensor based on surface plasmon resonance for enumeration of *Escherichia coli* in water samples. *Food Res. Int.* **2007**, *40*, 803–807. [[CrossRef](#)]
15. Guo, X.; Lin, C.S.; Chen, S.H.; Ye, R.; Wu, V.C.H. A piezoelectric immunosensor for specific capture and enrichment of viable pathogens by quartz crystal microbalance sensor, followed by detection with antibody-functionalized gold nanoparticles. *Biosens. Bioelectron.* **2012**, *38*, 177–183. [[CrossRef](#)] [[PubMed](#)]
16. Leahy, S.; Lai, Y. A cantilever biosensor based on a gap method for detecting *E. coli* in real time. *Sens. Actuators B Chem.* **2017**, *246*, 1011–1016. [[CrossRef](#)]
17. Felix, F.S.; Angnes, L. Electrochemical immunosensors—A powerful tool for analytical applications. *Biosens. Bioelectron.* **2018**, *102*, 470–478. [[CrossRef](#)]
18. Mollarasouli, F.; Kurbanoglu, S.; Ozkan, S.A. The Role of Electrochemical Immunosensors in Clinical Analysis. *Biosensors* **2019**, *9*, 86. [[CrossRef](#)]
19. Zhang, Z.; Zhou, J.; Du, X. Electrochemical Biosensors for Detection of Foodborne Pathogens. *Micromachines* **2019**, *10*, 222. [[CrossRef](#)]
20. Maalouf, R.; Fournier-Wirth, C.; Coste, J.; Chebib, H.; Saïkali, Y.; Vittori, O.; Errachid, A.; Cloarec, J.P.; Martelet, C.; Jaffrezic-Renault, N. Label-free detection of bacteria by electrochemical impedance spectroscopy: Comparison to surface plasmon resonance. *Anal. Chem.* **2007**, *79*, 4879–4886. [[CrossRef](#)]
21. Escamilla-Gómez, V.; Campuzano, S.; Pedrero, M.; Pingarrón, J.M. Gold screen-printed-based impedimetric immunobiosensors for direct and sensitive *Escherichia coli* quantisation. *Biosens. Bioelectron.* **2009**, *24*, 3365–3371. [[CrossRef](#)]
22. Geng, P.; Zhang, X.; Meng, W.; Wang, Q.; Zhang, W.; Jin, L.; Feng, Z.; Wu, Z. Self-assembled monolayers-based immunosensor for detection of *Escherichia coli* using electrochemical impedance spectroscopy. *Electrochim. Acta* **2008**, *53*, 4663–4668. [[CrossRef](#)]
23. Yang, H.; Zhou, H.; Hao, H.; Gong, Q.; Nie, K. Detection of *Escherichia coli* with a label-free impedimetric biosensor based on lectin functionalized mixed self-assembled monolayer. *Sens. Actuators B Chem.* **2016**, *229*, 297–304. [[CrossRef](#)]
24. Malvano, F.; Pilloton, R.; Albanese, D. Label-free impedimetric biosensors for the control of food safety—A review. *Int. J. Environ. Anal. Chem.* **2019**, *44*. [[CrossRef](#)]
25. Welch, N.G.; Scoble, J.A.; Muir, B.W.; Pigram, P.J. Orientation and characterization of immobilized antibodies for improved immunoassays (Review). *Biointerphases* **2017**, *12*, 02D301. [[CrossRef](#)] [[PubMed](#)]
26. Zhou, Y.; Fang, Y.; Ramasamy, R.P. Non-covalent functionalization of carbon nanotubes for electrochemical biosensor development. *Sensors* **2019**, *19*, 392. [[CrossRef](#)]
27. Sharma, S.; Byrne, H.; O’Kennedy, R.J. Antibodies and antibody-derived analytical biosensors. *Essays Biochem.* **2016**, *60*, 9–18.
28. Um, H.; Kim, M.; Lee, S.; Min, J.; Kim, H.; Choi, Y.; Kim, Y. Electrochemically oriented immobilization of antibody on poly-(2-cyano-ethylpyrrole)-coated gold electrode using a cyclic voltammetry. *Talanta* **2011**, *84*, 330–334. [[CrossRef](#)]
29. Alves, N.J.; Kiziltepe, T.; Bilgicer, B. Oriented surface immobilization of antibodies at the conserved nucleotide binding site for enhanced antigen detection. *Langmuir* **2012**, *28*, 9640–9648. [[CrossRef](#)]
30. Ho, J.A.; Hsu, W.; Liao, W.; Chiu, J.; Chen, M.; Chang, H.; Li, C. Ultrasensitive electrochemical detection of biotin using electrically addressable site-oriented antibody immobilization approach via aminophenyl boronic acid. *Biosens. Bioelectron.* **2010**, *26*, 1021–1027. [[CrossRef](#)]

31. Vashist, S.K.; Dixit, C.K.; MacCraith, B.D.; O’Kennedy, R. Effect of antibody immobilization strategies on the analytical performance of a surface plasmon resonance-based immunoassay. *Analyst* **2011**, *136*, 4431–4436. [[CrossRef](#)]
32. Rahman, M.A.; Shiddiky, M.J.A.; Park, J.S.; Shim, Y.B. An impedimetric immunosensor for the label-free detection of bisphenol A. *Biosens. Bioelectron.* **2007**, *22*, 2464–2470. [[CrossRef](#)]
33. Barton, A.C.; Collyer, S.D.; Davis, F.; Garifallou, G.; Tsekenis, G.; Tully, E.; Kennedy, R.O.; Gibson, T.; Millner, P.A.; Higson, S.P.J. Labelless AC impedimetric antibody-based sensors with pg mL^{-1} sensitivities for point-of-care biomedical applications. *Biosens. Bioelectron.* **2009**, *24*, 1090–1095. [[CrossRef](#)] [[PubMed](#)]
34. Ouerghi, O.; Touhami, A.; Jaffrezic-Renault, N.; Martelet, C.; Ouada, H.B.; Cosnier, S. Impedimetric immunosensor using avidin—Biotin for antibody immobilization. *Bioelectrochemistry* **2002**, *56*, 131–133. [[CrossRef](#)]
35. Lee, J.E.; Seo, J.H.; Kim, C.S.; Kwon, Y.; Ha, J.H.; Choi, S.S.; Cha, H.J. A comparative study on antibody immobilization strategies onto solid surface. *Korean J. Chem. Eng.* **2013**, *30*, 1934–1938. [[CrossRef](#)]
36. Inkpen, M.S.; Liu, Z.-F.; Li, H.; Campos, L.M.; Neaton, J.B.; Venkataraman, L. Non-chemisorbed gold–sulfur binding prevails in self-assembled monolayers. *Nat. Chem.* **2019**, *11*, 351–358. [[CrossRef](#)] [[PubMed](#)]
37. Sharafeldin, M.; Rusling, J.F. Influence of antibody immobilization strategy on carbon electrode immunoarrays. *Analyst* **2019**, *144*, 5108–5116. [[CrossRef](#)] [[PubMed](#)]
38. Fowler, J.M.; Stuart, M.C.; Wong, D.K.Y. Self-assembled layer of thiolated protein G as an immunosensor scaffold. *Anal. Chem.* **2007**, *79*, 350–354. [[CrossRef](#)] [[PubMed](#)]
39. Sun, X.; Du, S.; Wang, X.; Zhao, W.; Li, Q. A label-free electrochemical immunosensor for carbofuran detection based on a sol-gel entrapped antibody. *Sensors* **2011**, *11*, 9520–9531. [[CrossRef](#)]
40. Bereli, N.; Ertürk, G.; Tümer, M.A.; Denizli, A. Oriented immobilized anti-hIgG via Fc fragment-imprinted PHEMA cryogel for IgG purification. *Biomed. Chromatogr.* **2013**, *27*, 599–607. [[CrossRef](#)]
41. Moschallski, M.; Evers, A.; Brandstetter, T.; Rühle, J. Sensitivity of microarray based immunoassays using surface-attached hydrogels. *Anal. Chim. Acta* **2013**, *781*, 72–79. [[CrossRef](#)]
42. Yamazoe, H. Antibody immobilization technique using protein film for high stability and orientation control of the immobilized antibody. *Mater. Sci. Eng. C* **2019**, *100*, 209–214. [[CrossRef](#)]
43. Icoz, K.; Soylyu, M.C.; Canikara, Z.; Unal, E. Quartz-crystal Microbalance Measurements of CD19 Antibody Immobilization on Gold Surface and Capturing B Lymphoblast Cells: Effect of Surface Functionalization. *Electroanalysis* **2018**, *30*, 834–841. [[CrossRef](#)]
44. Barreiros dos Santos, M.; Agusil, J.P.; Prieto-Simón, B.; Sporer, C.; Teixeira, V.; Samitier, J. Highly sensitive detection of pathogen *Escherichia coli* O157:H7 by electrochemical impedance spectroscopy. *Biosens. Bioelectron.* **2013**, *45*, 174–180. [[CrossRef](#)] [[PubMed](#)]
45. Malvano, F.; Pilloton, R.; Albanese, D. Sensitive Detection of *Escherichia coli* O157:H7 in Food Products by Impedimetric Immunosensors. *Sensors* **2018**, *18*, 2168. [[CrossRef](#)] [[PubMed](#)]
46. Wan, J.; Ai, J.; Zhang, Y.; Geng, X.; Gao, Q.; Cheng, Z. Signal-off impedimetric immunosensor for the detection of *Escherichia coli* O157:H7. *Sci. Rep.* **2016**, *6*, 19806. [[CrossRef](#)] [[PubMed](#)]
47. Lin, D.; Pillai, R.G.; Lee, W.E.; Jemere, A.B. An impedimetric biosensor for *E. coli* O157:H7 based on the use of self-assembled gold nanoparticles and protein G. *Microchim. Acta* **2019**, *186*, 169. [[CrossRef](#)] [[PubMed](#)]
48. Chowdhury, A.D.; De, A.; Chaudhuri, C.R.; Bandyopadhyay, K.; Sen, P. Label free polyaniline based impedimetric biosensor for detection of *E. coli* O157:H7 Bacteria. *Sens. Actuators B Chem.* **2012**, *171–172*, 916–923. [[CrossRef](#)]
49. Vericat, C.; Vela, M.E.; Benitez, G.; Carro, P.; Salvarezza, R.C. Self-assembled monolayers of thiols and dithiols on gold: New challenges for a well-known system. *Chem. Soc. Rev.* **2010**, *39*, 1805–1834. [[CrossRef](#)]
50. Mandler, D.; Kraus-Ophir, S. Self-assembled monolayers (SAMs) for electrochemical sensing. *J. Solid State Electrochem.* **2011**, *15*, 1535. [[CrossRef](#)]
51. Chaki, N.K.; Vijayamohan, K. Self-assembled monolayers as a tunable platform for biosensor applications. *Biosens. Bioelectron.* **2002**, *17*, 1–12. [[CrossRef](#)]
52. Lee, C.Y.; Canavan, H.E.; Gamble, L.J.; Castner, D.G. Evidence of impurities in thiolated single-stranded DNA oligomers and their effect on DNA self-assembly on gold. *Langmuir* **2005**, *21*, 5134–5141. [[CrossRef](#)]
53. Butterworth, A.; Blues, E.; Williamson, P.; Cardona, M.; Gray, L.; Corrigan, D.K. SAM composition and electrode roughness affect performance of a DNA biosensor for antibiotic resistance. *Biosensors* **2019**, *9*, 22. [[CrossRef](#)] [[PubMed](#)]

54. Reimers, J.R.; Ford, M.J.; Marcuccio, S.M.; Ulstrup, J.; Hush, N.S. Competition of van der Waals and chemical forces on gold-sulfur surfaces and nanoparticles. *Nat. Rev. Chem.* **2017**, *1*, 0017. [[CrossRef](#)]
55. Häkkinen, H. The gold-sulfur interface at the nanoscale. *Nat. Chem.* **2012**, *4*, 443–455. [[CrossRef](#)] [[PubMed](#)]
56. Pensa, E.; Cortés, E.; Corthey, G.; Carro, P.; Vericat, C.; Fonticelli, M.H.; Benítez, G.; Rubert, A.A.; Salvarezza, R.C. The chemistry of the sulfur-gold interface: In search of a unified model. *Acc. Chem. Res.* **2012**, *45*, 1183–1192. [[CrossRef](#)] [[PubMed](#)]
57. Della Ventura, B.; Banchelli, M.; Funari, R.; Illiano, A.; De Angelis, M.; Taroni, P.; Amoresano, A.; Matteini, P.; Velotta, R. Biosensor surface functionalization by a simple photochemical immobilization of antibodies: Experimental characterization by mass spectrometry and surface enhanced Raman spectroscopy. *Analyst* **2019**, *144*, 6871–6880. [[CrossRef](#)] [[PubMed](#)]
58. Della Ventura, B.; Schiavo, L.; Altucci, C.; Esposito, R.; Velotta, R. Light assisted antibody immobilization for bio-sensing. *Biomed. Opt. Express* **2011**, *2*, 3223–3231. [[CrossRef](#)]
59. Gaglione, R.; Dell’Olmo, E.; Bosso, A.; Chino, M.; Pane, K.; Ascione, F.; Itri, F.; Caserta, S.; Amoresano, A.; Lombardi, A.; et al. Novel human bioactive peptides identified in Apolipoprotein B: Evaluation of their therapeutic potential. *Biochem. Pharmacol.* **2017**, *130*, 34–50. [[CrossRef](#)]
60. Funari, R.; Della Ventura, B.; Altucci, C.; Offenhäusser, A.; Mayer, D.; Velotta, R. Single Molecule Characterization of UV-Activated Antibodies on Gold by Atomic Force Microscopy. *Langmuir* **2016**, *32*, 8084–8091. [[CrossRef](#)]
61. Neves-Petersen, M.T.; Gryczynski, Z.; Lakowicz, J.; Fojan, P.; Pedersen, S.; Petersen, E.; Bjørn Petersen, S. High probability of disrupting a disulphide bridge mediated by an endogenous excited tryptophan residue. *Protein Sci.* **2002**, *11*, 588–600. [[CrossRef](#)]
62. Ellman, G.L. Tissue Sulfyd Groups. *Arch. Biochem. Biophys.* **1959**, *82*, 70–77. [[CrossRef](#)]
63. Funari, R.; Della Ventura, B.; Carrieri, R.; Morra, L.; Lahoz, E.; Gesuele, F.; Altucci, C.; Velotta, R. Detection of parathion and patulin by quartz-crystal microbalance functionalized by the photonics immobilization technique. *Biosens. Bioelectron.* **2015**, *67*, 224–229. [[CrossRef](#)] [[PubMed](#)]
64. Funari, R.; Della Ventura, B.; Schiavo, L.; Esposito, R.; Altucci, C.; Velotta, R. Detection of parathion pesticide by quartz crystal microbalance functionalized with UV-activated antibodies. *Anal. Chem.* **2013**, *85*, 6392–6397. [[CrossRef](#)] [[PubMed](#)]
65. Della Ventura, B.; Sakač, N.; Funari, R.; Velotta, R. Flexible immunosensor for the detection of salivary α -amylase in body fluids. *Talanta* **2017**, *174*, 52–58. [[CrossRef](#)] [[PubMed](#)]
66. Funari, R.; Terracciano, I.; Della Ventura, B.; Ricci, S.; Cardi, T.; D’Agostino, N.; Velotta, R. Label-Free Detection of Gliadin in Food by Quartz Crystal Microbalance-Based Immunosensor. *J. Agric. Food Chem.* **2017**, *65*, 1281–1289. [[CrossRef](#)]
67. Fulgione, A.; Cimafonte, M.; Della Ventura, B.; Iannaccone, M.; Ambrosino, C.; Capuano, F.; Proroga, Y.T.R.; Velotta, R.; Capparelli, R. QCM-based immunosensor for rapid detection of *Salmonella* Typhimurium in food. *Sci. Rep.* **2018**, *8*, 16137. [[CrossRef](#)]
68. Iarossi, M.; Schiattarella, C.; Rea, I.; De Stefano, L.; Fittipaldi, R.; Vecchione, A.; Velotta, R.; Della Ventura, B. Colorimetric Immunosensor by Aggregation of Photochemically Functionalized Gold Nanoparticles. *ACS Omega* **2018**, *3*, 3805–3812. [[CrossRef](#)]
69. Daniels, J.S.; Pourmand, N. Label-Free Impedance Biosensors: Opportunities and Challenges. *Electroanalysis* **2007**, *19*, 1239–1257. [[CrossRef](#)]



La borsa di dottorato è stata cofinanziata con risorse del
Programma Operativo Nazionale Ricerca e Innovazione 2014-2020 (CCI 2014IT16M2OP005),
Fondo Sociale Europeo, Azione I.1 “Dottorati Innovativi con caratterizzazione Industriale”



UNIONE EUROPEA
Fondo Sociale Europeo



*Ministero dell'Istruzione,
dell'Università e della Ricerca*

